

The Host Galaxies of Tidal Disruption Events

K. Decker French · Thomas Wevers ·
Jamie Law-Smith · Or Graur · Ann I.
Zabludoff

Received: date / Accepted: date

Abstract Recent studies of Tidal Disruption Events (TDEs) have revealed unexpected correlations between the TDE rate and the large-scale properties of the host galaxies. In this review, we present the host galaxy properties of all TDE candidates known to date and quantify their distributions. We consider throughout the differences between observationally-identified types of TDEs and differences from spectroscopic control samples of galaxies. We focus here on the black hole and stellar masses of TDE host galaxies, their star formation histories and stellar populations, the concentration and morphology of the optical light, the presence of AGN activity, and the extra-galactic environment

K. Decker French
Observatories of the Carnegie Institute for Science, 813 Santa Barbara St., Pasadena CA 91101, USA
E-mail: kfrench@carnegiescience.edu
ORCID: 0000-0002-4235-7337

Thomas Wevers
Institute of Astronomy, University of Cambridge, Madingley Road, Cambridge CB3 0HA, United Kingdom
E-mail: tw@ast.cam.ac.uk
ORCID: 0000-0002-4043-9400

Jamie Law-Smith
Department of Astronomy and Astrophysics, University of California, Santa Cruz, CA 95064, USA
E-mail: lawsmith@ucsc.edu
ORCID: 0000-0001-8825-4790

Or Graur
Harvard-Smithsonian Center for Astrophysics, 60 Garden Street, MA 02138, USA
E-mail: or.graur@cfa.harvard.edu
ORCID: 0000-0002-4391-6137

Ann Zabludoff
Steward Observatory, University of Arizona, 933 N Cherry Ave, Tucson, AZ 85721, USA
E-mail: aiz@email.arizona.edu
ORCID: 0000-0001-6047-8469

of the TDE hosts. We summarize the state of several possible explanations for the links between the TDE rate and host galaxy type. We present estimates of the TDE rate for different host galaxy types and quantify the degree to which rate enhancement in some types results in rate suppression in others. We discuss the possibilities for using TDE host galaxies to assist in identifying TDEs in upcoming large transient surveys and possibilities for TDE observations to be used to study their host galaxies.

1 Introduction

Tidal Disruption Events (TDEs) are observed when a star passes close enough to a supermassive black hole (SMBH) to be disrupted and torn apart by tidal forces. The rate of TDEs and the properties of the stars and SMBHs involved depend on the nuclear conditions of the host galaxies.

The mass of the SMBH will affect whether TDEs are observed and which stars can be tidally disrupted outside the event horizon (e.g., Hills 1975; Rees 1988; MacLeod et al. 2012; Law-Smith et al. 2017a). Because the tidal radius scales as $M_{\text{BH}}^{1/3}$, while the gravitational radius scales linearly with M_{BH} , stars will be swallowed whole if the SMBH is larger than the so-called Hills mass (Hills 1975), which is $\approx 10^8 M_{\odot}$ for a non spinning black hole and a Solar type star. The Hills mass also depends on the SMBH spin, such that a faster spinning SMBH can disrupt less massive stars at a given M_{BH} (Kesden 2012). The mass of the black hole is therefore an important parameter of a TDE. It can be estimated from observations because it is closely correlated with the mass and velocity dispersion of the galaxy’s stellar bulge (Magorrian et al. 1998; Ferrarese and Merritt 2000; Gültekin et al. 2009; Kormendy and Ho 2013; McConnell and Ma 2013). The mass of the stars available to be disrupted depends on the recent star formation history of the galaxy and the initial mass function. The mass of the disrupted star is much harder to infer from observations, although it has been argued that it leaves imprints on the UV/optical lightcurve (Lodato et al. 2009; Guillochon and Ramirez-Ruiz 2015; Mockler et al. 2019).

Stars will be perturbed in their orbits to pass within the tidal radius depending on the distribution function of the stars in that galaxy (Magorrian and Tremaine 1999). The parameter space of stars that can be tidally disrupted, called the loss cone, is thought to be re-filled mainly through two-body interactions, although other mechanisms may also play a non negligible role (see Stone et al. 2020, ISSI review). The stellar density profile in the vicinity of the SMBH and any deviations from an isotropic velocity / velocity dispersion field will hence affect the TDE rate (Magorrian and Tremaine 1999; Merritt and Poon 2004; Stone et al. 2018). As most TDEs are thought to be sourced from within the gravitational radius of influence of the black hole (Stone and Metzger 2016; this is typically 0.1-10 pc for galaxies with $M_{\text{BH}} \sim 10^{6-8} M_{\odot}$), the galaxy properties at these scales are likely to be most important in setting the TDE rate. However, the conditions in this region will be affected by the

evolution and merger history of the galaxy as a whole, and may therefore be correlated with larger scale galaxy properties.

Large transient surveys such as the Palomar Transient Factory (PTF; Law et al. 2009; Rau et al. 2009), Pan-STARRS (Chambers et al. 2016), the All Sky Automated Survey for SuperNovae (ASASSN; Shappee et al. 2014), and the Zwicky Transient Facility (ZTF; Bellm et al. 2019) in the optical, as well as the Roentgen Satellite (ROSAT) and the X-ray Multi-Mirror telescope (XMM; Jansen et al. 2001) in X-rays, and *Swift* in gamma rays have enabled the detections of tens of TDEs, providing a sample large enough to study population properties. In addition to the TDE properties themselves, these new samples of TDEs also allow us to study trends in their host galaxy properties. Arcavi et al. (2014) studied the host galaxies of seven UV/optical bright TDEs with broad H/He emission lines, and found many of the hosts showed E+A, or post-starburst, spectra. Such post-starburst spectra are characterized by a lack of strong emission lines, indicating low current star formation rates, but with strong Balmer absorption, indicating a recent burst of star formation (within the last \sim Gyr) that has now ended. Quiescent Balmer-strong galaxies, and the subset of post-starburst/E+A galaxies with less ambiguous star formation histories, are rare in the local universe, and yet are over-represented among TDE host galaxies (French et al. 2016; French et al. 2017; Law-Smith et al. 2017b; Graur et al. 2018).

The observed correlations between the pc-scale regions of stars which can be tidally disrupted and the kpc-scale star-formation histories and stellar concentrations are a puzzle, for which many possible solutions have been proposed. Here, we review the known host galaxy properties of TDEs observed to date and with published or archival host galaxy spectra in §2. We discuss possible drivers for the host galaxy preference in §3 and implications for the TDE rates in §4. We discuss possibilities for using the host galaxy information in future surveys to find more TDEs in §5 and study galaxy properties in §6 and conclude in §7.

1.1 TDEs Included in This Review

In this review, we have selected a list of TDEs to discuss from the sample compiled by Auchettl et al. (2017b) of X-ray and optical/UV - bright TDEs, as this sample has been used for recent host galaxy studies (Law-Smith et al. 2017b; Wevers et al. 2017; Graur et al. 2018). Given the focus of this chapter on the host galaxy properties, we only include TDEs for which a spectrum of the host galaxy has been published or is available from archival surveys. We have added three more recent TDEs for which host galaxy spectroscopy is available from before the TDE from SDSS and BOSS: AT2018dyk, AT2018bsi, and ASASSN18zj (aka AT2018hyz), as well as a new TDE with published host galaxy information (PS18kh, Holoien et al. 2018).

We note the important caveat that the classification of transient events as TDEs is complicated by the heterogeneous datasets obtained for each event.

For the purposes of this review we aim to balance including a large enough sample to reflect the range of published literature in this field with giving preference to the most well-justified claims of observed TDEs. We thus preserve the classifications of Auchettl et al. (2017b) for the X-ray and optical detected TDEs that rank the likelihood an event is a TDE based on the completeness of the data, and divide the data into a number of subsets. It is important to note that the host galaxy statistics may change depending on which subset of TDE candidates are used. We comment on the differences one obtains depending on the sample used throughout, though for some subclasses we are limited by small number statistics.

We list in Table 1 the TDEs considered in this review.

We divide the TDEs into two classes—X-ray bright and optical/UV bright—with several sub-categories. The X-ray bright TDEs are subdivided further into X-ray TDEs (Holoien et al. 2016b; Levan et al. 2011; Saxton et al. 2017; Holoien et al. 2016a), likely X-ray TDEs (Saxton et al. 2012; Esquej et al. 2007; Cenko et al. 2012; Maksym et al. 2010; Lin et al. 2015, 2017), and possible X-ray TDEs (Komossa and Greiner 1999; Gezari et al. 2008; Grupe et al. 1999; Ho et al. 1995; Greiner et al. 2000; Maksym et al. 2014) as done by Auchettl et al. (2017b). TDEs with no known or observed X-ray emission are classed as optical/UV TDEs (Brown et al. 2017; Blanchard et al. 2017; Tadhunter et al. 2017; Gezari et al. 2009; Chornock et al. 2014; Komossa et al. 2009; Wang et al. 2012; van Velzen et al. 2011; Yang et al. 2013; Holoien et al. 2016b; Arcavi et al. 2014; Blagorodnova et al. 2019; Arcavi et al. 2018; Gezari et al. 2018; Dong et al. 2018). TDEs requiring re-classification based on new X-ray data are re-classified (ASASSN-15oi, PS18kh; K. Auchettl, private communication).

TDEs that exhibited coronal lines (Komossa et al. 2009; Wang et al. 2012) or broad H/He lines (e.g., Arcavi et al. 2014) are also indicated. Three X-ray bright TDEs (ASASSN-14li, ASASSN-15oi, and PS18kh) additionally had significant optical observations, including broad H/He lines in their spectra, and are categorized as noted in the text. D3-13 is classed as a possible X-ray TDE, and also had significant optical/UV flux, but did not show broad H/He lines. We note that these classes are based on observational distinctions, which may or may not reflect physically different phenomena. Some optical/UV TDEs may have produced significant X-ray flux which was missed because of a lack of simultaneous X-ray observations. Indeed, the optical to X-ray luminosity ratios show significant variation in the events so far detected in both X-ray and optical light, and the observations of ASASSN-15oi by Gezari et al. (2017) demonstrate that X-ray emission can even be delayed well past the peak of the optical light curve, and would have been likely missed for many optical TDEs¹. Similarly, the coronal line detections may be a light echo from a previous TDE (Komossa and Merritt 2008), and the relation between these events and the others is still unclear. These classes represent those for which samples

¹ See e.g. Jonker et al. (2019) for more late-time X-ray detections of UV/optical TDEs; this article was posted to the arXiv during review of this article.

have been aggregated in the literature, and with adequate host galaxy localization and observations to study for the purposes of this chapter. We direct the reader to the other chapters in this review, especially those by Saxton et al., Arcavi et al., Zauderer et al., Alexander et al., and Zabludoff et al., (2020, ISSI review) for further discussion of TDE classification and the question of multiple TDE classes.

In particular, we note that the class of events including F01004 (Tadhunter et al. 2017) may be a type of nuclear phenomenon other than a TDE. Trakhtenbrot et al. (2019) argue against the TDE interpretation of this event as it has significantly narrower He lines than other broad H/He line events and the presence of Bowen fluorescence lines. However, Bowen fluorescence lines have now been found in other TDEs with broader H/He lines (Leloudas et al. 2019), indicating the space for observed TDE features may be broader than expected. The optical features of TDEs are discussed further in Arcavi et al. (2020, ISSI review), and a comparison of observational properties of observed TDE candidates with the spectrum of possible “imposters” is discussed further in Zabludoff et al. (2020, ISSI review).

We separate out 13 TDE host galaxies which are part of the SDSS main spectroscopic sample (indicated in Table 1) in some of the following analysis, as these host galaxies can be matched to the general galaxy population in a uniform way.

2 Known Host Galaxy Properties of all events

We consider here the host galaxy properties and trends of the TDE samples discussed above. We compare the stellar mass and black hole masses to expectations given the volume-corrected mass functions and expectations from an upper cutoff in the black hole mass from event horizon suppression (§2.1). We also consider the stellar populations and inferred recent star formation histories of the TDE hosts, and discuss the observed enhancement in post-starburst and quiescent Balmer-strong galaxies (§2.2). We discuss the morphologies and concentrations of the stellar light and observed trends toward higher central concentration on kpc scales in the TDE hosts (§2.3). The presence of on-going gas accretion and AGN activity in the TDE host galaxies, as well as possible biases against identifying TDEs in such host galaxies are also discussed (§2.4). We summarize the extragalactic environments of the TDE host galaxies, given the efforts to identify TDEs in galaxy clusters (§2.5).

The redshift range of the host galaxies affects the extent to which they can be studied. Most of the TDEs discovered to date are at low redshift, such that many of the TDE host galaxies have data from the SDSS. The redshift of all of the TDEs considered in this review (see Table 1) ranges from 0.01 to 0.4. The median redshift is $z = 0.08$, and the 50 percentile range is 0.05–0.15. This redshift range is necessarily biased by the surveys which have discovered TDEs so far. Future surveys, such as LSST, may find a larger sample of higher redshift TDEs, depending on how the intrinsic TDE rate changes with redshift. A study

Name	R.A.	Dec	z	Type	BL ^a	CL ^b
ASASSN14li ^c	12:48:15.23	+17:46:26.44	0.02058	X-ray TDE	1	0
Swift J1644	16:44:49.30	+57:34:51.00	0.3534	X-ray TDE	0	0
XMM J0740	07:40:08.09	−85:39:31.30	0.0173	X-ray TDE	0	0
ASASSN15oi	20:39:09.18	−30:45:20.10	0.0484	X-ray TDE	1	0
SDSS J1201 ^c	12:01:36.03	+30:03:05.52	0.146	Likely X-ray TDE	0	0
2MASX J0249	02:49:17.32	−04:12:52.20	0.0186	Likely X-ray TDE	0	0
PTF10iya	14:38:40.98	+37:39:33.45	0.22405	Likely X-ray TDE	0	0
SDSS J1311	13:11:22.15	−01:23:45.61	0.195	Likely X-ray TDE	0	0
SDSS J1323 ^c	13:23:41.97	+48:27:01.26	0.0875	Likely X-ray TDE	0	0
3XMM J1521	15:21:30.73	+07:49:16.52	0.17901	Likely X-ray TDE	0	0
3XMM J1500	15:00:52.07	+01:54:53.82	0.145	Likely X-ray TDE	0	0
PS18kh	07:56:54.53	+34:15:43.63	0.074	Likely X-ray TDE	1	0
RX J1242-A	12:42:38.54	−11:19:20.85	0.05	Possible X-ray TDE	0	0
RX J1242-B	12:42:38.16	−11:19:13.62	0.05	Possible X-ray TDE	0	0
RX J1420-A	14:20:24.39	+53:34:11.14	0.148	Possible X-ray TDE	0	0
RX J1420-B	14:20:24.52	+53:34:15.72	0.147	Possible X-ray TDE	0	0
SDSS J0159	01:59:57.64	+00:33:10.49	0.31167	Possible X-ray TDE	0	0
RBS 1032 ^c	11:47:26.80	+49:42:59.00	0.02604	Possible X-ray TDE	0	0
RX J1624	16:24:56.66	+75:54:56.09	0.0636	Possible X-ray TDE	0	0
NGC 5905	15:15:23.32	+55:31:01.59	0.01131	Possible X-ray TDE	0	0
GALEX D3-13	14:19:29.81	+52:52:06.37	0.3698	Possible X-ray TDE	0	0
iPTF16fml	00:29:57.01	+32:53:37.24	0.0163	Optical/UV TDE	1	0
PS16dtm ^c	01:58:04.75	−00:52:21.87	0.0804	Optical/UV TDE	0	0
F01004	01:02:50.01	−22:21:57.22	0.1178	Optical/UV TDE	0	0
GALEX D23H-1	23:31:59.54	+00:17:14.58	0.1855	Optical/UV TDE	0	0
PS1-11af	09:57:26.82	+03:14:00.94	0.4046	Optical/UV TDE	0	0
SDSS J0952 ^c	09:52:09.56	+21:43:13.24	0.0789	Optical/UV TDE	0	1
SDSS J1342 ^c	13:42:44.42	+05:30:56.14	0.0366	Optical/UV TDE	0	1
SDSS J1350 ^c	13:50:01.51	+29:16:09.71	0.0777	Optical/UV TDE	0	1
SDSS TDE1	23:42:01.41	+01:06:29.30	0.1359	Optical/UV TDE	0	0
SDSS TDE2	23:23:48.62	−01:08:10.34	0.2515	Optical/UV TDE	1	0
SDSS J0748 ^c	07:48:20.67	+47:12:14.23	0.0615	Optical/UV TDE	1	1
ASASSN14ae ^c	11:08:40.12	+34:05:52.23	0.0436	Optical/UV TDE	1	0
PTF09axc	14:53:13.08	+22:14:32.27	0.1146	Optical/UV TDE	1	0
PTF09djl	16:33:55.97	+30:14:16.65	0.184	Optical/UV TDE	1	0
PTF09ge ^c	14:57:03.18	+49:36:40.97	0.064	Optical/UV TDE	1	0
PS1-10jh	16:09:28.28	+53:40:23.99	0.1696	Optical/UV TDE	1	0
iPTF15af ^c	08:48:28.12	+22:03:33.58	0.079	Optical/UV TDE	1	0
iPTF16axa	17:03:34.36	+30:35:36.8	0.108	Optical/UV TDE	0	0
GALEX D1-9	02:25:17.00	−04:32:59.00	0.326	Optical/UV TDE	0	0
AT2018dyk ^c	15:33:08.02	+44:32:08.20	0.037	Optical/UV TDE	1	0
AT2018bsi	08:15:26.62	+45:35:31.95	0.051	Optical/UV TDE	1	0
ASASSN18zj ^c	10:06:50.74	+01:41:34.37	0.046	Optical/UV TDE	1	0

Table 1 TDEs included in this review. ^a Broad H/He lines observed during TDE. ^b Coronal lines observed. ^c Host galaxies with SDSS spectroscopy. Right ascension and declination are for the host galaxies.

by Kochanek (2016) predicts that the TDE rate will drop steeply with redshift between $z = 0$ and $z = 1$, based on the expected evolution of the host galaxy stellar populations, black hole masses, and merger rates. However, the rising fraction of post-starburst hosts with redshift (Yan et al. 2009; Snyder et al. 2011; Wild et al. 2016) may act to counter this effect. The blue continuum of

TDE emission may result in a negative k -correction (Cenko et al. 2016), which would result in a greater number of observed TDEs at higher redshift.

2.1 Host Galaxy Stellar Mass and Black Hole Mass

The black hole mass is one of the fundamental parameters for TDE studies, as it sets both the energetics (e.g. peak luminosity, accretion efficiency) and the dynamics (e.g. orbital timescales, relativistic effects) of the disruption. While theoretical predictions (Wang and Merritt 2004) suggest that TDEs should preferentially occur in the lowest mass galaxies still hosting SMBHs (10^4 – $10^6 M_\odot$), the observed distribution (using a heterogeneous set of measurements) was observed to peak around $10^7 M_\odot$ (e.g. Stone and Metzger 2016; Kochanek 2016). More recently, Wevers et al. (2017) presented systematic measurements of black hole masses using the M - σ relation for a sample of 12 optical TDEs, and found the peak in the TDE black hole mass distribution to be significantly lower, near $10^6 M_\odot$, consistent with theoretical predictions (taking into account the uncertainty in the calibration of the M - σ relation at the low mass end). In contrast to previous studies (e.g., Stone and Metzger 2016) which use scaling relations from photometric observations to infer black hole masses, Wevers et al. (2017) use spectroscopic observations of the bulge velocity dispersions. Black hole mass measurements from TDE light curves (Mockler et al. 2019) are consistent with measurements from galactic properties given the uncertainties in each set of measurements, but the number of TDE light curves with well-measured rises and thus more accurate black hole mass measurements is still limited.

van Velzen (2018) uses the BH masses from Wevers et al. (2017) to infer the BH mass and luminosity functions of TDEs. Correcting for selection effects such as survey depth, cadence and area, they find that the TDE rate is constant with black hole (or galaxy stellar) mass over two orders of magnitude from $M_\odot = 10^{5.5} - 10^{7.5}$. Given the uncertainties, the observed black hole mass function of TDE hosts could be consistent with either the expected black hole mass function over this mass range, or with the slightly steeper trend expected given the scaling of the TDE rate with black hole mass. The dearth of BH masses $\geq 10^8 M_\odot$ is consistent with the presence of BH event horizons, and the disappearance of the tidal radius for a main sequence $1 M_\odot$ star inside the event horizon.

While black hole masses are difficult and time-consuming to measure, stellar masses can be more easily measured using galaxy luminosities and stellar population estimates. The stellar masses of the host galaxies are roughly correlated with the black hole masses, via the black hole mass – bulge mass relation (e.g., McConnell and Ma 2013) and the correlation between galaxy stellar mass and bulge stellar mass (e.g., Mendel et al. 2014). For the host galaxies in the SDSS main spectroscopic sample, we plot a histogram of their stellar masses compared to the rest of the SDSS galaxies and the volume-corrected stellar mass function (SMF) in Figure 1. The TDE host galaxies are less massive than

Name	$\log(M_*)$ (M_\odot)	M_g (mag)	σ (km s^{-1})	$\log(M_{\text{BH}})$ (M_\odot)
X-ray TDEs				
ASASSN14li†	10.6	-18.8	81(2)	$6.23^{+0.39}_{-0.40}$
Swift J1644	-	-	-	-
XMM J0740	-	-	-	-
ASASSN15oi†	9.9	-19.3	61(7)	$5.71^{+0.60}_{-0.57}$
Likely X-ray TDEs				
SDSS J1201	10.4	-20.6	122(4)	$7.18^{+0.41}_{-0.41}$
2MASX J0249	9.1	-17.5	43(4)	$4.93^{+0.55}_{-0.53}$
PTF10iya	9.3	-20.0	-	-
SDSS J1311	8.7	-18.6	-	-
SDSS J1323	9.8	-18.9	75(4)	$6.15^{+0.46}_{-0.45}$
3XMM J1521	9.9	-19.2	58(2)	$5.61^{+0.41}_{-0.41}$
3XMM J1500	9.3	-19.1	59(3)	$5.64^{+0.45}_{-0.45}$
PS18kh†	9.6	-19.0	-	-
Possible X-ray TDEs				
RX J1242-A	10.3	-21.0	-	-
RX J1242-B	-	-	-	-
RX J1420-A	10.3	-20.3	131(13)	$7.33^{+0.56}_{-0.54}$
RX J1420-B	-	-	-	-
SDSS J0159	10.7	-21.8	124(10)	$7.21^{+0.52}_{-0.50}$
RBS 1032	9.0	-17.7	49(7)	$5.25^{+0.67}_{-0.62}$
RX J1624	10.4	-20.8	155(9)	$7.68^{+0.45}_{-0.45}$
NGC 5905	10.0	-20.2	97(5)	$6.69^{+0.45}_{-0.44}$
GALEX D3-13	10.7	-20.8	133(6)	$7.36^{+0.43}_{-0.44}$
Optical/UV TDEs				
iPTF16fml†	9.8	-19.8	55(2)	$5.50^{+0.42}_{-0.42}$
PS16dtm	9.6	-19.3	45(13)	$5.07^{+0.88}_{-1.06}$
F01004	9.8	-21.0	132(29)	$7.34^{+0.76}_{-0.86}$
GALEX D23H-1	10.3	-20.1	84(4)	$6.39^{+0.44}_{-0.44}$
PS1-11af	10.1	-20.1	-	-
SDSS J0952*	10.0	-20.2	-	-
SDSS J1342*	9.5	-19.0	72(6)	$6.06^{+0.51}_{-0.52}$
SDSS J1350*	-	-	-	-
SDSS TDE1	10.1	-19.2	126(7)	$7.25^{+0.45}_{-0.46}$
SDSS TDE2†	10.6	-20.6	-	-
SDSS J0748†*	9.9	-20.0	126(7)	$7.25^{+0.45}_{-0.46}$
ASASSN14ae†	10.8	-19.2	53(2)	$5.42^{+0.46}_{-0.46}$
PTF09axc†	10.0	-20.2	60(4)	$5.68^{+0.48}_{-0.49}$
PTF09djl†	10.1	-20.0	64(7)	$5.82^{+0.56}_{-0.58}$
PTF09ge†	10.1	-19.5	82(2)	$6.31^{+0.39}_{-0.39}$
PS1-10jh†	9.5	-18.1	65(3)	$5.85^{+0.44}_{-0.44}$
iPTF15af†	10.2	-18.0	106(2)	$6.88^{+0.38}_{-0.38}$
iPTF16axa	10.1	-19.4	82(3)	$6.34^{+0.42}_{-0.42}$
AT2018dyk†	10.6	-21.4	112(4)	$7.00^{+0.41}_{-0.42}$
AT2018bsi†	10.3	-20.8	-	-
ASASSN18zj†	9.5	-19.1	60(5)	$5.68^{+0.51}_{-0.52}$

Table 2 Table of properties of known TDE host galaxies discussed in §2.1. M_* (stellar mass) and M_g (g -band absolute magnitude) are calculated as in Wevers et al. (2019a). σ is the measured velocity dispersion, which is used to derive the black hole mass using the M - σ relation of Ferrarese and Ford (2005). Measurement uncertainties are given between parentheses. The uncertainties in M_{BH} are the linear addition of the measurement uncertainties and the scatter in the M - σ relation. Because the scatter in the M - σ relation is a systematic uncertainty and the uncertainty in the velocity dispersion measurements are statistical, we add them linearly.

. † Broad line TDEs (see Table 1). * Coronal line TDEs (see Table 1).

Sample size	M_*	M_g	M_{BH}
Optical	20	20	16
X-ray + likely X-ray	10	10	7
Possible X-ray	6	6	6
p-values			
Optical - X-ray	0.03 (0.09)	0.02 (0.02)	0.38 (0.42)
X-ray - pos. X-ray	0.15 (0.05)	0.03 (0.02)	0.06 (0.10)

Table 3 Summary of statistical comparison between samples for different host properties, including host galaxy stellar mass (M_*), absolute g -band magnitude (M_g) and the black hole mass (M_{BH}). We give the relevant sample sizes for each parameter. We test the hypothesis that the respective samples are drawn from the same parent distribution. The p-values of an Anderson-Darling test are given, as well as the p-values for a Kolmogorov-Smirnov test (in parentheses); values below 0.05 suggest that we can reject the hypothesis at >95 % significance. We note that these conclusions differ from those by Wevers et al. (2019a) due to the larger sample of TDEs considered here, as well as a different class division.

the typical SDSS galaxies, but with a typical stellar mass near M^* . This distribution is consistent with the TDE host galaxies being drawn from a volume limited sample of galaxies with stellar mass greater than $10^9 M_\odot$.

Are the distributions of host galaxy stellar mass or black hole mass different for different classes of TDEs? There are several predictions in the literature, and this question depends on the details of how stars are disrupted and accreted, and the origin of the observed emission. The inverse dependence of the accretion disk temperature on black hole mass suggests X-ray TDEs should have lower black hole masses than optical TDEs (Dai et al. 2015), but if rapid circularization is required to produce X-rays, higher mass black holes may be expected to produce more X-ray emission (Guillochon and Ramirez-Ruiz 2015). Alternatively, if the difference between the classes is related to a viewing angle effect (Dai et al. 2018), no difference in the host galaxy properties would be expected.

Wevers et al. (2019a) have measured the host galaxy absolute magnitudes of a large sample of optical and X-ray TDEs using SDSS and PS1 photometry. They used the kcorrect software (Blanton and Roweis 2017) and the Petrosian or Kron magnitudes for SDSS and PS1 to estimate the host absolute magnitude as well as the galaxy stellar mass for a sample of 35 TDEs and TDE candidates. These values are presented in Table 2 for all sources in the current sample. Using different subdivisions (and a smaller sample) of host galaxies than the ones used here, Wevers et al. (2019a) found that the host galaxy absolute magnitudes, stellar masses, and black hole masses for different TDE classes are consistent with being drawn from the same parent population.

The larger sample considered here allows us to repeat the analysis in Wevers et al. (2019a) with more statistical power (Figure 2; Table 2). We group the X-ray and likely X-ray hosts, the UV/optically discovered hosts and the possible X-ray hosts and perform pairwise Kolmogorov-Smirnov (KS) and Anderson-Darling (AD) tests for these 3 samples. For the X-ray and optical samples, we find that for both host galaxy stellar mass and absolute magnitude the hypothesis that they are drawn from the same parent distribution

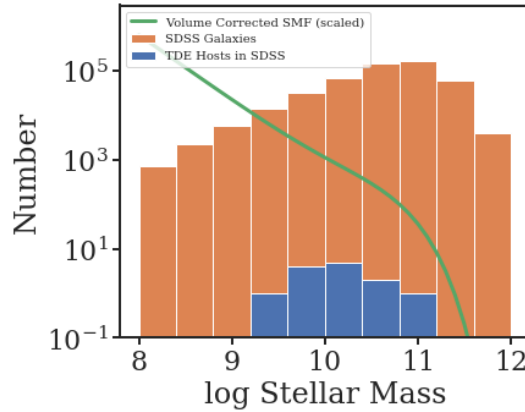


Fig. 1 Histogram of stellar masses for the SDSS main spectroscopic sample, with quality cuts as described in Law-Smith et al. (2017b) (orange), TDE host galaxies from the SDSS main spectroscopic sample (blue), and the volume corrected stellar mass function from Baldry et al. (2012). The TDE host galaxies are less massive than the typical SDSS galaxies, but with a typical stellar mass near M^* (the turnover in the stellar mass function, measured by Baldry et al. (2012) to be $10^{10.66} M_{\odot}$). This distribution is consistent with the TDE host galaxies being drawn from a volume limited sample of galaxies with stellar mass greater than $10^9 M_{\odot}$.

can be rejected. The KS and AD significance values are summarized in Table 3. The p-values for the X-ray and possible X-ray stellar mass comparison are higher, and we cannot reject the null hypothesis that they are drawn from the same parent distribution. For the latter, this could be due to the small size of the sample. The properties of the possible X-ray sources suggest significant contamination by AGN, which favour higher mass (both stellar mass and M_{BH}) and more luminous host galaxies. The difference with the results in Wevers et al. (2019a) can be explained by i) the larger sample considered here and ii) the different sample subdivision. In particular, the soft X-ray sample in Wevers et al. (2019a) consists of 6 likely and 6 possible X-ray TDE hosts, and the sources ASASSN-14li and ASASSN-15oi are considered as optical events.

Wevers et al. (2019a) also presented velocity dispersion measurements of an additional 19 TDE candidates, yielding a sample of 29 homogeneously measured black hole masses². Figure 2 shows a kernel density estimate (KDE) of the black hole mass distribution, divided by type. The KDE was calculated by representing each black hole mass estimate with a Gaussian function with a full width at half maximum (FWHM) equal to the measurement uncertainty (including both the velocity dispersion uncertainty and the scatter in the M - σ relation), and then summing over the respective samples.

² We note that the sample presented by Wevers et al. (2019a) contains a smaller but not completely overlapping sample to that presented in this review, due to differences in the TDE selection and differences in available data.

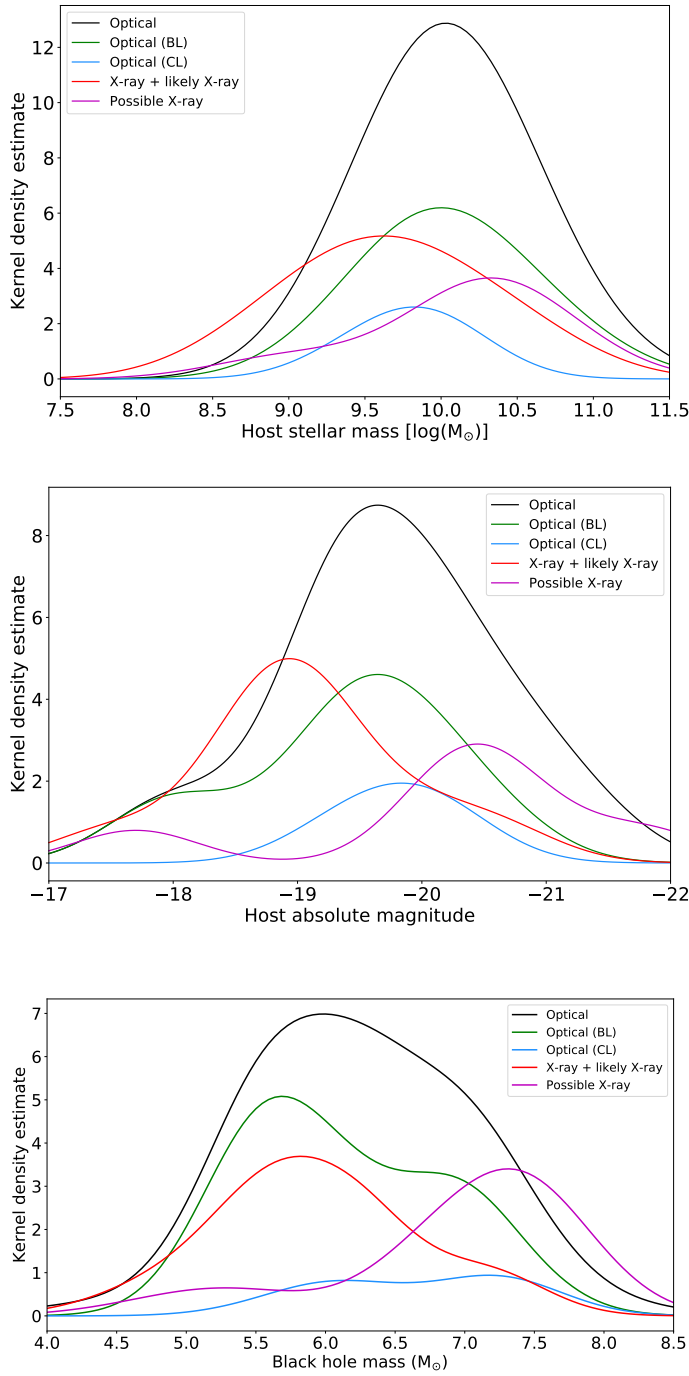


Fig. 2 Top: Kernel density estimate of TDE host galaxy stellar masses, sub-divided by TDE class. KDEs are calculated as in Wevers et al. (2019a), using Gaussians with width = 0.5 dex (the typical uncertainty on the host galaxy stellar mass measurements). Bulge to total light (B/T) corrections are applied (not individual measurements but a general prescription). The X-ray and optical/UV TDEs are consistent with being drawn from different parent samples, according to their Anderson-Darling statistic. **Middle:** Kernel density estimate of TDE host galaxy absolute magnitude, sub-divided by TDE class. KDEs are calculated as in Wevers et al. (2019a), using Gaussians with width = 0.5 dex (the typical uncertainty). The X-ray TDEs and optical TDEs are again consistent with being drawn from different parent samples. The possible X-ray TDE candidates are also distinct from the X-ray + likely X-ray samples as inferred from their Kolmogorov-Smirnov and Anderson-Darling tests. **Bottom:** Kernel density estimate of the black hole masses of X-ray and UV/optical selected TDEs, sub-divided by TDE class. The kernel size includes the velocity dispersion measurement as well as the intrinsic $M-\sigma$ scatter. No statistically significant differences are observed between the TDE classes. Interestingly, while the X-ray TDEs prefer host galaxies with lower stellar mass and absolute magnitude than the optical/UV TDEs, this trend is not seen in black hole mass. More observations of black hole masses for various classes of TDEs, especially X-ray TDEs, are required to test whether this effect is physical.

Using statistical tests to compare the distributions between X-ray and optical samples, we find no significant differences between the black hole mass distributions. This supports the idea that the apparent dichotomy between optical and X-ray selected TDEs could be related to (for example) viewing angle or geometry (Watarai et al. 2005; Coughlin and Begelman 2014; Dai et al. 2015; Metzger and Stone 2016; Roth et al. 2016; Dai et al. 2018), and that these events intrinsically belong to the same class. This is also supported by observations of UV/optical TDEs with deep X-ray upper limits: the detection of Bowen fluorescence lines in optical spectra implies that an ionizing (X-ray) radiation field exists, although no X-rays are actually observed (Leloudas et al. 2019). UV emission is not sufficient to excite the Bowen fluorescence lines for the one TDE (AT2018dyb) for which measurements are available. Emission line measurements presented by Leloudas et al. (2019) show that the Wien tail of the UV blackbody responsible for the UV/optical radiation is insufficient (by ~ 6 orders of magnitude) to explain the observed line fluxes. This suggests that the X-ray source is completely obscured along the line of sight.

While the black hole mass distribution is very similar, the host galaxy stellar mass and absolute magnitude are significantly lower for the X-ray sample, as we can reject the null hypothesis of a common parent sample at high significance. However, we caution that this effect could be due to the lesser number of TDE host galaxies with black hole mass measurements (Table 3). A larger sample of robust X-ray TDEs is required to draw robust statistical conclusions, and test whether optical/UV TDEs might have smaller black hole masses for their stellar masses (or whether X-ray TDEs have larger black hole masses for the stellar masses).

If the observed trends in stellar mass and absolute magnitude are driven by differences in the black hole mass distribution between the X-ray and optical samples, this suggests that smaller black holes have higher temperature accretion disks with higher X-ray luminosities, or a combination of this effect and a viewing angle effect are acting. Another possibility is that selection biases from the very different identification methods of TDEs in the optical vs. X-ray could lead to this effect. The light curve duration for TDEs may vary with black hole mass in different ways for X-ray compared to optical emission. Wen et al. (in prep) find lower mass black holes to have longer duration super-*eddington* plateaus in their predicted X-ray light curves. Lin et al. (2018) have found one such example of a long duration X-ray light curve from an event around a small SMBH. If it were the case that smaller black holes have longer-duration light curves in the X-ray compared to the optical, coarser cadence surveys in the X-ray would be biased against detecting TDEs in more massive black holes. Differences between TDEs found in optical vs. X-ray surveys will need to be studied further in the era of *eROSITA* and *LSST*.

Wevers et al. (2019a) also consider a class of hard X-ray selected TDE candidates (which are not included in the sample discussed here), finding these host galaxies to have significantly different black hole mass distributions, as well as absolute magnitude and stellar mass distributions. However, these conclusions are based on a sample of 5 hard X-ray TDE candidate host galaxies,

and a larger sample is needed to confirm these findings and understand the cause of these potential differences.

2.2 Star Formation Rates, Star Formation Histories, and Stellar Populations

Next, we consider the current star formation rates, the past star formation history, and the stellar populations of the TDE host galaxies. While the stellar populations in the nucleus may be far removed from those of the bulk of the host galaxy, the galaxy-wide stellar populations trace the formation and evolution of the host galaxy and are closely tied to the morphologies, kinematics, interstellar medium properties, and merger histories of the host galaxies.

Star formation rates (SFRs) for host galaxies are calculated using various tracers of short-lived massive O and B stars. While many SFR tracers from the UV to the radio work well for galaxies with significant star formation, these tracers can be heavily biased in galaxies with rapidly changing SFRs (as many of the TDE host galaxies are thought to have), in dusty galaxies, or in galaxies influenced by AGN activity.

We consider here SFRs of TDE host galaxies derived using $H\alpha$ luminosities from the SDSS, and correct for extinction and aperture using the corrections from the MPA-JHU SDSS catalogues (Brinchmann et al. 2004; Tremonti et al. 2004). The SFRs from this catalogue use the D4000 break to estimate the SFRs for galaxies with non-star-forming emission line ratios, like those of many of the TDE hosts (see §2.4). While the D4000-sSFR correlation will lead to accurate SFRs on average for large samples, individual galaxies will have high uncertainties. Our use of $H\alpha$ here thus is more accurate for galaxies without strong AGN, but will be in general biased towards higher values for galaxies with additional $H\alpha$ emission from non-star-forming sources. We convert the $H\alpha$ luminosities to SFRs using $\eta = 5.4 \times 10^{-42} \text{ M}_{\odot} \text{ yr}^{-1} / (\text{ergs s}^{-1})$ (Kennicutt and Evans 2012). We compare the TDE hosts to galaxies from the SDSS main spectroscopic survey in SFR–stellar mass space in Figure 3. While several of the TDE hosts are at the lower SFR edge of the “main sequence” of star forming galaxies, most are quiescent, with low SFRs.

We also consider the optical colours of the TDE hosts in the context of the colour magnitude relation. The $u - r$ colours and M_r absolute magnitudes are plotted in Figure 4. The TDE hosts occupy a range of red, blue, and green-valley host galaxies. Because the colours are affected by both the current SFR and recent star formation history (SFH), we explore the physical interpretation of these quantities below.

The quiescent SFRs paired with green colours of many of the TDE hosts is suggestive of an intermediate stellar population and a recent decline in the SFH of the host. Indeed, a large number of TDEs have been observed in E+A or post-starburst galaxies. The large number of post-starburst host galaxies was first observed by Arcavi et al. (2014) in a sample of UV/optical bright TDEs with broad H/He lines. The presence of even one post-starburst galaxy amongst the hosts would be unusual given the rarity of post-starburst galaxies.

Name	H α [Å]	σ (H α) [Å]	Lick H δ_A [Å]	σ (Lick H δ_A) [Å]	SFR M $_{\odot}$ yr $^{-1}$	Type
X-ray TDEs						
ASASSN14li†	-0.6	0.5	5.7	0.6	0.01	PSB
Swift J1644	-2.5	0.8	4.7	1.1	–	QBS
XMM J0740	-0.3	0.6	0.4	0.4	–	Quiescent
ASASSN15oi†	0.1	0.3	1.9	0.7	–	QBS
Likely X-ray TDEs						
SDSS J1201	0.7	0.3	-1.1	2.4	–	Quiescent
2MASX J0249	-5.7	0.6	0.4	0.5	–	SF
PTF10iya	-20.5	0.6	2.9	0.9	–	SF
SDSS J1311	-2.1	1.5	3.6	1.1	–	QBS
SDSS J1323	-0.2	0.5	-1.2	1.5	0.01	Quiescent
3XMM J1521	0.8	1.1	-1.5	2.4	–	Quiescent
3XMM J1500	-45.1	0.8	1.4	1.7	–	SF
Possible X-ray TDEs						
RX J1242-A	1.1	0.8	0.9	1.2	–	Quiescent
RX J1242-B	-0.9	0.9	-0.4	2.7	–	Quiescent
RX J1420-A	-0.2	0.9	-2.8	2.0	0.03	Quiescent
RX J1420-B	-71.6	1.7	5.8	3.4	0.54	SF
SDSS J0159	-19.9	0.8	1.7	1.0	5.25	SF
RBS 1032	-0.5	0.4	4.1	0.4	0.0	QBS
RX J1624	0.6	1.3	-1.1	2.1	–	Quiescent
NGC 5905	-28.4	0.1	–	–	–	SF
Optical/UV TDEs						
iPTF16fnl†	0.8	0.6	5.8	0.3	–	PSB
PS16dtm	-31.8	0.4	-0.2	1.1	0.26	SF
F01004	-47.0	0.2	-0.2	0.8	–	SF
GALEX D23H-1	-13.3	0.9	4.3	1.5	–	SF
PS1-11af	0.7	1.2	1.5	1.4	–	QBS
SDSS J0952*	-27.8	0.4	-2.0	1.1	1.6	SF
SDSS J1342*	-15.1	0.5	-1.0	1.3	0.07	SF
SDSS J1350*	-20.3	0.4	0.9	1.3	0.55	SF
SDSS TDE1	1.2	1.0	-1.3	1.3	–	Quiescent
SDSS TDE2†	-4.5	0.5	3.7	0.6	–	SF
SDSS J0748†*	-11.4	1.0	1.2	0.8	0.87	SF
ASASSN14ae†	-0.7	0.4	3.4	0.8	0.01	QBS
PTF09axc†	-1.1	0.7	4.9	0.4	–	PSB
PTF09djl†	-0.3	0.7	4.7	0.5	–	PSB
PTF09ge†	-1.7	0.8	0.3	0.7	0.05	Quiescent
PS1-10jh†	-0.5	0.7	1.7	0.8	–	QBS
iPTF15aff†	-1.7	0.3	1.3	1.9	0.02	QBS
iPTF16axa	-1.1	1.7	0.2	1.5	–	Quiescent
PS18kh	-0.11	0.47	0.16	0.56	–	Quiescent
AT2018dyk†	-2.17	0.11	-0.27	0.48	2.54	Quiescent
AT2018bsi†	-5.25	0.69	-0.73	0.47	–	SF
ASASSN18zj†	-0.35	0.14	5.43	0.41	0.01	PSB

Table 4 Table of properties of known TDE host galaxies discussed in §2.2. Negative values indicate emission and positive values indicate absorption for the H α and H δ measurements. SFRs are only calculated when SDSS MPA-JHU catalogue data are available. To be classified as quiescent, quiescent Balmer-strong (QBS), or post-starburst (PSB), galaxies are required to have H α EW > -3 Å. Galaxies with stronger H α emission are labeled as star-forming (SF). Galaxies with strong Balmer absorption (Lick H δ_A > 1.31 Å) are classified as QBS, and a subset of these are classified as PSB if they meet the threshold of H δ_A - σ (H δ_A) > 4 Å. 5/41 (12%) host galaxies are post-starburst galaxies and 13/41 (32%) are either QBS or PSB. Of the 4 X-ray TDEs, 3 (75%) are QBS and 1 (25%) is PSB. Of the 15 broad H/He line TDEs, 9 (60%) are QBS and 5 (33%) are PSB. We consider the effects of these choices of dividing criteria in §2.2. † Broad line TDEs (see Table 1). * Coronal line TDEs (see Table 1).

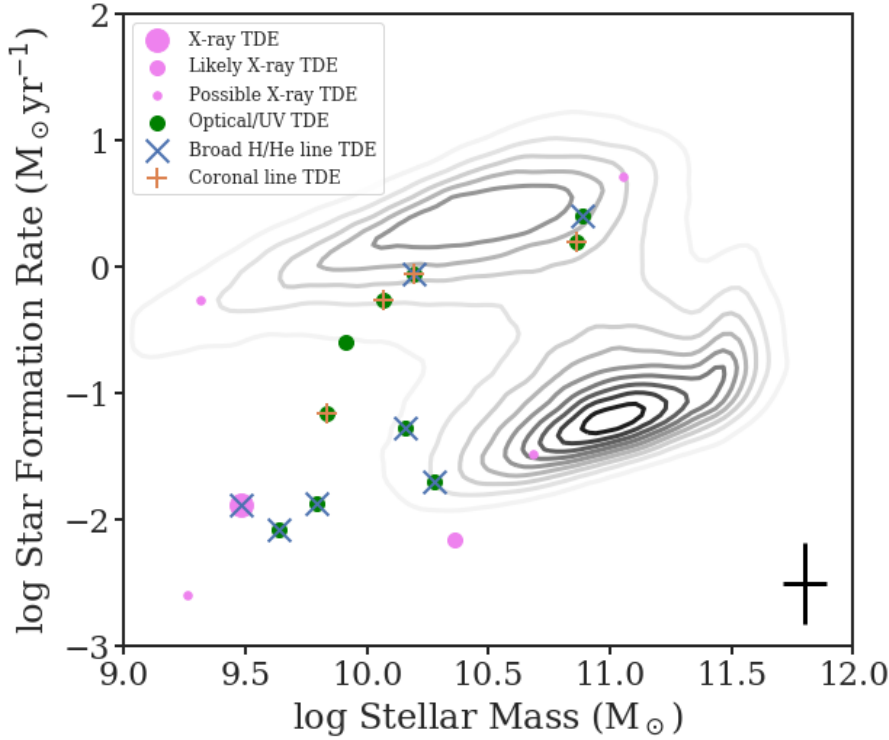


Fig. 3 Star formation rates vs. stellar masses for the SDSS main spectroscopic sample (grey contours) and the different classes of TDE hosts considered here. Stellar masses are from the MPA-JHU catalogue for all samples, as well as SFRs for the SDSS sample. We determine the TDE host SFRs based on $H\alpha$ fluxes as described in §2.2. A characteristic error-bar is shown in the bottom right. While several of the TDE hosts are at the lower SFR edge of the “main sequence” of star forming galaxies, most are quiescent, with low SFRs. We note that the SDSS sample has not been volume corrected; for a more detailed analysis of the stellar mass distributions of the TDE hosts compared to a volume-limited sample, see §2.1. Thus, for the typical black hole masses of TDEs, the host galaxies lie in a relatively sparse region on this diagram due to the magnitude-limited nature of the SDSS comparison sample used here.

The over-representation of post-starburst galaxies in TDE hosts was then quantified by French et al. (2016), who used tracers sensitive to recent star formation on different scales to assess the recent star formation history of the host galaxies. One such comparison is to use the $H\alpha$ emission as a tracer for the current star formation on ~ 10 Myr timescales and the Balmer absorption as a tracer for star formation on timescales of ~ 1 Gyr. This method of using $H\alpha$ emission vs. Lick $H\delta_A$ has been used by many (French et al. 2016; Law-Smith et al. 2017b; Graur et al. 2018) to study the recent star formation histories of TDE host galaxies.

There are many ways to quantify the current SFR in galaxies, as described above. Many methods that are sensitive to post-starburst galaxies use $H\alpha$

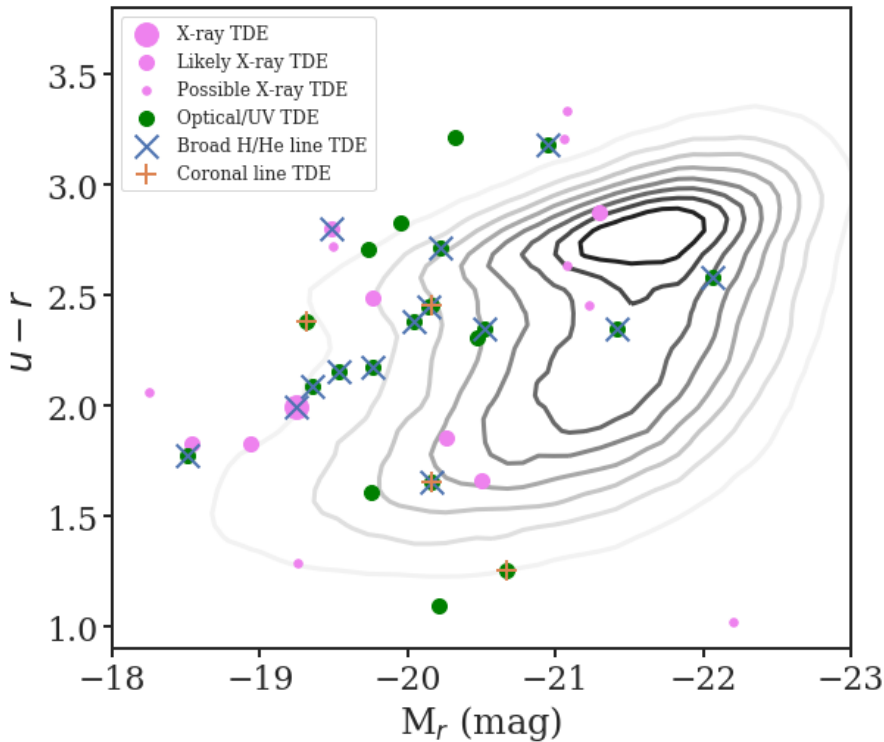


Fig. 4 Optical colour magnitude relation of TDE host galaxies and the SDSS main spectroscopic sample. All TDE hosts with SDSS photometry are plotted here. We note that the SDSS sample has not been volume corrected; for a more detailed analysis of the absolute magnitude distributions of the TDE hosts compared to a volume-limited sample, see §2.1. The TDE hosts occupy a range of red, blue, and green-valley host galaxies. Because the colours are affected by both the current SFR and recent star formation history (SFH), we explore the physical interpretation of these quantities below.

emission or O[II] emission if the red end of the rest-frame spectra are not available. Other methods allow for residual star formation using a PCA analysis (Wild et al. 2010) or a BPT diagram analysis (Alatalo et al. 2016). French et al. (2016) require $H\alpha$ EW $< 3 \text{ \AA}$ in emission in the rest frame to be considered quiescent. This corresponds to a specific SFR $\lesssim 1 \times 10^{-11} \text{ yr}^{-1}$, well below the main sequence of star-forming galaxies (e.g., Elbaz et al. 2011). The $H\alpha$ emission is also corrected for stellar Balmer absorption, which is significant for post-starburst quiescent Balmer-strong galaxies.

The moderate lifetime of A stars means that the presence of a large A star population is indicative of a burst of star formation within the last Gyr. A star spectra show strong Balmer absorption, which can be best traced using the $H\gamma$, $H\delta$, or $H\epsilon$ lines. French et al. (2016) use the Lick $H\delta_A$ index and its uncertainty $\sigma(H\delta_A)$, which is optimized for the stellar absorption from A stars (Worthey and Ottaviani 1997), has lower emission filling than $H\beta$,

and smooth nearby continuum regions. The more bursty the SFH, i.e. the greater fraction of stellar mass produced over a shorter time, the higher $H\delta$ absorption will be. A stricter cut of $H\delta_A - \sigma(H\delta_A) > 4 \text{ \AA}$ will select galaxies with recent starbursts creating $> 3\%$ of their current stellar mass over 25–200 Myr (referred to as post-starburst galaxies throughout), and a weaker cut of $H\delta_A > 1.31 \text{ \AA}$ (referred to as quiescent Balmer-strong galaxies throughout) will select galaxies with recent epochs of star formation which created $> 0.1\%$ of their current stellar mass over 25–1000 Myr (French et al. 2017, 2018).

We plot these SFH tracers in Figure 5 for various subsamples of TDEs. The TDE host galaxies span a range of SFHs from star-forming galaxies, to quiescent galaxies which have been quiescent for at least the past Gyr, and galaxies which had significant star-formation within the last Gyr but are currently quiescent. This last category consists of “post-starburst” or “quiescent Balmer-strong” galaxies as defined above.

Several TDE host galaxies in the classes of the coronal line TDEs and optical/UV TDEs without coronal or broad lines have low $H\delta$ absorption for their $H\alpha$ emission compared to the rest of the galaxies in the SDSS spectroscopic sample. This may not be due to a physical difference between the host galaxies, and might instead be due to filling of the $H\delta$ line by residual TDE emission, as discussed by Graur et al. (2018). Another possibility is contamination from the nearby Bowen fluorescence line NIII $\lambda 4100$ (Blagorodnova et al. 2018; Leloudas et al. 2019; Trakhtenbrot et al. 2019).

The over-representation of a galaxy type among the TDE host galaxies can be determined using its rate in the TDE host galaxies compared to its rate in a general galaxy sample. We describe here the analyses done by various groups, and summarize in Table 5. French et al. (2016) find that 38% of a sample of eight UV/optical H/He broad line TDE hosts meet a post-starburst selection criterion with a rate of only 0.2% in the general galaxy population. Similarly, 75% of the same TDE host galaxies meet a quiescent Balmer-strong selection criterion with a rate of 2.3% in the general galaxy population. These rates imply overdensities of $33^{+7}_{-11} \times$ in quiescent Balmer-strong galaxies and $190^{+115}_{-100} \times$ in post-starburst galaxies.

Graur et al. (2018) considered the over-enhancement rates for several additional categories of observed TDEs using a similar but slightly different parent galaxy sample and post-starburst/ quiescent Balmer-strong definitions. For an updated sample of UV/optical bright H/He broad line TDEs, the over-enhancement rates are $34^{+22}_{-14} \times$ in quiescent Balmer-strong galaxies and $110^{+80}_{-50} \times$ in post-starburst galaxies, consistent with the rate enhancements found by French et al. (2016).

The over-enhancement rates in post-starburst galaxies for the X-ray bright TDEs are weaker than for the UV/optical broad line TDEs, though this comparison is limited by small number statistics. For the set of X-ray TDEs, “likely” X-ray TDEs, and “possible” X-ray TDEs identified in Auchettl et al. (2017a), Graur et al. (2018) find the over-enhancement rates to be $18^{+13}_{-9} \times$ in quiescent Balmer-strong galaxies and $18^{+22}_{-18} \times$ in post-starburst galaxies.

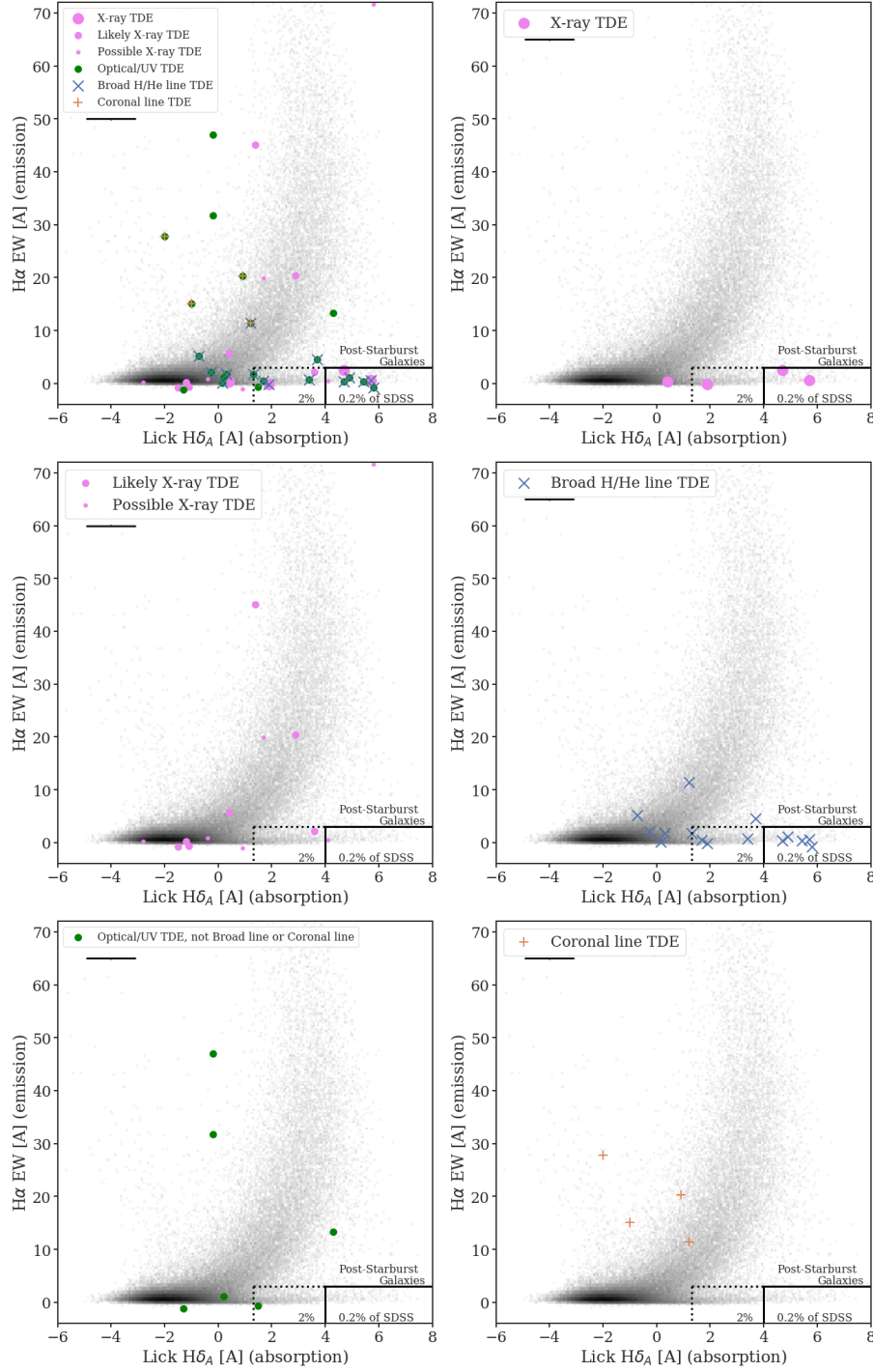


Fig. 5 Spectral indices tracing the recent star formation histories of TDE hosts and SDSS galaxies (updated from French et al. 2016; Graur et al. 2018). We plot $H\alpha$ EW (sensitive to current star formation) vs. Lick $H\delta_A$ absorption (sensitive to star formation over the past Gyr) for each galaxy. Galaxies with low current star formation, yet significant star formation over the past Gyr form the post-starburst/quiescent Balmer-strong “spur” in the lower right. TDEs, especially the X-ray and broad H/He line classes, are over-represented among the post-starburst and quiescent Balmer-strong galaxies.

Overenhancement	Galaxy Sample ^a	TDE Sample ^b	Source
$33^{+7}_{-11} \times$	QBS	H/He broad line	[1]
$190^{+115}_{-100} \times$	PSB	H/He broad line	[1]
$34^{+24}_{-14} \times$	QBS	H/He broad line	[2]
$110^{+80}_{-50} \times$	PSB	H/He broad line	[2]
$18^{+13}_{-9} \times$	QBS	X-ray, likely, possible	[2]
$18^{+22}_{-18} \times$	PSB	X-ray, likely, possible	[2]
$23^{+21}_{-13} \times$	QBS	X-ray, likely	[2]
$29^{+41}_{-29} \times$	PSB	X-ray, likely	[2]
$17^{+12}_{-8} \times$	QBS	Optical	[2]
$50^{+38}_{-29} \times$	PSB	Optical	[2]
$18^{+8}_{-7} \times$	QBS	X-ray, likely, possible, optical	[2]
$35^{+21}_{-17} \times$	PSB	X-ray, likely, possible, optical	[2]
$20-80 \times$	QBS/PSB	X-ray, likely, possible, optical	[3]
$40-120 \times$	QBS/PSB	X-ray, H/He broad line	[3]

Table 5 Summary of TDE rate overenhancement found in various samples of galaxies and TDE classifications. ^a We note that the definitions of Quiescent Balmer-Strong (QBS) and Post-Starburst (PSB) vary slightly between French et al. (2016) and Graur et al. (2018), and in this review we present the overenhancement as a function of the Balmer strength (see Fig 7). ^b Similarly, the TDEs used in each classification vary. For the TDEs included in the two calculations for this review, see Table 1. [1] French et al. (2016) [2] Graur et al. (2018) [3] This review.

These rates are higher once the “possible” X-ray TDEs are excluded, many of which have ambiguous light curves and may be AGN flares. Considering only the X-ray and “likely” X-ray TDEs, the over-enhancement rates are $23^{+21}_{-13} \times$ in quiescent Balmer-strong galaxies and $29^{+41}_{-29} \times$ in post-starburst galaxies. These rate enhancements for the post-starburst sample are driven by the one X-ray (including the “likely” and “possible” samples) TDE that meets the strictest post-starburst criterion, ASASSN-14li.

We present classifications for the TDE hosts discussed in this review in Table 4, using the criteria described above. 5/41 (12%) host galaxies are post-starburst galaxies and 13/41 (32%) are either quiescent Balmer-strong or post-starburst. Of the 4 X-ray TDEs, 3 (75%) are quiescent Balmer-strong and 1 (25%) is post-starburst. Of the 15 broad H/He line TDEs, 9 (60%) are quiescent Balmer-strong and 5 (33%) are post-starburst.

To account for the dependence of the TDE rate enhancement on the definition of “post-starburst” or “quiescent Balmer-strong” we plot in Figure 6 the cumulative distribution of quiescent SDSS galaxies and quiescent TDE hosts with stronger Balmer absorption than the value on the x-axis. For both the full set of TDE hosts considered here as well as the subsets of the broad H/He line TDEs and the X-ray TDEs with the strongest post-starburst enhancement, there is a significant difference in the distributions between the quiescent SDSS galaxies and TDE hosts. We also demonstrate the effect of the criteria for post-starburst or quiescent Balmer-strong on the TDE enhancement rate over normal quiescent galaxies in Figure 7. For the full set of TDE hosts, the enhancement rate ranges between 20-80 \times that of normal quiescent galaxies.

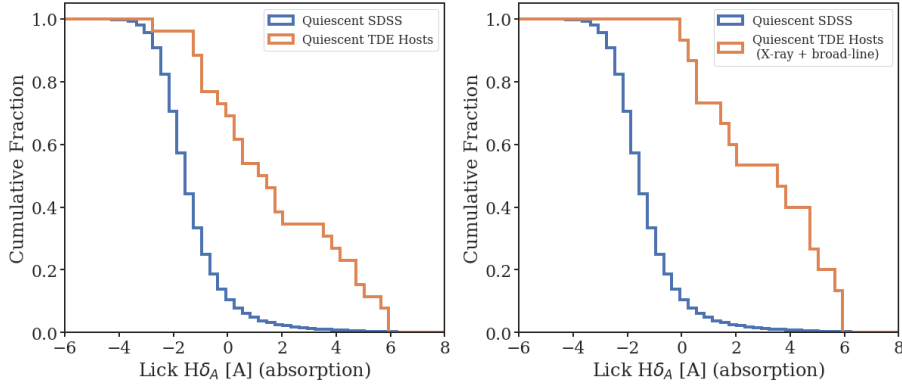


Fig. 6 Cumulative distribution of quiescent SDSS galaxies and quiescent TDE hosts with stronger Balmer absorption than the limit of the x-axis. For both the full set of TDE hosts considered here (left) as well as the subsets of the broad H/He line TDEs and the X-ray TDEs with the strongest post-starburst enhancement (right), there is a significant difference in the distributions between the quiescent SDSS galaxies and TDE hosts.

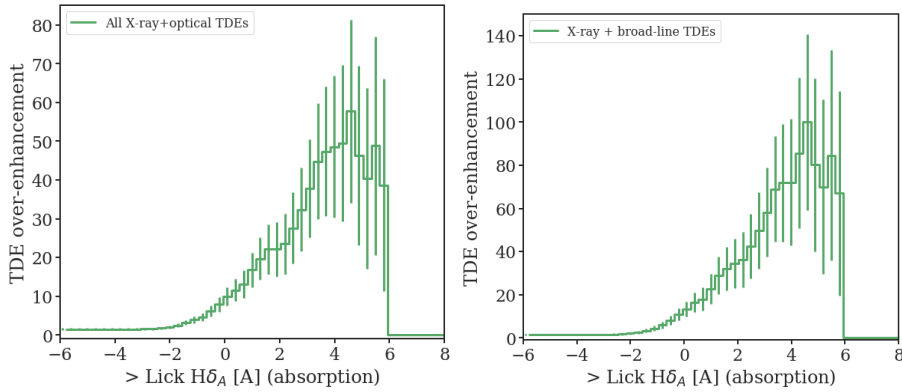


Fig. 7 Effect of the criteria for post-starburst or quiescent Balmer-strong on the TDE enhancement rate over normal quiescent and star-forming galaxies. For the full set of TDE hosts (left), the enhancement rate ranges for 20-80 \times that of normal quiescent and star-forming galaxies. For the broad H/He line TDEs and the X-ray TDEs (right), the enhancement rate ranges for 40-120 \times that of normal quiescent and star-forming galaxies. We note again that these TDE classifications are tentative and subject to a number of observational biases. More observations of the host galaxies for a large sample of well-characterized TDEs are needed to overcome these uncertainties and the small-number statistics limiting our precision here.

For the broad H/He line TDEs and the X-ray TDEs, the enhancement rate ranges from 40-120 \times that of normal quiescent and star-forming galaxies. We note again that these TDE classifications are tentative and subject to a number of observational biases. More observations of the host galaxies for a large sample of well-characterized TDEs are needed to overcome these uncertainties and the small-number statistics limiting our precision here.

Law-Smith et al. (2017b) consider the post-starburst and quiescent Balmer-strong galaxy over-enhancement rates in a somewhat different subset of the Auchettl et al. (2017a) X-ray and optical TDEs, but control the galaxy parent sample on different properties to test whether selection effects drive the observed rate enhancements. Controlling on bulge mass (and thus likely black hole mass), redshift, surface brightness, Sérsic index, or bulge to total light ratio can affect the relative post-starburst or quiescent Balmer-strong galaxy rate by $\leq 2\times$, within the error on the rates due to small number statistics.

Controlling on bulge colour has the largest possible effect on the observed post-starburst or quiescent Balmer-strong rates, decreasing the observed rate enhancements by factors of ~ 4 for the post-starburst galaxies and ~ 2.5 for the quiescent Balmer-strong galaxies, depending on what other factors are controlled for. This may be due to selection effects against finding TDEs in dustier and thus redder galaxies, or by the unique stellar populations in post-starburst galaxies, which cause them to lie in the optical green valley (Wong et al. 2012). If we control on properties which are strongly correlated with post-starburst and quiescent Balmer-strong galaxies, such as green optical colors or high central concentrations, we expect that the residual enhancement of the TDE rate in such hosts would be diminished by construction. The TDE enhancement rates in such hosts are thus consistent (given the small number statistics) between the studies of French et al. (2016), Law-Smith et al. (2017b) and Graur et al. (2018).

While the Balmer absorption is a proxy for the recent SFH, detailed stellar population fitting can be used to determine the nature of the recent SFH using the information from the full galaxy SED. French et al. (2017) fit stellar population models to the UV/optical host galaxy photometry and optical Lick indices to determine the time elapsed since the recent starburst, the fraction of mass produced in the starburst, and the duration of the recent starburst (French and Zabludoff 2018), for a sample of host galaxies of broad H/He line TDEs. While the lower Balmer absorption “quiescent Balmer-strong” galaxies could have had weaker H δ absorption due to longer-duration bursts, older bursts, or weaker bursts, stellar population modelling by French et al. (2017) determined that this effect is driven by the fact that quiescent Balmer-strong TDE hosts had weaker starbursts than most post-starburst galaxies. While most post-starburst galaxies have formed $\sim 3 - 50\%$ of their stellar mass in their recent starbursts, the quiescent Balmer-strong (and non-post-starburst) hosts had burst mass fractions of $0.5 - 2\%$. The post-starburst and quiescent Balmer-strong TDE hosts have ages ranging from 60 Myr to 1 Gyr since the recent starbursts ended. This large range in age suggests the enhanced TDE rate is not limited to a specific time in their host’s post-starburst evolution. When compared to the total sample of post-starburst and quiescent Balmer-strong galaxies, French et al. (2017) observed a statistically insignificant dearth of TDEs in older (> 600 Myr) post-starburst galaxies. The evolution of the TDE rate enhancement after a starburst implied by this early small sample is consistent with several models for explaining the enhanced TDE rate during this phase (Stone et al. 2018, discussed further in §4).

TDEs may also be over-represented in starbursting host galaxies. However, the extreme dust extinction present in the nucleus of starburst galaxies as well as the co-existence of AGN activity make detecting such TDEs difficult. Either a lucky dust-free sightline or transient detections in the NIR are required to find TDEs in starburst galaxies. Both such scenarios have been observed. Tadhunter et al. (2017) observed a light-curve over 10 years and a serendipitous appearance of broad He lines similar to those observed in other TDEs in a starburst galaxy³. Mattila et al. (2018) observed a jet launched from the nucleus of the starburst galaxy Arp 299 believed to be caused by a TDE, with a transient discovered in NIR AO imaging. Arp 299 has a stellar population consistent with evolving to a typical post-starburst galaxy, with an starburst age of 70-260 Myr since the starburst began and 9-29% of the total stellar mass formed in the on-going starburst (Pereira-Santaella et al. 2015).

Tadhunter et al. (2017) estimate the TDE rate to be enhanced in such galaxies by 1000-10,000 \times , to one per century or even one per decade per galaxy. From the observations thus far, it is unclear whether the TDE rate is enhanced during both the starburst and post-starburst phases, with selection effects biasing against observing TDEs in starburst galaxies, or if the TDE rate enhancement peak lags in time after the starburst. Upcoming infrared and radio surveys for TDEs, as well as concerted efforts to disambiguate TDEs from AGN will be necessary to resolve this question.

2.3 Concentration and Morphology of Stellar Light; Stellar Kinematics

The TDE rate is expected to depend on various physical properties of the SMBH and the stellar population in its vicinity, including the mass of the SMBH, the density of stars within its loss cone, and their velocity dispersion. Unfortunately, it is exceedingly hard to observationally probe the parsec-scale region of influence, except for the most nearby SMBHs. However, some global host-galaxy properties, on kpc scales, are known to be correlated with local properties in galactic nuclei. The most fundamental of these is the M - σ relation, which relates the mass of the SMBH, M , to the host galaxy stellar velocity dispersion, σ (e.g., Kormendy and Richstone 1995; Magorrian et al. 1998; Gebhardt et al. 2000; Tremaine et al. 2002; McConnell and Ma 2013). Moreover, these central stellar velocity dispersions have been shown to be correlated over galactic scales (Cappellari et al. 2006).

Graur et al. (2018) compared a sample of 11 TDE host galaxies with surface stellar mass densities and velocity dispersions computed from galaxy properties measured by the Sloan Digital Sky Survey (SDSS; York et al. 2000; Kauffmann et al. 2003; Brinchmann et al. 2004) to a volume-limited sample of SDSS galaxies with galaxy properties measured by the same pipeline. Their TDE host galaxies had surface stellar mass densities in the range $\Sigma_{M_*} =$

³ This event is included in our catalogue (F01004), although its classification as a TDE is controversial. Trakhtenbrot et al. (2019) argue it may not be a true TDE, although the space for observed TDE features may be broader than expected (Leloudas et al. 2019).

Name	Sérsic n^a	M_{BH}^b	A^c	$\log(\Sigma_{M_*})^d$	σ_v^e (km/s)
X-ray TDEs					
ASASSN-14li†	4.91	6.17	0.015	$10.1^{+0.2}_{-0.2}$	63 ± 3
Likely X-ray TDEs					
SDSSJ1201	5.61	—	0.008	$9.5^{+0.2}_{-0.3}$	122 ± 4
SDSSJ1323	5.03	6.52	0.002	$9.5^{+0.2}_{-0.2}$	75 ± 10
3XMM J1521	—	—	—	$9.5^{+0.2}_{-0.3}$	62 ± 14
Possible X-ray TDEs					
RX J1420-A	—	—	—	$9.7^{+0.2}_{-0.2}$	131 ± 13
RX J1420-B	—	—	—	$7.4^{+0.3}_{-0.3}$	168 ± 52
SDSSJ0159	—	—	—	< 9.9	128 ± 17
RBS1032	2.24	5.62	0.018	$9.5^{+0.2}_{-0.2}$	36 ± 9
NGC 5905	—	—	—	$10.1^{+0.3}_{-0.2}$	97 ± 5
GALEX D3-13	—	—	—	$9.4^{+0.2}_{-0.2}$	133 ± 6
Optical/UV TDEs					
iPTF16fml†	—	—	—	$9.6^{+0.3}_{-0.3}$	55 ± 2
PS16dtm	—	—	—	$9.4^{+0.2}_{-0.2}$	45 ± 13
GALEX D23-H1	—	—	—	$9.2^{+0.2}_{-0.2}$	86 ± 14
SDSSJ0952*	7.98	7.04	0.011	< 10.4	—
SDSSJ1342*	2.56	6.51	0.012	$9.7^{+0.3}_{-0.2}$	72 ± 6
SDSSJ1350*	4.57	7.47	0.003	$9.3^{+0.3}_{-0.3}$	—
SDSS TDE1	—	—	—	$9.5^{+0.2}_{-0.2}$	137 ± 12
SDSSJ0748†*	1.53	6.58	0.011	$9.5^{+0.2}_{-0.2}$	126 ± 7
ASASSN-14ae†	2.61	5.56	0.013	$9.5^{+0.2}_{-0.2}$	41 ± 6
PTF09axc†	—	—	—	$9.2^{+0.2}_{-0.2}$	60 ± 4
PTF09djl†	—	—	—	$9.1^{+0.3}_{-0.3}$	64 ± 7
PTF-09ge†	4.03	6.26	0.019	$9.2^{+0.2}_{-0.2}$	59 ± 9
PS1-10jh†	—	—	—	$8.7^{+0.3}_{-0.4}$	65 ± 3
iPTF15af†	3.54	7.29	0.01	$9.5^{+0.2}_{-0.2}$	98 ± 11
iPTF16axa	—	—	—	$9.4^{+0.2}_{-0.2}$	82 ± 3
AT2018dyk†	2.48	7.74	0.034	—	—
ASASSN18zj†	1.98	5.92	0.009	—	—

Table 6 Table of properties of known TDE host galaxies discussed in §2.3. ^a Sérsic indices from Mendel et al. (2014) fits. ^b Black hole masses from Law-Smith et al. (2017b). ^c Residual asymmetry measures from Simard et al. (2011). ^d Surface stellar mass density, computed as $\Sigma_{M_*} = \log[(M_*/r_{50}^2)/(M_\odot/\text{kpc}^2)]$ by Graur et al. (2018). ^e Stellar velocity dispersions from SDSS Portsmouth pipeline or Wevers et al. (2017). † Broad line TDEs (see Table 1). * Coronal line TDEs (see Table 1).

$10^{9-10} M_\odot \text{ kpc}^2$. The star-forming TDE hosts were significantly denser than the star-forming control sample. This effect was not significant for quiescent galaxies, which already tend to have high surface stellar mass densities. Graur et al. (2018) also measured surface stellar mass densities for a similar sample of 9 TDE host galaxies with velocity dispersions measured by Wevers et al. (2017), and found that they too had values in the range $10^{9-10} M_\odot \text{ kpc}^2$ with one exception: PS1-10jh, which had a surface stellar mass density of $\log(\Sigma_{M_*}/M_\odot \text{ kpc}^2) = 8.7^{+0.3}_{-0.4}$. Both of these samples, in purple and gray markers, respectively, are shown in Figure 8. Because the volume-corrected quiescent galaxies have a different stellar mass distribution than the star-

forming galaxy sample, we also compare the Σ_{M_\star} and velocity dispersion for a comparison sample cut in stellar mass to be $M_\star > 10^9 M_\odot$ in order to match the TDE host galaxies. Even after removing the low mass galaxies, the TDE hosts still have higher stellar surface densities than the volume-corrected comparison sample.

While the preference of TDE hosts for galaxies with high surface stellar mass densities was statistically significant (at least for star-forming galaxies), there was no significant dependence on the galaxy central stellar velocity dispersion. Only the quiescent host galaxies showed a hint that their velocity dispersions might be lower than those of the quiescent galaxies in the control sample. It remains to be seen whether this effect proves to be significant in a larger sample.

Law-Smith et al. (2017b) also compared kpc-scale indicators of stellar mass concentration for a sample of 10 TDE hosts with data from the Simard et al. (2011) and Mendel et al. (2014) SDSS catalogues, comparing the Sérsic indices of the TDE host galaxies and SDSS comparison galaxies to the black hole masses inferred from the $M - \sigma$ relation. The TDE host galaxies have Sérsic indices in the top 10–15% of the comparison sample in bins of black hole mass, indicating the TDE host galaxies have more concentrated stellar populations. In this review, we add data for two new TDEs (ASASSN-18zj and AT2018dyk) with archival SDSS information. We also perform a volume correction for the SDSS comparison sample using the volume calculations of Mendel et al. (2014) in order to compare this analysis to that of Graur et al. (2018). The updated Sérsic index–black hole mass plots are shown in Figure 8. The volume correction accounts for the larger number of galaxies with low black hole mass, but the same trend of TDE host galaxies having higher Sérsic indices for their black hole masses is seen. We find that 50% of the TDE host galaxies have Sérsic indices in the top 20% of the volume-corrected SDSS galaxies with $M_{\text{BH}} 10^5 - 10^6 M_\odot$, top 10% of the volume-corrected SDSS galaxies with $M_{\text{BH}} 10^6 - 10^7 M_\odot$, and top 30% of the volume-corrected SDSS galaxies with $M_{\text{BH}} 10^7 - 10^8 M_\odot$. If we only compare to the volume-corrected SDSS galaxies with quiescent levels of star formation ($\text{SFR} < 1 M_\odot \text{ yr}^{-1}$), we find the same result for $M_{\text{BH}} 10^5 - 10^7 M_\odot$, but no significant enhancement of TDE hosts in higher Sérsic index galaxies with black hole masses $M_{\text{BH}} 10^7 - 10^8 M_\odot$.

A similar trend is also seen if the bulge to total light ratio is used as a proxy for stellar concentration instead of the Sérsic index (Law-Smith et al. 2017b). However, the Sérsic index measurements from Simard et al. (2011) have lower errors and thus allow finer binning and a more detailed comparison for our analyses.

The analyses by Law-Smith et al. (2017b) and Graur et al. (2018) have established that TDE hosts are more concentrated on galaxy-wide (kpc) scales. We discuss possible mechanisms for the stellar concentration affecting the TDE rate, and the interplay between this effect and the trend with star formation history in Section 3.1, as post-starburst and quiescent Balmer-strong galaxies are also known to have high central concentrations of stellar light.

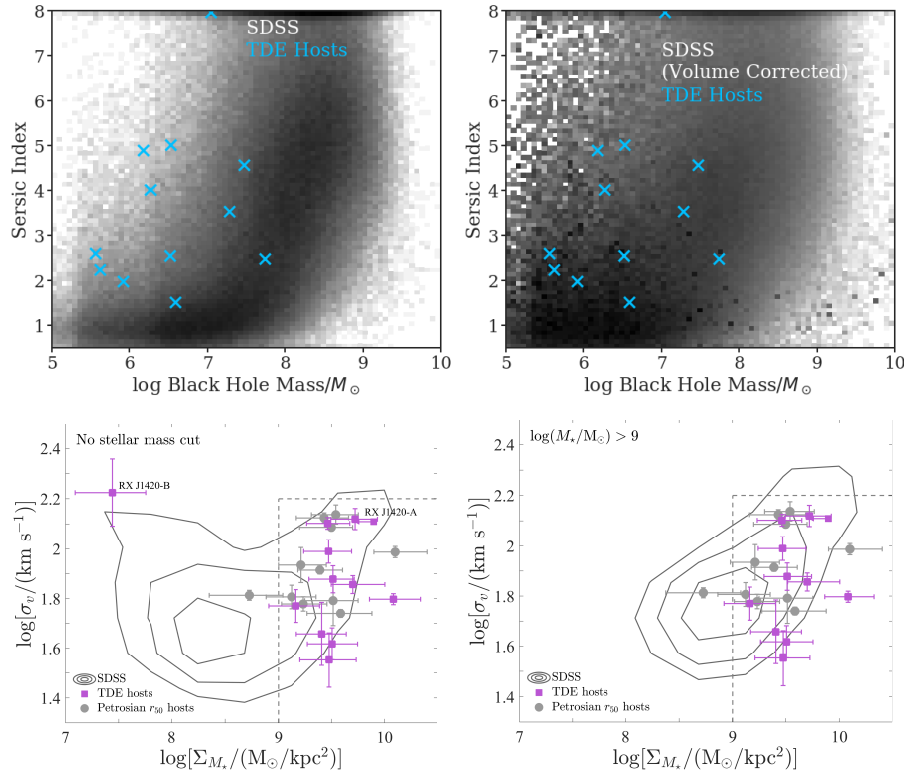


Fig. 8 **Top Left:** Black hole masses inferred from the $M - \sigma$ relation vs. Sérsic indices from Simard et al. (2011) for the SDSS main galaxy sample and the SDSS TDE hosts, adapted from (Law-Smith et al. 2017b). The TDE hosts have high Sérsic indices for their black hole masses. **Top Right:** Adapted from Law-Smith et al. (2017b) with volume corrections from Mendel et al. (2014) as done in the bottom left plot. Despite the large number of low black hole mass galaxies inferred from the volume correction, the TDE hosts still lie at high Sérsic indices for their black hole masses, compared with the rest of the galaxy sample. **Bottom Left:** Updated from Graur et al. (2018), TDE host galaxies (symbols) significantly prefer galaxies with high surface stellar mass densities, relative to a volume-limited SDSS sample (contours). New measurements for NGC 5905 and SDSS J1201 have been added to these plots. Contours represent the 25th, 50th, and 84th percentiles of the volume-weighted background galaxy distribution. Host galaxies marked by purple squares have galaxy properties measured by the same pipeline as the SDSS control sample. Host galaxies marked by grey circles differ from the SDSS control sample because their stellar surface densities are measured using Petrosian radii rather than Sérsic half-light radii, and some have velocity dispersions measured by Wevers et al. (2017) instead of the SDSS pipeline. The TDE host galaxies are significantly denser than the control sample (although this trend depends on whether the galaxies are star-forming or not – see text). **Bottom Right:** (Reproduced by permission of the AAS.) From Graur et al. (2018), same as the previous panel, but with a stellar mass cut to include only galaxies with similar stellar masses as the TDE host galaxies. Contours again represent the 25th, 50th, and 84th percentiles of the volume-weighted background galaxy distribution. As before, the TDE host galaxies have a significantly higher distribution of stellar surface mass densities. While the axes in these plots are not strictly analogous to those in the top plots, both analyses demonstrate that the TDE hosts have higher stellar concentrations than expected given their velocity dispersion or inferred black hole mass. Data from this Figure can be found in Table 6.

We also consider here the quantitative morphologies of the TDE host galaxies in asymmetry - concentration space. Spiral galaxies and elliptical galaxies separate in this space with elliptical galaxies having higher concentrations and spiral galaxies having higher asymmetries (Abraham et al. 1996). Mergers can be further identified, with higher asymmetries than individual galaxies (Conselice et al. 2003). Post-starburst galaxies often show signs of recent mergers, but at several hundred Myr past coalescence, their asymmetries as measured using HST imaging have lessened to be between those of elliptical and spiral galaxies (Yang et al. 2008, Figure 5 reproduced in this review).

Law-Smith et al. (2017b) have compiled a sample of morphological indicators for the TDE host galaxies as well as the SDSS main spectroscopic sample, using the catalogues of Simard et al. (2011). We compare the concentration to the residual asymmetries (Simard et al. 2002) for the SDSS galaxies and TDE host galaxies in Figure 9, using the Sérsic index as a proxy for concentration. We separate out star-forming, quiescent, and quiescent Balmer-strong galaxies to identify trends in this space. The star-forming galaxies have high asymmetries and low Sérsic indices, while the quiescent galaxies have Sérsic indices of $\sim 3 - 5$ and low asymmetries. The quiescent Balmer-strong galaxies show high Sérsic indices⁴, with a tail extending down to the quiescent galaxies, and low asymmetries. The TDE hosts are distributed like the quiescent galaxies, with one source (SDSSJ0952) having a high Sérsic index of $n \sim 8$. The shift towards higher asymmetry for the post-starburst or quiescent Balmer-strong galaxies is not observed in the residual asymmetries from the SDSS imaging as it was in the total light asymmetries from the HST imaging; this is likely due to the greater sensitivity of the HST data to low surface brightness tidal features. Yang et al. (2008) found that many of the tidal features observed with HST imaging would not be observable with ground-based imaging. Thus, the lack of high asymmetries in the TDE host sample does not rule out a recent merger, even a recent major merger. Higher resolution imaging and a variety of new measures of galaxy asymmetry (e.g., Pawlik et al. 2015) will be required to determine whether the TDE host galaxies have the trend towards intermediate asymmetries indicative of recent mergers, as seen in the HST imaging of post-starburst galaxies.

⁴ See above for a more thorough discussion of the Sérsic indices of TDE hosts, accounting for trends in stellar mass and black hole mass.

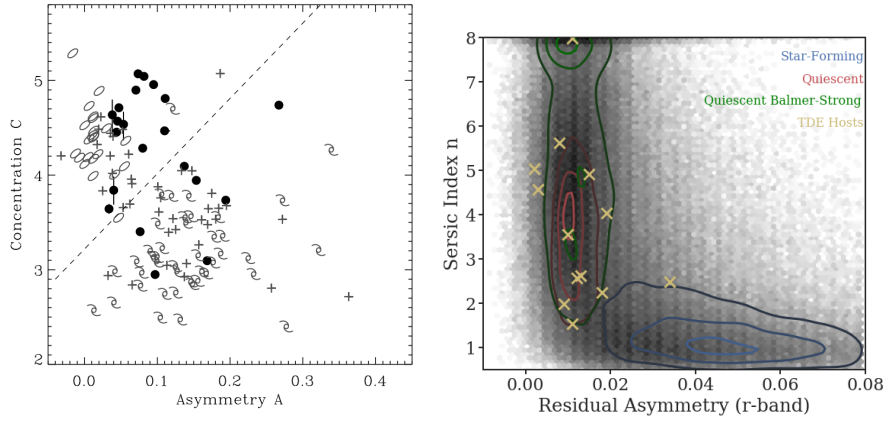


Fig. 9 Left: (Reproduced by permission of the AAS.) From Yang et al. (2008), showing the concentration and asymmetry trends for star-forming (spiral symbols), quiescent (elliptical symbols), intermediate spirals (plus signs), and post-starburst galaxies (filled circles) from HST imaging. The post-starburst sample has high concentrations of stellar light, comparable to or higher than the quiescent galaxies, and asymmetries stronger than the quiescent galaxies, but less pronounced than the star-forming galaxies. Right: Adapted from Law-Smith et al. (2017b), we plot the Sérsic index vs. the r -band residual asymmetry. In contrast to the left-hand panel, the residual asymmetries are calculated after the best-fit smooth galaxy model has already been subtracted. The residual asymmetries are calculated by Simard et al. (2002, 2011) and are denoted RA1.2 in the GIM2D output tables. Contours are plotted for the subsamples of star-forming (blue), quiescent (red), and quiescent Balmer-strong galaxies (green). TDE hosts are plotted as yellow crosses. The star-forming galaxies have high asymmetries and low Sérsic indices, whereas the quiescent galaxies have Sérsic indices of $\sim 3 - 5$ and low asymmetries. The quiescent Balmer-strong galaxies show high Sérsic indices, with a tail extending down to the quiescent galaxies. The TDE hosts follow the quiescent galaxy distribution, with one outlier (SDSSJ0952) at high Sérsic index ($n \sim 8$). Higher resolution imaging is required to determine whether the TDE host galaxies show the trend towards intermediate asymmetries indicative of recent mergers, as seen in the HST imaging of post-starburst galaxies. Data from this panel can be found in Table 6.

Name	H α	H β	[NII]6584	[SII]6717+6731	[OIII]5007	BPT Class ^a	W1-W2 ^b	SDSS Notes ^c
X-ray TDEs								
ASASSN14li†	47.7	22.8	42.5	17.7	89.3	AGN/Seyfert	0.01±0.04	GALAXY BROADLINE
Swift J1644	—	—	—	—	—	—	—	—
XMM J0740	—	—	—	—	—	—	0.01±0.03	—
ASASSN15oi†	—	—	—	—	—	—	0.06±0.06	—
Likely X-ray TDEs								
SDSS J1201	—	—	—	—	—	—	0.22±0.07	—
2MASX J0249	40.5	11.0	10.9	8.7	27.1	composite	0.05±0.04	—
PTF10iya	—	—	—	—	—	—	0.73±0.14	—
SDSS J1311	—	—	—	—	—	—	—	—
SDSS J1323	2.5	4.8	—	5.3	0.6	—	0.08±0.06	QSO
3XMM J1521	—	—	—	—	—	—	0.07±0.26	—
3XMM J1500	—	—	—	—	—	—	0.37±0.46	—
PS18kh†	—	—	—	—	—	—	-0.13±0.12	—
Possible X-ray TDEs								
RX J1242-A	—	—	—	—	—	—	-0.03±0.04	—
RX J1242-B	—	—	—	—	—	—	—	—
RX J1420-A	5.0	2.5	1.2	5.1	0.4	SF	0.12±0.06	ROSAT D
RX J1420-B	87.0	64.7	13.2	203.7	45.6	SF	—	ROSAT D
SDSS J0159	30.5	6.5	19.2	12.4	13.4	AGN/Seyfert	0.53±0.07	QSO STARBURST BROADLINE
RBS 1032	6.7	2.3	3.6	1.7	6.3	AGN/Seyfert	0.09±0.05	GALAXY
RX J1624	—	—	—	—	—	—	0.06±0.05	—
NGC 5905	23.6	6.4	13.5	6.4	2.9	composite	0.15±0.03	—
Optical/UV TDEs								
iPTF16fml†	—	—	—	—	—	—	0.01±0.05	—
PS16dtm ^d	287.3	82.5	70.9	82.5	166.4	SF	0.44±0.07	GALAXY STARFORMING
F01004	—	—	—	—	—	—	1.63±0.03	—
GALEX D23H-1	21.2	5.9	15.2	7.6	2.1	composite	0.36±0.13	—
PS1-11af	—	—	—	—	—	—	—	—
SDSS J0952*	620.7	188.4	580.4	77.9	163.4	composite	1.02±0.04	QSO BROADLINE
SDSS J1342*	311.0	70.6	62.3	55.4	82.8	SF	1.08±0.03	GALAXY STARFORMING
SDSS J1350*	202.7	48.4	193.1	36.0	49.3	AGN/LINER	0.87±0.03	GALAXY BROADLINE
SDSS TDE1	—	—	—	—	—	—	0.2±0.24	—
SDSS TDE2†	—	—	—	—	—	—	0.52±0.14	—
SDSS J0748†*	149.6	51.6	55.9	46.8	11.4	SF	0.77±0.03	GALAXY STARFORMING
ASASSN14ae†	13.2	6.0	7.3	1.9	37.8	AGN/Seyfert	0.15±0.05	GALAXY
PTF09axc†	—	—	—	—	—	—	0.15±0.08	—
PTF09djl†	—	—	—	—	—	—	0.33±0.56	—
PTF09ge†	17.8	1.8	16.8	13.1	12.1	AGN/Seyfert	0.13±0.04	GALAXY
PS1-10jh†	—	—	—	—	—	—	<0.88	—
iPTF15af†	9.0	—	—	—	2.4	—	0.18±0.08	GALAXY
iPTF16axa	—	—	—	—	—	—	0.29±0.18	—
AT2018dyk†	120.4	20.3	182.2	98.4	67.6	AGN/LINER	0.03±0.03	GALAXY
AT2018bsi†	—	—	—	—	—	—	0.09±0.05	—
ASASSN18zj†	9.3	7.9	5.4	—	8.7	composite	0.15±0.05	GALAXY

Table 7 Table of properties of known TDE host galaxies discussed in §2.4. Fluxes are in units of 10^{-17} ergs/s/cm². ^a Classification from [NII]-BPT diagram. ^b WISE 3.4 μ m - 4.6 μ m colours. We **bold** those values that meet the Stern et al. (2012) WISE AGN criteria. ^c SDSS **targettype** and **subclass** notes indicating the presence of broadline AGN or QSO like spectra. ^d While the host galaxy of PS16dtm is classed as SF on the [NII]-BPT diagram, it is a Seyfert I (Blanchard et al. 2017). † Broad line TDEs (see Table 1). * Coronal line TDEs (see Table 1).

2.4 AGN Activity

We consider here the possibility that some TDEs may occur in an environment with a pre-existing accretion disk. We have compiled a BPT (Baldwin et al. 1981) diagram in Figure 10 showing the TDE host galaxies as well as galaxies from the SDSS main spectroscopic survey. We include TDE host galaxies with SDSS spectra as described above, as well as galaxies with emission line ratios measured by French et al. (2017) and Wevers et al. (2019a). These emission line fluxes are shown in Table 7. We classify galaxies into star-forming, composite, and AGN Seyfert II or LINER based on the classifications of Kewley et al. (2001) and Kauffmann et al. (2003). These classifications are subject to a number of caveats, and represent the likely dominant ionisation source in the aperture probed by the spectrum. However, many galaxies in the AGN region of the BPT diagram, especially those with relatively weak emission lines, may instead have ionisation consistent with an origin from shocks or evolved stars (e.g., Rich et al. 2015; Yan and Blanton 2012). “Composite” galaxies lie in between the star-forming and AGN regions and could be a mix of star-formation and other ionisation sources. The TDE host galaxies occupy a range of star-formation dominated, AGN-dominated, and ambiguous ionisation source galaxies.

Another way of identifying AGN, especially those obscured by dust, is to look for signatures of hot dust from the WISE 3.4–4.6 μm colours. Stern et al. (2012) identify a WISE colour cut of $\text{WISE } 3.4\text{--}4.6 > 0.8$ Vega mag to indicate the presence of an AGN. We present these WISE colours in Table 7, identifying four TDE hosts which meet this criterion: the hosts of F01004, SDSS J0952, SDSS J1342, and SDSS J1350. The first host galaxy is currently experiencing a starburst (Tadhunter et al. 2017). The latter three galaxies all hosted TDEs with observed coronal line emission.

The BPT analysis described above selects narrow-line AGN (Seyfert II galaxies), or obscured AGN, as does the infrared selection. When the broad-line regions of AGN are visible, this provides another way to identify them from their optical spectra. In Table 7, we also list notes from the SDSS to indicate broad-line or QSO emission. Five TDE host galaxies have such notes, with varying overlap with those galaxies classified as AGN from the BPT or WISE colour analyses. AGN selection using any of these methods is neither pure nor complete. One may note that the host galaxy of PS16dtm, a Narrow-line Seyfert I galaxy (Blanchard et al. 2017), is not selected as an AGN using a BPT or WISE colour analysis, and requires further analysis of the optical spectrum to identify the broad components of the Balmer lines. The connection between TDEs and Narrow line Seyfert I galaxies requires further study (Wevers et al. 2019b). Such galaxies make up only $\sim 15\%$ of all Seyfert I galaxies (Williams et al. 2002) and have been observed to have optical flares similar to TDEs (Kankare et al. 2017). Some of these events may even belong to a different class of transient (Frederick et al. 2019).

Caution should be taken in interpreting these results given the selection effects against identifying TDEs in AGN host galaxies. We discuss the role of

AGN in either enhancing the TDE rate or as the source of selection effects against identifying TDEs in such host galaxies in §3.3. TDEs will be more difficult to identify in AGN due to selection against AGN flares and higher levels of dust obscuration. These effects may also bias the types of AGN TDEs are found in. Further study will be needed to fully understand these effects.

Furthermore, we note that spectra taken after the TDE may be contaminated by residual TDE emission, depending on how long the emission persists for. Brown et al. (2016) found that narrow $H\alpha$ emission can persist for a year after the TDE, but after several years, Wevers et al. (2019a) find no residual narrow line emission. French et al. (2017) noted a tentative offset in $H\alpha$ equivalent width and $[NII]-6584/H\alpha$ emission ratio between the few events with spectroscopy before vs. after the TDE. French et al. (2017) found the host galaxies with spectroscopy from after the TDE to have higher $H\alpha$ equivalent widths and $[NII]-6584/H\alpha$ emission ratios than the host galaxies with spectroscopy from before the TDE, although this analysis was limited by the small number of events and the lack of events with spectra from both before and well-after the TDEs. In the sample considered in this review, we note the host galaxies with spectra taken before the TDE contain more Seyferts and the host galaxies with spectra taken after the TDE contain more star-forming and composite classifications. However, this comparison is still limited by small number statistics and selection effects between the various TDE detection methods used. A systematically collected set of follow-up spectra will be needed to better understand the presence of narrow line emission in the decade after a TDE.

Further insight into the presence or absence of AGN in TDE host galaxies requires spatially resolved emission line maps from IFU data. We present one example here; the host galaxy of AT2018dyk was observed as part of the MaNGA survey (Bundy et al. 2015). This host galaxy is in the AGN regions of the BPT diagrams in Figure 10, and in Figure 11 we see that there is indeed a central $[OIII]$ -bright source, and that the outskirts of the galaxy have ionisation dominated by star formation.

The host galaxy of the TDE ASASSN-14li additionally shows evidence of past AGN activity, with large extended ionized regions visible in $[OIII] 5007$ and $[NII] 6584$ lines, seen in MUSE observations (Prieto et al. 2016, Figure 12). Given the light travel time to these narrow-line regions, their ionisation implies strong AGN activity $10^4 - 10^5$ years in the past. Such extended ionized features have been seen around other galaxies in large imaging surveys (“voorwerps” Lintott et al. 2009; Keel et al. 2017) and around other post-starburst galaxies in narrow-band imaging (Schweizer et al. 2013; Watkins et al. 2018). These instances of recent AGN activity in galaxies lacking strong current AGN activity further complicate our understanding of the co-existence of gas and stellar accretion by supermassive black holes in galactic nuclei, raising questions regarding the timescale for TDE rate enhancements compared to AGN duty cycles. The host galaxy of ASASSN-14li furthermore has a persistent radio source discovered in the FIRST survey which may also indicate on-going low-level AGN activity (Holoien et al. 2016a).

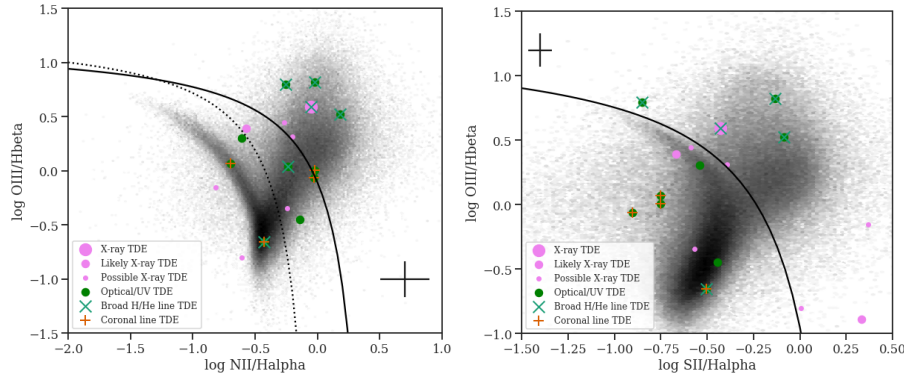


Fig. 10 BPT (Baldwin et al. 1981) diagrams of emission line ratios indicative of ionisation from AGN or star formation in the TDE host galaxies and SDSS main galaxy spectroscopic sample. Galaxies to the lower left of the dotted and solid lines have ionisation dominated by star formation. Galaxies to the upper right of the dotted lines have ionisation dominated by AGN, although those with relatively weak emission lines may instead have ionisation from shocks or evolved stars (e.g., Rich et al. 2015; Yan and Blanton 2012). The dotted line is the observed star formation - AGN separation from Kauffmann et al. (2003) and the solid lines are the theoretical maximum starburst lines from Kewley et al. (2001). Characteristic error bars are shown in each panel. The TDE host galaxies occupy a range of star-formation dominated, AGN-dominated, and ambiguous hosts.

2.5 Environment

We consider here the extragalactic environments of the TDE host galaxies, as many mechanisms which act to change the other galaxy properties considered in this section can only act in dense cluster-scale environments. Several TDEs have been found in targeted X-ray surveys of dense galaxy clusters. J1311 (Maksym et al. 2010) was found in a search for TDEs in Abell 1689. While it is not included in our analysis due to the lack of a host galaxy spectrum, “Wings” (Maksym et al. 2013) was found in Abell 1795.

In addition to possible selection biases towards finding TDEs in clusters, post-starburst galaxies are known to lie preferentially in group environments (Zabludoff et al. 1996). While groups like the Local Group are the most common galaxy environment, the groups favored by post-starburst galaxies tend to be virialized and more massive than the Local Group, with low enough velocity dispersions and high enough galaxy densities to make galaxy-galaxy mergers and tidal interactions likely (Zabludoff et al. 1996).

We cross match the catalogue in Table 1 with the Abell cluster catalogue (Abell et al. 1989), to check for host galaxies within 25 arcminutes of a cluster with a similar redshift (velocities within 3000 km/s of the host galaxy redshift). We find one additional TDE host galaxy, PTF09axc, to be associated with the cluster Abell 1986.

To test for TDE host galaxies in less rich clusters and groups, we cross match our TDE host galaxy catalogue with the group and cluster catalogue of Tempel et al. (2014). Of the 41 host galaxies, 14 are matched with the

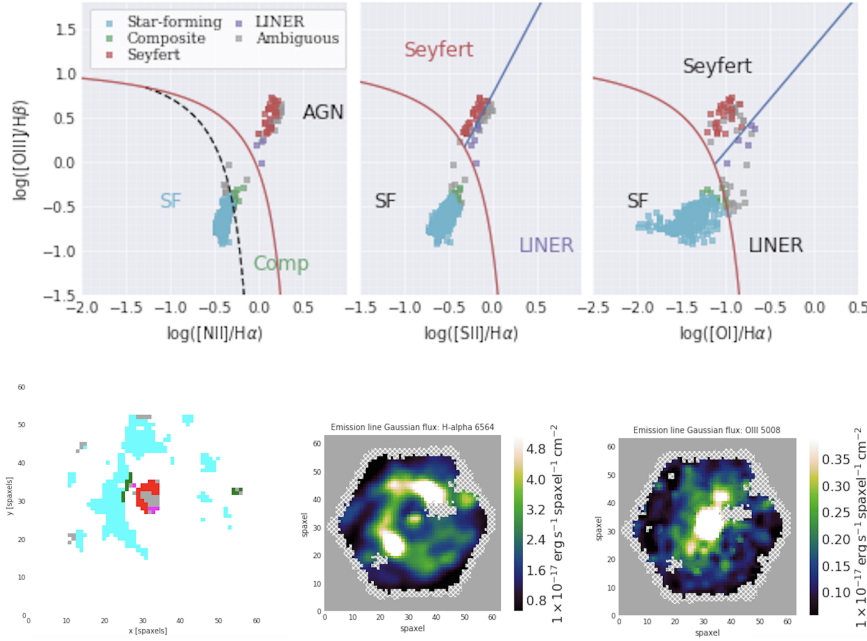


Fig. 11 Spatially resolved BPT diagram, $H\alpha$ map, and $[OIII]5007$ map for the host galaxy of TDE AT2018dyk, made using Marvin (Cherinka et al. 2018). Points are colored blue, green, red, dark grey, or light grey based on their classification as star-forming, composite, Seyfert, LINER, or ambiguous. This host galaxy is in the AGN regions of the BPT diagrams in Figure 10, and here we see that there is indeed a central $[OIII]$ -bright source, and that the outskirts of the galaxy have ionisation dominated by star formation. Obtaining data like this for additional TDE hosts, especially those for which the ionisation source is ambiguous, or there is evidence for unusual AGN properties, will help further our understanding of the co-existence of TDEs and AGN.

Tempel et al. (2014) catalogue. Seven are the only galaxy in their halo⁵, six are associated with groups of 1-6 additional galaxies⁶, and one is part of a cluster of 52 galaxies (SDSS J1350). Given the set of 14 TDE host galaxies in the Tempel et al. (2014) catalogue, and their full sample of galaxies, we find no evidence to suggest that the TDE host galaxies prefer different environments than the general galaxy sample. Using either a Kolmogorov-Smirnov or Anderson-Darling test, we cannot reject the hypothesis their environment richnesses are drawn from the same distribution.

3 Possible Drivers for Host Galaxy Preferences

There are several possible causes for the observed TDE rate enhancement in the host galaxy types discussed above. Many of these scenarios predict TDE

⁵ ASASSN14li, RBS1032, SDSS J1342, SDSS J0748, ASASSN14ae, ASASSN18zj

⁶ SDSS J1323, NGC 5905, SDSS J0952, PTF09ge, AT2018dyk, AT2018bsi

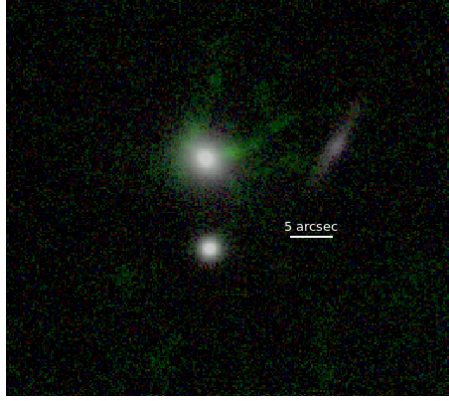


Fig. 12 Three-colour RGB image constructed from a MUSE datacube of the host galaxy of ASASSN-14li. The red and blue components of this RGB image are from red and blue continuum regions and green is from the [OIII] 5007 line. Extended ionized features are observed via the [OIII] 5007 line extending beyond the continuum-dominated bulk of the galaxy, and are likely from past AGN activity $10^4 - 10^5$ years ago (Prieto et al. 2016). The star observed below the galaxy and the edge-on galaxy to the right are not associated with the TDE host galaxy. Recent AGN activity in galaxies lacking strong current AGN activity further complicates our understanding of the co-existence of gas and stellar accretion by supermassive black holes in galaxies, raising questions of the timescale for TDE rate enhancements compared to AGN duty cycles.

enhancements in both post-starburst hosts and centrally concentrated hosts, such as a central overdensity or mechanisms related to galaxy-galaxy mergers.

3.1 Increased Stellar Concentration / Central Overdensities

The TDE rate depends on the number of stars which can be scattered into center-crossing orbits, and so a high central stellar density will result in a high TDE rate. For a Nuker surface-brightness profile, the inner stellar slope γ is found to correlate with the TDE rate as $\dot{N}_{\text{TDE}} \propto \gamma^{0.705}$ in a sample of early type galaxies from Lauer et al. (2007) (Stone and Metzger 2016). A high central stellar concentration may be correlated with high concentrations on larger $\sim \text{kpc}$ scales. As discussed above in §2.3, TDEs are overrepresented in galaxies with high Sérsic indices for their black hole masses (Law-Smith et al. 2017b) and in galaxies with high stellar surface densities on scales of the half-light radius (Graur et al. 2018). An increased TDE rate due to a merger-induced stellar overdensity is seen in simulations by Pfister et al. (2019), although at very early stages in the merger, before the coalescence of the two black holes.

If high stellar concentrations drive the TDE rate enhancement in high Sérsic index or stellar surface density galaxies, it may also explain the rate enhancement in post-starburst galaxies. Post-starburst galaxies have high Sérsic indices (Yang et al. 2004; Quintero et al. 2004; Yang et al. 2008) as the recent starbursts are centrally concentrated, likely due to stars formed from gas infall

in the recent merger, and the young/intermediate A stars dominate the light. Once the bright young stellar population in post-starburst galaxies fades, the bulge properties are consistent with evolving to normal early type galaxies, but the stellar concentrations on scales close to the black hole radius of influence have not been measured in samples of post-starburst galaxies. However, the nearby post-starburst galaxy NGC 3156 has HST imaging with high enough resolution to measure the central slope of the Nuker profile, and Stone and van Velzen (2016) find the slope to be steeper than any of the early type galaxies studied previously by Stone and Metzger (2016). Given the lack of a similar TDE rate enhancement in early type galaxies, something must change in the central galaxy concentration or dynamics in the few Gyrs after the post-starburst phase.

The evolution of a central overdensity with time was studied by Stone et al. (2018), who model the stellar density profile as $\rho \propto r^{-\gamma}$, and determine how γ changes with time. Given the post-burst ages of the post-starburst TDE hosts (French et al. 2017), the TDE rate enhancement and its tentative evolution with time could be explained if $\gamma \geq 2.5$. The predictions made by this model can be tested with larger samples of post-starburst TDE hosts in the LSST and perhaps even ZTF eras.

Based on the supposition that the TDE rate should depend on the density of stars in the SMBH loss cone, along with their velocity dispersions, Graur et al. (2018) assumed those local properties would be correlated with their global, kpc-scale counterparts, and that the TDE rate would depend on the latter as $R_{\text{TDE}} \propto \Sigma_{M_*}^\alpha \times \sigma_v^\beta$, where Σ_{M_*} is the surface stellar mass density on the scale of the half-light radius and σ_v is the kpc-scale velocity dispersion. By comparing their sample of TDE host galaxies with a volume-limited control sample drawn from the SDSS, Graur et al. (2018) estimated the values of the power-law indices to be $\hat{\alpha} = 0.9 \pm 0.2$ and $\hat{\beta} = -1.0 \pm 0.6$ using SDSS fiber measurements of the central few kpc, and assuming these global properties correlate with the properties on the smaller scales of the stars in the SMBH loss cone.

Wang and Merritt (2004) find that the TDE rate of an isothermal sphere ($\rho \propto r^{-2}$) depends on the SMBH mass, M_\bullet , and local velocity dispersion, σ , as $R_{\text{TDE}} \propto M_\bullet^{-\alpha} \times \sigma^\eta$. The average surface stellar mass density of the stars orbiting the SMBH is $\Sigma = M_\bullet / \pi r_h^2 = \sigma^4 / \pi G^2 M_\bullet$, where $r_h = GM_\bullet / \sigma^2$ is the size of the star cluster (Peebles 1972), and G is the gravitational constant. This allows us to rewrite the TDE rate as $R_{\text{TDE}} \propto \Sigma^\alpha \times \sigma^{\eta-4\alpha}$. Using the Graur et al. (2018) estimates for α and $\beta = \eta - 4\alpha$, the values measured from the data, $\alpha = 0.9 \pm 0.2$ and $\eta = 2.6 \pm 1.0$ are consistent with the theoretical predictions, $\alpha = 1$ and $\eta = 3.5$ (Wang and Merritt 2004). This suggests that the TDE rate is indeed driven by the dynamical relaxation of stars into the loss cone of the SMBH.

Could both the preference of TDE hosts to be in post-starburst or quiescent Balmer-strong host galaxies and the preference for host galaxies with high central concentrations be driven by the same effect? Similar galaxy over-representations can be found in both Sérsic index–black hole mass and in

H α emission–H δ absorption, where $\geq 60\%$ of TDEs are found in $\sim 2\%$ of the parameter space (i.e., at high H δ absorption and low H δ emission, or at high Sérsic index and low black hole mass)⁷. Of the five TDE host galaxies considered by Law-Smith et al. (2017b) with high Sérsic indices and low black hole masses, three are post-starburst or quiescent Balmer-strong, and two (PTF09ge and SDSSJ123) are not. Of the seven quiescent Balmer-strong galaxies considered by French et al. (2016), two (ASASSN-14li and ASASSN-14ae) also meet the high Sérsic index and low black hole mass criteria, and the remaining five do not have sufficient data to determine an accurate Sérsic index or bulge mass. Larger numbers of observed TDEs and more detailed analyses of low concentration post-starburst hosts or high concentration non-bursty host galaxies will be an important test of which mechanisms most affect the TDE rate.

3.2 Black Hole Binary

After a galaxy–galaxy merger, the supermassive black hole from each galaxy will inspiral and coalesce. The influence of supermassive black hole binary dynamics on TDEs is the subject of another chapter in this review (Coughlin et al. 2019, ISSI review). We summarize here the relevant points from Coughlin et al. (2019, ISSI review) for the present discussion of the host galaxies.

The TDE rate can be very high (of order 1 per year) for a short (~ 1 Myr) period during coalescence when the secondary black hole approaches the cusp of stars around the primary, at \sim pc scale separations. As inspiral continues, the TDE rate will then drop below that of an isolated black hole, and rise once more to a modest rate enhancement of $\sim 2 - 10\times$ that of an isolated black hole once the binary has reached mpc separations. The lightcurves of TDEs can be altered in the case of a tightly bound binary where the debris stream interacts with the companion supermassive black hole. However, if most of the TDEs around black holes in coalescing binaries happens at pc-scale separations, the debris streams will be on significantly smaller scales, and the TDE lightcurves will show no evidence of the companion supermassive black hole. Thus, we are unlikely to see observational effects from the secondary black hole at separations of the same spatial scales which will boost the TDE rate.

The main observable difference between this explanation for the TDE rate enhancement in post-starburst or centrally-concentrated galaxies and the others, is the TDE rate per galaxy. If the TDE rate is very high ($\sim 0.1 - 1$ per year per galaxy) for a Myr, we should observe a high instance of repeat TDEs per host galaxy, especially over the 10 year run of LSST. The other mechanisms for enhancing the TDE rate described in this section would act over 100 Myr - 1 Gyr, with more modest TDE rates per galaxy, and instances of repeat TDEs would be rare. No repeated TDEs have been observed to date,

⁷ Although the details of this will depend on the TDE samples and comparison samples used, see previous discussions in §2.2 and §2.3.

which means either there are no observed cases where the TDE rate is as high as 1 per several years, or systems hosting multiple TDEs within several years are obscured by dust or otherwise produce a different observational signature than the TDEs discussed in this review.

For now, the likelihood that supermassive black hole binary effects are driving the observed host galaxy distributions can be probed statistically. French et al. (2017) measured the star formation histories for a sample of six post-starburst TDE host galaxies to determine the time since the recent starbursts. If the starburst coincides with the coalescence of the two galaxies, this can also constrain the time since the supermassive black holes started to inspiral on kpc-scales. Most of the TDE host galaxies are less than 600 Myr since starburst. For a secondary to have in-spiraled to pc-scales in 600 Myr, that mass ratio of the two galaxies must be more equal than 12:1 given the dynamical friction timescales. This constrains the TDE rate enhancement in supermassive black hole binaries to be more strongly dependent on the mass ratio than the merger rate, since minor mergers with mass ratios less equal than 12:1 are more common than major mergers. Stone et al. (2018) also argue against the possibility of supermassive black hole binaries causing the observed rate enhancement in post-starburst galaxies by constructing an expected delay time distribution of TDEs after a starburst. Many more TDEs would be expected at times > 1 Gyr after a starburst, but the observed host galaxies have younger ages. Unless the timescale between the merger and the starburst is fine-tuned, compared to the dynamical friction timescale, the observed host galaxies are not compatible with rate enhancement from a black hole binary scenario.

3.3 Circumnuclear Gas

If a supermassive black hole is surrounded by a circumnuclear gas disk, this may act to enhance the TDE rate as stars interact with the disk. Kennedy et al. (2016) predict the TDE rate could be increased by up to $10\times$ by the presence of such a disk. This effect may co-exist with the other mechanisms for affecting the TDE rate discussed here, as mergers are expected to trigger AGN activity (e.g., Treister et al. 2012) as well as bursts of centrally-concentrated star formation.

However, there are a number of selection effects which may hinder the identification of TDEs in host galaxies with pre-existing circumnuclear gas disks. As discussed by Law-Smith et al. (2017b), Wevers et al. (2019a), and others, observational searches for TDEs will select against AGN host galaxies while trying to avoid classifying AGN flares from variations in the gas accretion rate as TDEs, and many TDEs in AGN host galaxies will be heavily extinguished by dust. One possibility for identifying TDEs in AGN host galaxies with heavy dust obscuration is through multi-epoch radio observations. Mattila et al. (2018) identify a TDE in Arp 299, a Seyfert II galaxy and dust-obscured LIRG (Pereira-Santaella et al. 2015), via a growing radio jet in one of the two nuclei in this merging system. Identifying the accretion of an indi-

vidual star in an AGN with a high gas accretion rate may prove unfeasible, or only possible to assess statistically.

3.4 Other Dynamical or Secular Effects

There are several other effects that might increase the TDE rate in post-merger galaxies, causing the observed host galaxy preferences. A more complete description of these effects can be found in the chapter of this review by Stone et al. (2020, ISSI review); we very briefly mention two mechanisms here. First, a radial anisotropy of the orbits after a merger would increase the rate of TDEs. Stone et al. (2018) modeled the dependence of the rate enhancement on the time since the starburst, parameterizing the radial anisotropy as $\beta \equiv 1 - \frac{T_{\perp}}{2T_{\parallel}}$, where T_{\perp} and T_{\parallel} are the kinetic energies of the tangential and radial motion, respectively⁸. Stone et al. (2018) find that the observed host galaxies could be explained if $\beta > 0.6$. A triaxial nuclear potential (Merritt and Poon 2004) could have a similar effect of enhancing the TDE rate after a nuclear starburst. Second, Madigan et al. (2018) predict an enhanced TDE rate that declines with time after a nuclear starburst due to the formation of an eccentric stellar disk, where the TDE rate would be increased due to secular effects and could potentially reach $0.1 - 1 \text{ gal}^{-1} \text{ yr}^{-1}$. However, the timescale over which this effect might produce a high TDE rate is uncertain. The high spatial and spectral resolution of next-generation 30-m class telescopes will provide crucial tests of these mechanisms in nearby TDE hosts.

4 Implications for TDE Rates

The variation in TDE rates by host galaxy type has implications for the relative TDE rates in different types of galaxies. The TDE rate averaged across all galaxy types is observed to be $\sim 10^{-4}$ per galaxy per year (van Velzen 2018). We quantify the TDE rates in quiescent Balmer-strong and post-starburst galaxies compared to normal quiescent galaxies in Figure 13, and how this depends on the definition of “Balmer-strong”. The TDE rate in quiescent Balmer-strong and post-starburst galaxies is $1\text{--}3 \times 10^{-3}$ per galaxy per year, depending on the threshold used to define such galaxies. An enhancement in the TDE rate in certain galaxies will necessarily result in a decreased TDE rate in other galaxies given a measurement of the total TDE rate. Is this lowered rate enough to cause tension with theoretical predictions for the TDE rate in normal quiescent galaxies ($\sim \text{few} \times 10^{-4}$ per galaxy per year, e.g., Stone and Metzger 2016)? Depending on the definition of “Balmer-strong” vs. “normal” quiescent galaxies, the TDE rate in normal quiescent galaxies is $0.3 - 1 \times 10^{-4}$ per galaxy per year. We stress here that despite the enhanced TDE rates observed in post-starburst and quiescent Balmer-strong galaxies, the number

⁸ β is defined such that if all orbits are purely radial, $\beta = 1$, and if all orbits are purely tangential, $\beta = -\infty$.

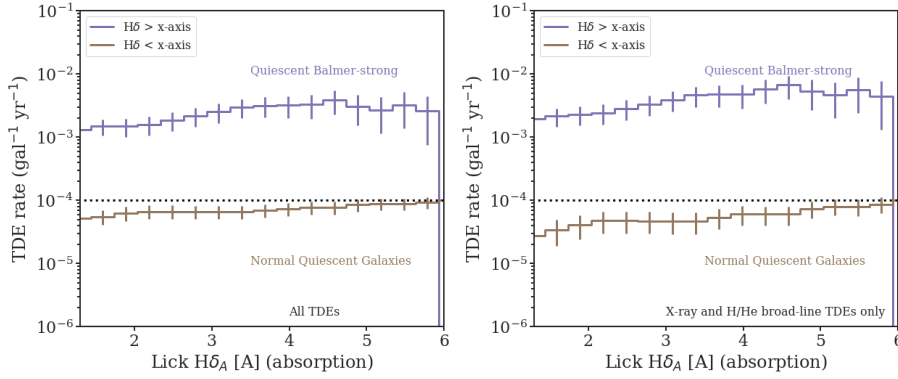


Fig. 13 TDE rate (scaled to a fiducial value of 10^{-4} per galaxy per year as measured by e.g., van Velzen 2018) in quiescent galaxies above and below each value of $H\delta$ absorption. While the rate enhancement in quiescent Balmer-strong and post-starburst galaxies results in higher TDE rates, the resulting suppression of TDE rates in quiescent galaxies that do not meet a given $H\delta$ absorption threshold is mild, at $< 3\times$.

of TDEs in normal galaxies is still high enough to avoid a crisis in their TDE rates. The large number of galaxies which do not meet the quiescent Balmer-strong or post-starburst selection compensates for the lower TDE rate in such “normal” galaxies. This rate suppression of $\lesssim 3\times$ in normal quiescent galaxies is comparable to the uncertainties in predicting the theoretical TDE rate and determining the observed TDE rate in various surveys.

5 Using the Host Galaxy Information in Transient Surveys

5.1 Identifying TDEs using a priori Host Galaxy Information

In addition to being used to understand what drives the TDE rates, the unique properties of TDE host galaxies may be useful for selecting candidate TDEs for spectroscopic follow-up observations in large transient surveys. The large volume of transient alerts faced by current and future surveys such as ZTF and LSST means that not all transients can be followed up for spectroscopic confirmation and further study with triggered space-based observations and high cadence photometry. Methods to flag likely TDEs will be essential for future TDE studies. One method to flag likely TDE candidates is to use a priori information about their likely host galaxies. Transients discovered in pre-identified likely TDE host galaxies, based on (for example) E+A spectroscopic signatures or concentration indices, can then be systematically classified with dedicated spectroscopic observations to efficiently select TDEs for further photometric and spectroscopic monitoring.

For transient surveys in the Northern hemisphere where transient detections will have a significant overlap with large spectroscopic surveys (especially SDSS), the detailed properties of likely host galaxies can be used to predict

which candidate detections are likely TDEs, supernovae, or other transient phenomenon, and flag interesting objects for follow-up. However, a significant portion of the LSST footprint will not be covered by large spectroscopic surveys, so photometric criteria will be useful.

A technique of selecting likely TDEs for followup based on the colour (and thus star formation rate) of the host galaxy is used by iPTF/ZTF (Hung et al. 2018) in order to reduce contamination by supernovae. Further cuts on the recent star formation history or concentration of host galaxies may further refine this selection, independent of the physical reason for the enhanced TDE rate in such galaxies.

French and Zabludoff (2018) present a method for identifying likely TDE candidates using photometrically-identified quiescent Balmer-strong galaxies. A Random Forest classifier trained on spectroscopically-identified quiescent Balmer-strong galaxies can be used to detect such galaxies in LSST using LSST photometry in addition to archival photometry from *GALEX* and *WISE*. Because these galaxies have low star formation rates and thus low supernova rates, contamination from other transients will be low.

Other possible methods for identifying likely TDE hosts can use photometric information on the light concentration, given by either the Sérsic index or bulge fraction that may predict a TDE overabundance in a related set of likely host galaxies (see discussion in §3.1). For instance, choosing nuclear transients in high-Sérsic galaxies could significantly increase the success of confirming TDEs.

There are several important benefits to selecting TDEs for spectroscopic follow-up. In addition to identifying a large number of events, this method can identify TDEs with properties that diverge from the known set of TDEs. The small number of optical/UV bright TDEs studied to date already show a large variety in their peak magnitude, colour evolution, and decline timescale (Holoien et al. 2016a; Blagorodnova et al. 2017; Wevers et al. 2017). Furthermore, a priori selection of the likely host galaxies means candidate events can be followed-up early, even before a light curve is obtained. Early time light curve information will enable more detailed modeling, and may be able to be used to measure black hole masses (Mockler et al. 2019).

Any method for selecting transient events for follow-up based on the host galaxy properties will bias the host galaxy properties of the resulting sample. Thus, these selection methods are complementary to other methods which are un-targeted or use information on the transient properties alone.

6 Galaxy Studies Using TDEs

Current and upcoming transient surveys, such as LSST in the optical and eROSITA in the X-ray, are expected to detect hundreds to thousands of TDEs each year (van Velzen et al. 2011; Khabibullin et al. 2014). In light of the theoretical predictions and observational evidence that these TDEs should occur in the lowest mass galaxies still harbouring black holes (Wang and Merritt

2004), TDEs could become beacons for studying the black hole mass functions and spin distributions of quiescent supermassive black holes.

While measuring velocity dispersions of large samples of increasingly faint galaxies will become prohibitively expensive, alternatives are emerging to measure the black hole mass. For example, it is expected that the shape of a TDE lightcurve depends mainly on the mass of the black hole and the mass of the disrupted star. Mockler et al. (2019) exploit this by using lightcurve models to infer the black hole mass under some assumptions for the mass of the disrupted star. They show that this method yields similar uncertainties when compared to other ways of estimating the black hole mass (e.g. galaxy scaling relations), while further improvements (such as including realistic models for the stellar structure) could decrease potential systematic effects. This can provide the opportunity to measure black hole masses of galaxies that are too faint for velocity dispersion measurements, as well as large samples of galaxies, as long as the lightcurve is well sampled around peak and ideally in more than one filter.

These mass measurements will be invaluable for TDE demographics studies, but can also potentially contribute to other areas of galaxy evolution, such as the cosmic growth of SMBHs in quiescent galaxies and the BH occupation fraction and mass function of dwarf galaxies. On the high end of the mass function, observed TDE rates will be affected by the presence of an event horizon cutoff, as a consequence of the tidal radius becoming smaller than the event horizon and making disruptions invisible to outside observers. A main sequence star disrupted by a Schwarzschild black hole of mass $\geq 10^8 M_\odot$ will not produce an observable flare. However, the spin of the SMBH will affect this cutoff mass, such that TDEs would still be observable around $10^8 - 10^9 M_\odot$ SMBHs at high ($a \sim 0.9 - 0.999$) spins (Kesden 2012; Leloudas et al. 2016). A large number of TDEs with black hole masses $\geq 10^8 M_\odot$ would imply a large fraction of supermassive black holes with high spin parameters. The spin distribution for supermassive black holes has implications for their accretion and merger history, as coherent gas accretion is expected to spin up black holes while frequent mergers will spin them down (e.g., Volonteri et al. 2003; Hughes and Blandford 2003). The effect of the spin distribution on the observed TDE rate is discussed further by Stone et al. (2020, ISSI review). The possibilities for observing TDEs in dwarf galaxies with intermediate mass black holes are discussed by Maguire et al. (2020, ISSI review).

7 Summary and Discussion

We have summarized the observed host galaxy properties of X-ray bright and optical/UV bright TDEs and discussed the possible physical mechanisms that could drive the observed correlations between host galaxy properties and the TDE rate. While the black hole masses of TDEs have similar distributions between X-ray and optical/UV bright TDEs, compiling a large sample of known TDEs allows us to identify a significant shift in the stellar masses and abso-

lute magnitude distributions between the two samples, with optical/UV TDEs having higher stellar masses than the X-ray TDEs. This may be due to an underlying trend in black hole mass we do not yet have the statistical power to resolve. Future work on determining the black hole masses of new TDEs and understanding the selection effects of TDEs identified in the X-ray or optical will be needed.

Most TDE host galaxies are quiescent, with little current star formation, and TDEs are over-represented in galaxies with post-starburst or quiescent Balmer-strong star formation histories. We present new estimates of the TDE rate enhancement in these samples depending on the definition of these classes and the types of TDEs considered. For the TDE host galaxies considered in this review, 5/41 (12%) are post-starburst galaxies and 13/41 (32%) are either quiescent Balmer-strong or post-starburst. Of the 4 X-ray TDEs, 3 (75%) are quiescent Balmer-strong and 1 (25%) is post-starburst. Of the 15 broad H/He line TDEs, 9 (60%) are quiescent Balmer-strong and 5 (33%) are post-starburst. We note again that these TDE classifications are tentative and subject to a number of observational biases. More observations of the host galaxies for a large sample of well-characterized TDEs are needed to overcome these uncertainties and the small-number statistics limiting our precision here. While controlling for some galaxy properties, notably bulge color and central concentration, can reduce the TDE enhancement rate in post-starburst or quiescent Balmer-strong galaxies, these properties are strongly correlated with galaxy SFH during the post-starburst phase. The TDE enhancement rates in such hosts are thus consistent (given the small number statistics) between the studies of French et al. (2016), Law-Smith et al. (2017b) and Graur et al. (2018). While the rate enhancement in quiescent Balmer-strong and post-starburst galaxies results in higher TDE rates, the resulting suppression of TDE rates in normal quiescent galaxies is mild, at $< 3\times$.

TDE host galaxies have higher concentrations of stellar light than expected given their stellar mass or black hole mass. We aggregate here observations from many sources of TDE host galaxy optical light concentrations, and present new versions of two analyses from the literature. We consider the effect of volume-correcting the SDSS comparison sample on the result by Law-Smith et al. (2017b) that TDE host galaxies have high Sérsic indices for their black hole masses, finding that despite the large number of low black hole mass galaxies inferred from the volume correction, the TDE hosts still lie at high Sérsic indices for their black hole masses, compared with the rest of the galaxy sample. We also add measurements for two additional TDE host galaxy velocity dispersions from Wevers et al. (2019a) to the analysis of Graur et al. (2018) that shows TDE hosts have high stellar surface densities for their velocity dispersions, and find the conclusions unchanged.

The ionisation states of TDE host galaxies span a range from star-formation dominated to AGN-dominated, and we identify many TDE host galaxies with signs of on-going gas accretion by the SMBH. However, given the significant selection biases affecting this distribution, and the uncertainties in identifying especially low-luminosity AGN or LINERs, we urge caution in its interpreta-

tion. The extra-galactic environments of TDE host galaxies show no signs of being different than the general galaxy population or the post-starburst galaxy population, but this comparison is especially limited by the small numbers of TDE hosts with well-studied extra-galactic environments.

We summarize the state of several possible explanations for the links between the TDE rate and host galaxy type, including the effect of stellar overdensities, black hole binaries, circumnuclear gas, and dynamical or secular effects. We present estimates of the TDE rate for different host galaxy types and quantify the degree to which rate enhancement in some groups results in rate suppression in others. We discuss the possibilities for using TDE host galaxies to assist in identifying TDEs in upcoming large transient surveys and possibilities for TDE observations to be used to study their host galaxies.

We note that the TDEs considered here are a relatively small number of events, with classifications subject to observational and selection biases which may change in future studies of TDEs.

We identify the following as important open questions in this field:

1. What is the primary driver of the observed correlations between galaxy-scale host properties and the TDE rate?
2. What are the distributions of stellar mass and the stellar kinematics of TDE host galaxies within the radius of gravitational influence of their supermassive black holes?
3. Do the same physical effects drive the observed enhanced TDE rates in post-starburst or quiescent Balmer-strong galaxies and galaxies with high central concentrations?
4. Are the high central concentrations at kpc scales of optical stellar light seen in TDE hosts correlated with high central concentrations of stars at the nucleus?
5. What is the unobscured TDE rate in starburst galaxies? Does the enhancement during the post-starburst phase arise from a higher absolute rate during this phase or simply a higher observed rate due to dust obscuration during the starburst phase and/or selection bias against AGN in starburst galaxies?
6. How does the presence of an existing AGN of varying accretion rates affect the rates and observability of TDEs?
7. What is the connection between TDEs and Narrow-Line Seyfert Is?
8. What is the connection between TDEs and the LINER-like emission present in most post-starburst or quiescent Balmer-strong galaxies? What can cases where a host galaxy has pre-TDE spectroscopy tell us about the evolution of narrow line emission from TDEs vs. AGN?
9. Are there differences in the host galaxies depending on the type of TDE?
10. What drives the observed difference in stellar mass between the optical and X-ray bright TDEs? Is the difference due to a difference in intrinsic black hole mass? Are the observed trends affected by selection bias in how TDEs are identified in the optical vs. X-ray?

11. How can we best use our understanding of TDE host galaxies to study supermassive black holes and their host galaxies using new observations from next-generation surveys like LSST and *eROSITA*? How can we best compare the samples of TDEs discovered using LSST vs. *eROSITA*?

Planned time-domain programs in the next decade will discover hundreds to thousands of new TDEs and will enable the detailed study of TDEs and their host galaxies with significantly greater statistical power.

Acknowledgements We thank the referees for their detailed feedback and helpful suggestions, which have improved this review.

The authors thank ISSI for their support and hospitality and the review organizers for their leadership in coordinating this set of reviews.

K.D.F. is supported by Hubble Fellowship grant HST-HF2-51391.001-A, provided by NASA through a grant from the Space Telescope Science Institute (STScI), which is operated by the Association of Universities for Research in Astronomy, Inc., under NASA contract NAS5-26555. A.I.Z. acknowledges support from NASA through STScI grant HST-GO-14717.001-A. T.W. is funded in part by European Research Council grant 320360 and by European Commission grant 730980. O.G. is supported by an NSF Astronomy and Astrophysics Fellowship under award AST-1602595.

Funding for SDSS-III has been provided by the Alfred P. Sloan Foundation, the Participating Institutions, the National Science Foundation, and the U.S. Department of Energy Office of Science. The SDSS-III website is <http://www.sdss3.org/>. SDSS-III is managed by the Astrophysical Research Consortium for the Participating Institutions of the SDSS-III Collaboration, including the University of Arizona, the Brazilian Participation Group, Brookhaven National Laboratory, University of Cambridge, Carnegie Mellon University, University of Florida, the French Participation Group, the German Participation Group, Harvard University, the Instituto de Astrofísica de Canarias, the Michigan State/Notre Dame/JINA Participation Group, Johns Hopkins University, Lawrence Berkeley National Laboratory, Max Planck Institute for Astrophysics, Max Planck Institute for Extraterrestrial Physics, New Mexico State University, New York University, the Ohio State University, Pennsylvania State University, University of Portsmouth, Princeton University, the Spanish Participation Group, University of Tokyo, University of Utah, Vanderbilt University, University of Virginia, University of Washington, and Yale University.

This publication makes use of data products from the Wide-field Infrared Survey Explorer (Wright et al. 2010), which is a joint project of the University of California, Los Angeles, and the Jet Propulsion Laboratory/California Institute of Technology, funded by the National Aeronautics and Space Administration.

This work made use of the IPython package (Pérez and Granger 2007). This research made use of SciPy (Jones et al. 2001). This research made use of Astropy, a community-developed core Python package for Astronomy (Astropy Collaboration et al. 2013). This research made use of NumPy (Van Der Walt et al. 2011).

References

- G.O. Abell, J. Corwin Harold G., R.P. Olowin, A Catalog of Rich Clusters of Galaxies. The Astrophysical Journal Supplement Series **70**, 1 (1989). doi:10.1086/191333
- R.G. Abraham, S. van den Bergh, K. Glazebrook, R.S. Ellis, B.X. Santiago, P. Surma, R.E. Griffiths, The Morphologies of Distant Galaxies. II. Classifications from the Hubble Space Telescope Medium Deep Survey. The Astrophysical Journal Supplement Series **107**, 1 (1996). doi:10.1086/192352
- K. Alatalo, S.L. Cales, J.A. Rich, P.N. Appleton, L.J. Kewley, M. Lacy, L. Lanz, A.M. Medling, K. Nyland, Shocked Poststarburst Galaxy Survey I: Candidate Poststarburst Galaxies with Emission Line Ratios Consistent with Shocks. The Astro-

- physical Journal Supplement Series **224**, 38 (2016). doi:10.3847/0067-0049/224/2/38. <http://arxiv.org/abs/1601.05085> <http://dx.doi.org/10.3847/0067-0049/224/2/38>
- I. Arcavi, J. Burke, K.D. French, A. Zabludoff, D. Hiramatsu, C. McCully, D.A. Howell, G. Hosseinzadeh, S. Valenti, FLOYDS Classification of AT 2018dyk/ZTF18aaajupnt as a Possible Tidal Disruption Event. *The Astronomer's Telegram* **11953**, 1 (2018)
- I. Arcavi, A. Gal-Yam, M. Sullivan, Y.-C. Pan, S.B. Cenko, A. Hosh, E.O. Ofek, A. De Cia, L. Yan, C.-W. Yang, D.A. Howell, D. Tal, S.R. Kulkarni, S.P. Tendulkar, S. Tang, D. Xu, A. Sternberg, J.G. Cohen, J.S. Bloom, P.E. Nugent, M.M. Kasliwal, D.A. Perley, R.M. Quimby, A.A. Miller, C.A. Theissen, R.R. Laher, A Continuum of H- to He-Rich Tidal Disruption Candidates with a Preference for E+A Galaxies. *The Astrophysical Journal* **793**(1), 38 (2014). doi:10.1088/0004-637X/793/1/38. <http://adsabs.harvard.edu/abs/2014ApJ...793...38A>
- Astropy Collaboration, T.P. Robitaille, E.J. Tollerud, P. Greenfield, M. Droettboom, E. Bray, T. Aldcroft, M. Davis, A. Ginsburg, A.M. Price-Whelan, W.E. Kerzendorf, A. Conley, N. Crighton, K. Barbary, D. Muna, H. Ferguson, F. Grollier, M.M. Parikh, P.H. Nair, H.M. Unther, C. Deil, J. Woillez, S. Conseil, R. Kramer, J.E.H. Turner, L. Singer, R. Fox, B.A. Weaver, V. Zabalza, Z.I. Edwards, K. Azalee Bostroem, D.J. Burke, A.R. Casey, S.M. Crawford, N. Dencheva, J. Ely, T. Jenness, K. Labrie, P.L. Lim, F. Pierfederici, A. Pontzen, A. Ptak, B. Refsdal, M. Servillat, O. Streicher, Astropy: A community Python package for astronomy. *Astron. & Astrophys.* **558**, 33 (2013). doi:10.1051/0004-6361/201322068
- K. Auchettl, J. Guillochon, E. Ramirez-Ruiz, New physical insights about Tidal Disruption Events from a comprehensive observational inventory at X-ray wavelengths. *The Astrophysical Journal* **838**(2), 149 (2017a). doi:10.3847/1538-4357/aa633b. <http://arxiv.org/abs/1611.02291> <http://dx.doi.org/10.3847/1538-4357/aa633b>
- K. Auchettl, E. Ramirez-Ruiz, J. Guillochon, Comparison of the X-ray emission from Tidal Disruption Events with those of Active Galactic Nuclei (2017b). <http://arxiv.org/abs/1703.06141>
- I.K. Baldry, S.P. Driver, J. Loveday, E.N. Taylor, L.S. Kelvin, J. Liske, P. Norberg, A.S.G. Robotham, S. Brough, A.M. Hopkins, S.P. Bamford, J.A. Peacock, J. Bland-Hawthorn, C.J. Conselice, S.M. Croom, D.H. Jones, H.R. Parkinson, C.C. Popescu, M. Prescott, R.G. Sharp, R.J. Tuffs, Galaxy And Mass Assembly (GAMA): the galaxy stellar mass function at $z < 0.06$. *Mon. Not. R. Astron. Soc.* **421**, 621–634 (2012). doi:10.1111/j.1365-2966.2012.20340.x
- J.A. Baldwin, M.M. Phillips, R. Terlevich, Classification parameters for the emission-line spectra of extragalactic objects. *Publications of the Astronomical Society of the Pacific* **93**, 5 (1981). doi:10.1086/130766. <http://adsabs.harvard.edu/abs/1981PASP...93...5B>
- E.C. Bellm, S.R. Kulkarni, M.J. Graham, R. Dekany, R.M. Smith, R. Riddle, F.J. Masci, G. Helou, T.A. Prince, S.M. Adams, C. Barbarino, T. Barlow, J. Bauer, R. Beck, J. Belicki, R. Biswas, N. Blagorodnova, D. Bodewits, B. Bolin, V. Brinnel, T. Brooke, B. Bue, M. Bulla, R. Burruss, S.B. Cenko, C.-K. Chang, A. Connolly, M. Coughlin, J. Cromer, V. Cunningham, K. De, A. Delacroix, V. Desai, D.A. Duev, G. Eadie, T.L. Farnham, M. Feeney, U. Feindt, D. Flynn, A. Franckowiak, S. Frederick, C. Fremling, A. Gal-Yam, S. Gezari, M. Giomi, D.A. Goldstein, V.Z. Golkhou, A. Goobar, S. Groom, E. Hachopian, D. Hale, J. Henning, A.Y.Q. Ho, D. Hover, J. Howell, T. Hung, D. Huppenkothen, D. Imel, W.-H. Ip, Ž. Ivezić, E. Jackson, L. Jones, M. Juric, M.M. Kasliwal, S. Kaspi, S. Kaye, M.S.P. Kelley, M. Kowalski, E. Kramer, T. Kupfer, W. Landry, R.R. Laher, C.-D. Lee, H.W. Lin, Z.-Y. Lin, R. Lunnan, M. Giomi, A. Mahabal, P. Mao, A.A. Miller, S. Monkevitz, P. Murphy, C.-C. Ngeow, J. Nordin, P. Nugent, E. Ofek, M.T. Patterson, B. Penprase, M. Porter, L. Rauch, U. Rebbapragada, D. Reiley, M. Rigault, H. Rodriguez, J. van Roestel, B. Rusholme, J. van Santen, S. Schulze, D.L. Shupe, L.P. Singer, M.T. Soumagnac, R. Stein, J. Surace, J. Sollerman, P. Szkody, F. Taddia, S. Terek, A. Van Sistine, S. van Velzen, W.T. Vestrand, R. Walters, C. Ward, Q.-Z. Ye, P.-C. Yu, L. Yan, J. Zolkower, The Zwicky Transient Facility: System Overview, Performance, and First Results. *Publ. Astron. Soc. Pac.* **131**(995), 018002 (2019). doi:10.1088/1538-3873/aaecbe
- N. Blagorodnova, S. Gezari, T. Hung, S.R. Kulkarni, S.B. Cenko, D.R. Pasham, L. Yan, I. Arcavi, S. Ben-Ami, B.D. Bue, T. Cantwell, Y. Cao, A.J. Castro-Tirado, R. Fender, C. Fremling, A. Gal-Yam, A.Y.Q. Ho, A. Hosh, G. Hosseinzadeh, M.M. Kasliwal,

- A.K.H.H. Kong, R.R. Laher, G. Leloudas, R. Lunnan, F.J. Masci, K. Mooley, J.D. Neill, P. Nugent, M. Powell, A.F. Valeev, P.M. Vreeswijk, R. Walters, P. Wozniak, iPTF16fnl: a faint and fast tidal disruption event in an E+A galaxy. *The Astrophysical Journal* **844**(46) (2017). doi:10.3847/1538-4357/aa7579. <http://arxiv.org/abs/1703.00965><http://dx.doi.org/10.3847/1538-4357/aa7579>
- N. Blagorodnova, S.B.C.S.R. Kulkarni, I. Arcavi, J.S. Bloom, G. Duggan, A.V. Filippenko, C. Fremling, A. Horeh, G. Hosseinzadeh, E. Karamahmetoglu, A. Levan, F.J. Masci, P.E. Nugent, D.R. Pasham, S. Veilleux, R. Walters, L. Yan, W. Zheng, The Broad Absorption Line Tidal Disruption Event iPTF15af: Optical and Ultraviolet Evolution. arXiv e-prints, 1809–07446 (2018)
- N. Blagorodnova, S.B. Cenko, S.R. Kulkarni, I. Arcavi, J.S. Bloom, G. Duggan, A.V. Filippenko, C. Fremling, A. Horeh, G. Hosseinzadeh, E. Karamahmetoglu, A. Levan, F.J. Masci, P.E. Nugent, D.R. Pasham, S. Veilleux, R. Walters, L. Yan, W. Zheng, The Broad Absorption Line Tidal Disruption Event iPTF15af: Optical and Ultraviolet Evolution. *Astrophys. J.* **873**(1), 92 (2019). doi:10.3847/1538-4357/ab04b0
- P.K. Blanchard, M. Nicholl, E. Berger, J. Guillochon, R. Margutti, R. Chornock, K.D. Alexander, J. Leja, M.R. Drout, PS16dtm: A Tidal Disruption Event in a Narrow-line Seyfert 1 Galaxy. *The Astrophysical Journal* **843**(2), 106 (2017). doi:10.3847/1538-4357/aa77f7. <http://arxiv.org/abs/1703.07816> <http://dx.doi.org/10.3847/1538-4357/aa77f7>
- M.R. Blanton, S. Roweis, *kcorrect: Calculate K-corrections between observed and desired bandpasses*, 2017
- J. Brinchmann, S. Charlot, S.D.M. White, C. Tremonti, G. Kauffmann, T. Heckman, J. Brinkmann, The physical properties of star-forming galaxies in the low-redshift Universe. *Mon. Not. R. Astron. Soc.* **351**, 1151–1179 (2004). doi:10.1111/j.1365-2966.2004.07881.x
- J.S. Brown, T.W.-S. Holoien, K. Auchettl, K.Z. Stanek, C.S. Kochanek, B.J. Shappee, J.L. Prieto, D. Grupe, The Long Term Evolution of ASASSN-14li. *Monthly Notices of the Royal Astronomical Society* **446**(4), 4904–4916 (2016). <http://arxiv.org/abs/1609.04403>
- J.S. Brown, C.S. Kochanek, T.W.-S. Holoien, K.Z. Stanek, K. Auchettl, B.J. Shappee, J.L. Prieto, N. Morrell, E. Falco, J. Strader, L. Chomiuk, R. Post, S. Villanueva, S. Mathur, S. Dong, P. Chen, S. Bose, The Ultraviolet Spectroscopic Evolution of the Low-Luminosity Tidal Disruption Event iPTF16fnl (2017). <http://arxiv.org/abs/1704.02321>
- K. Bundy, M.A. Bershad, D.R. Law, R. Yan, N. Drory, N. MacDonald, D.A. Wake, B. Cherinka, J.R. Sánchez-Gallego, A.-M. Weijmans, D. Thomas, C. Tremonti, K. Masters, L. Coccatto, A.M. Diamond-Stanic, A. Aragón-Salamanca, V. Avila-Reese, C. Badenes, J. Falcón-Barroso, F. Belfiore, D. Bizyaev, G.A. Blanc, J. Bland-Hawthorn, M.R. Blanton, J.R. Brownstein, N. Byler, M. Cappellari, C. Conroy, A.A. Dutton, E. Emsellem, J. Etherington, P.M. Frinchaboy, H. Fu, J.E. Gunn, P. Harding, E.J. Johnston, G. Kauffmann, K. Kinemuchi, M.A. Klaene, J.H. Knapen, A. Leauthaud, C. Li, L. Lin, R. Maiolino, V. Malanushenko, E. Malanushenko, S. Mao, C. Maraston, R.M. McDermid, M.R. Merrifield, R.C. Nichol, D. Oravetz, K. Pan, J.K. Parejko, S.F. Sanchez, D. Schlegel, A. Simmons, O. Steele, M. Steinmetz, K. Thanjavur, B.A. Thompson, J.L. Tinker, R.C.E. van den Bosch, K.B. Westfall, D. Wilkinson, S. Wright, T. Xiao, K. Zhang, Overview of the SDSS-IV MaNGA Survey: Mapping nearby Galaxies at Apache Point Observatory. *Astrophys. J.* **798**, 7 (2015). doi:10.1088/0004-637X/798/1/7
- M. Cappellari, R. Bacon, M. Bureau, M.C. Damen, R.L. Davies, P.T. de Zeeuw, E. Emsellem, J. Falcón-Barroso, D. Krajnović, H. Kuntschner, R.M. McDermid, R.F. Peletier, M. Sarzi, R.C.E. van den Bosch, G. van de Ven, The SAURON project - IV. The mass-to-light ratio, the virial mass estimator and the Fundamental Plane of elliptical and lenticular galaxies. *Mon. Not. R. Astron. Soc.* **366**, 1126–1150 (2006). doi:10.1111/j.1365-2966.2005.09981.x
- S.B. Cenko, J.S. Bloom, S.R. Kulkarni, L.E. Strubbe, A.A. Miller, N.R. Butler, R.M. Quimby, A. Gal-Yam, E.O. Ofek, E. Quataert, L. Bildsten, D. Poznanski, D.A. Perley, A.N. Morgan, A.V. Filippenko, D.A. Frail, I. Arcavi, S. Ben-Ami, A. Cucchiara, C.D. Fassnacht, Y. Green, I.M. Hook, D.A. Howell, D.J. Lagattuta, N.M. Law, M.M. Kasliwal, P.E. Nugent, J.M. Silverman, M. Sullivan, S.P. Tendulkar, O. Yaron, PTF10iya:

- a short-lived, luminous flare from the nuclear region of a star-forming galaxy. *Monthly Notices of the Royal Astronomical Society* **420**(3), 2684–2699 (2012). doi:10.1111/j.1365-2966.2011.20240.x. <http://adsabs.harvard.edu/abs/2012MNRAS.420.2684C>
- S.B. Cenko, A. Cucchiara, N. Roth, S. Veilleux, J.X. Prochaska, L. Yan, J. Guillochon, W.P. Maksym, I. Arcavi, N.R. Butler, A.V. Filippenko, A.S. Fruchter, S. Gezari, D. Kasen, A.J. Levan, J.M. Miller, D.R. Pasham, E. Ramirez-Ruiz, L.E. Strubbe, N.R. Tanvir, F. Tombesi, An Ultraviolet Spectrum of the Tidal Disruption Flare ASASSN-14li. arXiv:1601.03331, 8 (2016). <http://arxiv.org/abs/1601.03331>
- K.C. Chambers, E.A. Magnier, N. Metcalfe, H.A. Flewelling, M.E. Huber, C.Z. Waters, L. Denneau, P.W. Draper, D. Farrow, D.P. Finkbeiner, C. Holmberg, J. Koppenhoefer, P.A. Price, R.P. Saglia, E.F. Schlafly, S.J. Smartt, W. Sweeney, R.J. Wainscoat, W.S. Burgett, T. Grav, J.N. Heasley, K.W. Hodapp, R. Jedicke, N. Kaiser, R.-P. Kudritzki, G.A. Luppino, R.H. Lupton, D.G. Monet, J.S. Morgan, P.M. Onaka, C.W. Stubbs, J.L. Tonry, E. Banados, E.F. Bell, R. Bender, E.J. Bernard, M.T. Botticella, S. Casertano, S. Chastel, W.-P. Chen, X. Chen, S. Cole, N. Deacon, C. Frenk, A. Fitzsimmons, S. Gezari, C. Goessl, T. Goggia, B. Goldman, E.K. Grebel, N.C. Hambly, G. Hasinger, A.F. Heavens, T.M. Heckman, R. Henderson, T. Henning, M. Holman, U. Hopp, W.-H. Ip, S. Isani, C.D. Keyes, A. Koekemoer, R. Kotak, K.S. Long, J.R. Lucey, M. Liu, N.F. Martin, B. McLean, E. Morganson, D.N.A. Murphy, M.A. Nieto-Santisteban, P. Norberg, J.A. Peacock, E.A. Pier, M. Postman, N. Primak, C. Rae, A. Rest, A. Riess, A. Riffeser, H.W. Rix, S. Roser, E. Schilbach, A.S.B. Schultz, D. Scolnic, A. Szalay, S. Seitz, B. Shiao, E. Small, K.W. Smith, D. Soderblom, A.N. Taylor, A.R. Thakar, J. Thiel, D. Thilker, Y. Urata, J. Valenti, F. Walter, S.P. Watters, S. Werner, R. White, W.M. Wood-Vasey, R. Wyse, The Pan-STARRS1 Surveys. arXiv:1612.05560 (2016). <http://arxiv.org/abs/1612.05560>
- B. Cherinka, B.H. Andrews, J. Sánchez-Gallego, J. Brownstein, M. Argudo-Fernández, M. Blanton, K. Bundy, A. Jones, K. Masters, D.R. Law, K. Rowlands, A.-M. Weijmans, K. Westfall, R. Yan, Marvin: A Toolkit for Streamlined Access and Visualization of the SDSS-IV MaNGA Data Set. arXiv e-prints (2018)
- R. Chornock, E. Berger, S. Gezari, B.A. Zauderer, A. Rest, L. Chomiuk, A. Kamble, A.M. Soderberg, I. Czekala, J. Dittmann, M. Drout, R.J. Foley, W. Fong, M.E. Huber, R.P. Kirshner, A. Lawrence, R. Lunnan, G.H. Marion, G. Narayan, A.G. Riess, K.C. Roth, N.E. Sanders, D. Scolnic, S.J. Smartt, K. Smith, C.W. Stubbs, J.L. Tonry, W.S. Burgett, K.C. Chambers, H. Flewelling, K.W. Hodapp, N. Kaiser, E.A. Magnier, D.C. Martin, J.D. Neill, P.A. Price, R. Wainscoat, THE ULTRAVIOLET-BRIGHT, SLOWLY DECLINING TRANSIENT PS1-11af AS A PARTIAL TIDAL DISRUPTION EVENT. *The Astrophysical Journal* **780**(1), 44 (2014). doi:10.1088/0004-637X/780/1/44. <http://adsabs.harvard.edu/abs/2014ApJ...780...44C>
- C.J. Conselice, S.C. Chapman, R.A. Windhorst, Evidence for a Major Merger Origin of High-Redshift Submillimeter Galaxies. *Astrophys. J.* **596**, 5–8 (2003). doi:10.1086/379109
- E.R. Coughlin, M.C. Begelman, Hyperaccretion during Tidal Disruption Events: Weakly Bound Debris Envelopes and Jets. *Astrophys. J.* **781**(2), 82 (2014). doi:10.1088/0004-637X/781/2/82
- L. Dai, J.C. McKinney, M.C. Miller, Soft X-Ray Temperature Tidal Disruption Events from Stars on Deep Plunging Orbits. *Astrophys. J.* **812**(2), 39 (2015). doi:10.1088/2041-8205/812/2/L39
- L. Dai, J.C. McKinney, N. Roth, E. Ramirez-Ruiz, M.C. Miller, A unified model for tidal disruption events (2018). <http://arxiv.org/abs/1803.03265>
- S. Dong, S. Bose, P. Chen, T.G. Brink, T. de Jaeger, A.V. Filippenko, W. Zheng, Spectroscopic Classification of ASASSN-18zj with the Lick 3-m Shane Telescope. *The Astronomer’s Telegram* **12198**, 1 (2018)
- D. Elbaz, M. Dickinson, H.S. Hwang, T. Diaz-Santos, G. Magdis, B. Magnelli, D.L. Borgne, F. Galliano, M. Pannella, P. Chianal, L. Armus, V. Charmandaris, E. Daddi, H. Aussel, P. Popesso, J. Kartaltepe, B. Altieri, I. Valtchanov, D. Coia, H. Dannerbauer, K. Dasyra, R. Leiton, J. Mazzarella, V. Buat, D. Burgarella, R.-R. Chary, R. Gilli, R.J. Ivison, S. Juneau, E. LeFloc’h, D. Lutz, G.E. Morrison, J. Mullaney, E. Murphy, A. Pope, D. Scott, D. Alexander, M. Brodwin, D. Calzetti, C. Cesarsky, S. Charlot, H. Dole, P. Eisenhardt, H.C. Ferguson, N. Foerster-Schreiber, D. Frayer, M. Giavalisco, M. Huynh,

- A.M. Koekemoer, C. Papovich, N. Reddy, C. Surace, H. Teplitz, M.S. Yun, G. Wilson, GOODS-Herschel: an infrared main sequence for star-forming galaxies. *Astronomy & Astrophysics* **533**, 119 (2011). <http://arxiv.org/abs/1105.2537>
- P. Esquej, R.D. Saxton, M.J. Freyberg, A.M. Read, B. Altieri, M. Sanchez-Portal, G. Hasinger, Candidate tidal disruption events from the XMM-Newton slew survey. *Astronomy and Astrophysics* **462**(3), 49–52 (2007). doi:10.1051/0004-6361:20066072. <http://adsabs.harvard.edu/abs/2007A%2526A...462L..49E>
- L. Ferrarese, H. Ford, Supermassive Black Holes in Galactic Nuclei: Past, Present and Future Research. *Space Sci. Rev.* **116**, 523–624 (2005). doi:10.1007/s11214-005-3947-6
- L. Ferrarese, D. Merritt, A Fundamental Relation between Supermassive Black Holes and Their Host Galaxies. *Astrophys. J.* **539**, 9–12 (2000). doi:10.1086/312838
- S. Frederick, S. Gezari, M.J. Graham, S.B. Cenko, S. van Velzen, D. Stern, N. Blagorodnova, S.R. Kulkarni, L. Yan, K. De, U.C. Fremling, T. Hung, E. Kara, D.L. Shupe, C. Ward, E.C. Bellm, R. Dekany, D.A. Duev, U. Feindt, M. Giomi, T. Kupfer, R.R. Laher, F.J. Masci, A.A. Miller, C.-C. Ngeow, M.T. Patterson, M. Porter, B. Rusholme, J. Sollerman, R. Walters, A New Class of Changing-Look LINERs. arXiv e-prints, 1904–10973 (2019)
- K.D. French, A.I. Zabludoff, Identifying Tidal Disruption Events via Prior Photometric Selection of Their Preferred Hosts. *Astrophys. J.* **868**, 99 (2018). doi:10.3847/1538-4357/aaea64
- K.D. French, I. Arcavi, A. Zabludoff, Tidal Disruption Events Prefer Unusual Host Galaxies. *ApJ* **818**, 21 (2016). doi:10.3847/2041-8205/818/1/L21. <http://arxiv.org/abs/1601.04705> <http://dx.doi.org/10.3847/2041-8205/818/1/L21>
- K.D. French, I. Arcavi, A. Zabludoff, The Post-starburst Evolution of Tidal Disruption Event Host Galaxies. *Astrophys. J.* **835**, 176 (2017). doi:10.3847/1538-4357/835/2/176
- K.D. French, Y. Yang, A.I. Zabludoff, C.A. Tremonti, Clocking the Evolution of Post-starburst Galaxies: Methods and First Results. *Astrophys. J.* **862**, 2 (2018). doi:10.3847/1538-4357/aacb2d
- K. Gebhardt, R. Bender, G. Bower, A. Dressler, S.M. Faber, A.V. Filippenko, R. Green, C. Grillmair, L.C. Ho, J. Kormendy, T.R. Lauer, J. Magorrian, J. Pinkney, D. Richstone, S. Tremaine, A Relationship between Nuclear Black Hole Mass and Galaxy Velocity Dispersion. *Astrophys. J. Lett.* **539**, 13–16 (2000). doi:10.1086/312840
- S. Gezari, S.B. Cenko, I. Arcavi, X-ray Brightening and UV Fading of Tidal Disruption Event ASASSN-15oi (2017). <http://arxiv.org/abs/1712.03968>
- S. Gezari, S. Basa, D.C. Martin, G. Bazin, K. Forster, B. Milliard, J.P. Halpern, P.G. Friedman, P. Morrissey, S.G. Neff, D. Schiminovich, M. Seibert, T. Small, T.K. Wyder, UV/Optical Detections of Candidate Tidal Disruption Events by GALEX and CFHTLS. *Astrophys. J.* **676**(2), 944–969 (2008). doi:10.1086/529008
- S. Gezari, S. van Velzen, S.B. Cenko, M. Graham, N. Blagorodnova, T. Hung, L. Yan, S. Kulkarni, ZTF Discovery of a Tidal Disruption Event at $z=0.051$. The Astronomer’s Telegram **12035**, 1 (2018)
- S. Gezari, T. Heckman, S.B. Cenko, M. Eracleous, K. Forster, T.S. Gonçalves, D.C. Martin, P. Morrissey, S.G. Neff, M. Seibert, D. Schiminovich, T.K. Wyder, LUMINOUS THERMAL FLARES FROM QUIESCENT SUPERMASSIVE BLACK HOLES. The Astrophysical Journal **698**(2), 1367–1379 (2009). doi:10.1088/0004-637X/698/2/1367. <http://adsabs.harvard.edu/abs/2009ApJ...698.1367G>
- O. Graur, K.D. French, H.J. Zahid, J. Guillochon, K.S. Mandel, K. Auchettl, A.I. Zabludoff, A Dependence of the Tidal Disruption Event Rate on Global Stellar Surface Mass Density and Stellar Velocity Dispersion. *Astrophys. J.* **853**, 39 (2018). doi:10.3847/1538-4357/aaa3fd
- J. Greiner, R. Schwarz, S. Zharikov, M. Orto, RX J1420.4+5334 - another tidal disruption event? *Astron. & Astrophys.* **362**, 25–28 (2000)
- D. Grupe, H.-C. Thomas, K.M. Leighly, RX J1624.9+7554: a new X-ray transient AGN. *Astron. & Astrophys.* **350**, 31–34 (1999)
- J. Guillochon, E. Ramirez-Ruiz, A Dark Year for Tidal Disruption Events. *Astrophys. J.* **809**, 166 (2015). doi:10.1088/0004-637X/809/2/166
- K. Gültekin, D.O. Richstone, K. Gebhardt, T.R. Lauer, S. Tremaine, M.C. Aller, R. Bender, A. Dressler, S.M. Faber, A.V. Filippenko, R. Green, L.C. Ho, J. Kormendy, J. Magorrian, J. Pinkney, C. Siopis, The $M-\sigma$ and $M-L$ Relations in Galactic Bulges,

- and Determinations of Their Intrinsic Scatter. *Astrophys. J.* **698**(1), 198–221 (2009). doi:10.1088/0004-637X/698/1/198
- J.G. Hills, Possible power source of Seyfert galaxies and QSOs. *Nature* **254**(5498), 295–298 (1975). doi:10.1038/254295a0. <http://adsabs.harvard.edu/abs/1975Natur.254..295H>
- L.C. Ho, A.V. Filippenko, W.L. Sargent, A Search for “Dwarf” Seyfert Nuclei. II. an Optical Spectral Atlas of the Nuclei of Nearby Galaxies. *The Astrophysical Journal Supplement Series* **98**, 477 (1995). doi:10.1086/192170
- T.W.-S. Holoien, C.S. Kochanek, J.L. Prieto, D. Grupe, P. Chen, D. Godoy-Rivera, K.Z. Stanek, B.J. Shappee, S. Dong, J.S. Brown, U. Basu, J.F. Beacom, D. Bersier, J. Brimacombe, E.K. Carlson, E. Falco, E. Johnston, B.F. Madore, G. Pojmanski, M. Seibert, ASASSN-15oi: A Rapidly Evolving, Luminous Tidal Disruption Event at 216 Mpc. arXiv:1602.01088, 17 (2016a). <http://arxiv.org/abs/1602.01088>
- T.W.-S. Holoien, C.S. Kochanek, J.L. Prieto, K.Z. Stanek, S. Dong, B.J. Shappee, D. Grupe, J.S. Brown, U. Basu, J.F. Beacom, D. Bersier, J. Brimacombe, A.B. Danilet, E. Falco, Z. Guo, J. Jose, G.J. Herczeg, F. Long, G. Pojmanski, G.V. Simonian, D.M. Szczygieł, T.A. Thompson, J.R. Thorstensen, R.M. Wagner, P.R. Woźniak, Six months of multiwavelength follow-up of the tidal disruption candidate ASASSN-14li and implied TDE rates from ASAS-SN. *Monthly Notices of the Royal Astronomical Society* **455**(3), 2918–2935 (2016b). doi:10.1093/mnras/stv2486. <http://adsabs.harvard.edu/abs/2016MNRAS.455.2918H>
- T.W.-S. Holoien, M.E. Huber, B.J. Shappee, M. Eracleous, K. Auchettl, J.S. Brown, M.A. Tucker, K.C. Chambers, C.S. Kochanek, K.Z. Stanek, A. Rest, D. Bersier, R.S. Post, G. Aldering, K.A. Ponder, J.D. Simon, E. Kankare, D. Dong, G. Hallinan, J. Bulger, T.B. Lowe, E.A. Magnier, A.S.B. Schultz, C.Z. Waters, M. Willman, D. Wright, D.R. Young, S. Dong, J.L. Prieto, T.A. Thompson, L. Denneau, H. Flewelling, A.N. Heinze, S.J. Smartt, K.W. Smith, B. Stalder, J.L. Tonry, H. Weiland, PS18kh: A New Tidal Disruption Event with a Non-Axisymmetric Accretion Disk. arXiv e-prints, 1808–02890 (2018)
- S.A. Hughes, R.D. Blandford, Black Hole Mass and Spin Coevolution by Mergers. *Astrophys. J.* **585**, 101–104 (2003). doi:10.1086/375495
- T. Hung, S. Gezari, S.B. Cenko, S. van Velzen, N. Blagorodnova, L. Yan, S.R. Kulkarni, R. Lunnan, T. Kupfer, G. Leloudas, A.K.H. Kong, P.E. Nugent, C. Fremling, R.R. Laher, F.J. Masci, Y. Cao, R. Roy, T. Petrushevska, Sifting for Sapphires: Systematic Selection of Tidal Disruption Events in iPTF. *The Astrophysical Journal Supplement Series* **238**, 15 (2018). doi:10.3847/1538-4365/aad8b1
- F. Jansen, D. Lumb, B. Altieri, J. Clavel, M. Ehle, C. Erd, C. Gabriel, M. Guainazzi, P. Gondoin, R. Much, R. Munoz, M. Santos, N. Scharrel, D. Texier, G. Vacanti, XMM-Newton observatory. I. The spacecraft and operations. *Astron. & Astrophys.* **365**, 1–6 (2001). doi:10.1051/0004-6361:20000036
- E. Jones, T. Oliphant, P. Peterson, Others, *SciPy: Open source scientific tools for Python*, 2001. <http://www.scipy.org/>
- P.G. Jonker, N.C. Stone, A. Generozov, S. van Velzen, B. Metzger, Implications from Late-Time X-ray Detections of Optically Selected Tidal Disruption Events: State Changes, Unification, and Detection Rates. arXiv e-prints, 1906–12236 (2019)
- E. Kankare, R. Kotak, S. Mattila, P. Lundqvist, M.J. Ward, M. Fraser, A. Lawrence, S.J. Smartt, W.P.S. Meikle, A. Bruce, J. Harmanen, S.J. Hutton, C. Inserra, T. Kangas, A. Pastorello, T. Reynolds, C. Romero-Cañizales, K.W. Smith, S. Valenti, K.C. Chambers, K.W. Hodapp, M.E. Huber, N. Kaiser, R.-P. Kudritzki, E.A. Magnier, J.L. Tonry, R.J. Wainscoat, C. Waters, A population of highly energetic transient events in the centres of active galaxies. *Nature Astronomy* **1**, 865–871 (2017). doi:10.1038/s41550-017-0290-2
- G. Kauffmann, T.M. Heckman, S.D.M. White, S. Charlot, C. Tremonti, J. Brinchmann, G. Bruzual, E.W. Peng, M. Seibert, M. Bernardi, M. Blanton, J. Brinkmann, F. Castander, I. Csábai, M. Fukugita, Z. Ivezic, J.A. Munn, R.C. Nichol, N. Padmanabhan, A.R. Thakar, D.H. Weinberg, D. York, Stellar masses and star formation histories for 10^5 galaxies from the Sloan Digital Sky Survey. *Mon. Not. R. Astron. Soc.* **341**, 33–53 (2003). doi:10.1046/j.1365-8711.2003.06291.x
- G. Kauffmann, T.M. Heckman, C. Tremonti, J. Brinchmann, S. Charlot, S.D.M. White, S.E. Ridgway, J. Brinkmann, M. Fukugita, P.B. Hall, Ž. Ivezić, G.T. Richards, D.P.

- Schneider, The host galaxies of active galactic nuclei. *Monthly Notices of the Royal Astronomical Society* **346**(4), 1055–1077 (2003). doi:10.1111/j.1365-2966.2003.07154.x. <http://adsabs.harvard.edu/abs/2003MNRAS.346.1055K>
- W.C. Keel, C.J. Lintott, W.P. Maksym, V.N. Bennert, S.D. Chojnowski, A. Moiseev, A. Smirnova, K. Schawinski, L.F. Sartori, C.M. Urry, A. Pancoast, M. Schirmer, B. Scott, C. Showley, K. Flatland, Fading AGN Candidates: AGN Histories and Outflow Signatures. *Astrophys. J.* **835**(2), 256 (2017). doi:10.3847/1538-4357/835/2/256
- G.F. Kennedy, Y. Meiron, B. Shukirgaliyev, T. Panamarev, P. Berczik, A. Just, R. Spurzem, Star-disc interaction in galactic nuclei: orbits and rates of accreted stars. *Monthly Notices of the Royal Astronomical Society* **460**, 240–255 (2016). doi:10.1093/mnras/stw908. <http://arxiv.org/abs/1604.05309> <http://dx.doi.org/10.1093/mnras/stw908>
- R.C. Kennicutt, N.J. Evans, Star Formation in the Milky Way and Nearby Galaxies. *Annual Review of Astronomy and Astrophysics* **50**, 531–608 (2012). doi:10.1146/annurev-astro-081811-125610
- M. Kesden, Tidal-disruption rate of stars by spinning supermassive black holes. *Phys. Rev. D* **85**(2), 024037 (2012). doi:10.1103/PhysRevD.85.024037
- L.J. Kewley, M.A. Dopita, R.S. Sutherland, C.A. Heisler, J. Trevena, Theoretical Modeling of Starburst Galaxies. *The Astrophysical Journal* **556**(1), 121–140 (2001). doi:10.1086/321545. <http://iopscience.iop.org/0004-637X/556/1/121/fulltext/>
- I. Khabibullin, S. Sazonov, R. Sunyaev, SRG/eROSITA prospects for the detection of stellar tidal disruption flares. *Mon. Not. R. Astron. Soc.* **437**(1), 327–337 (2014). doi:10.1093/mnras/stt1889
- C.S. Kochanek, Tidal Disruption Event (TDE) Demographics. *Monthly Notices of the Royal Astronomical Society* **461**, 371–384 (2016). doi:10.1093/mnras/stw1290. <http://arxiv.org/abs/1601.06787> <http://dx.doi.org/10.1093/mnras/stw1290>
- S. Komossa, H. Zhou, A. Rau, M. Dopita, A. Gal-Yam, J. Greiner, J. Zuther, M. Salvato, D. Xu, H. Lu, R. Saxton, M. Ajello, NTT, Spitzer, and Chandra Spectroscopy of SDSSJ095209.56+214313.3: The Most Luminous Coronal-line Supernova Ever Observed, or a Stellar Tidal Disruption Event? *Astrophys. J.* **701**, 105–121 (2009). doi:10.1088/0004-637X/701/1/105
- S. Komossa, J. Greiner, Discovery of a giant and luminous X-ray outburst from the optically inactive galaxy pair RX J1242.6-1119. *Astron. & Astrophys.* **349**, 45–48 (1999)
- S. Komossa, D. Merritt, Tidal Disruption Flares from Recoiling Supermassive Black Holes. *The Astrophysical Journal* **683**(1), 21–24 (2008). doi:10.1086/591420. <http://adsabs.harvard.edu/abs/2008ApJ...683L..21K>
- J. Kormendy, D. Richstone, Inward Bound—The Search For Supermassive Black Holes In Galactic Nuclei. *ARA&A* **33**, 581 (1995). doi:10.1146/annurev.aa.33.090195.003053
- J. Kormendy, L.C. Ho, Coevolution (Or Not) of Supermassive Black Holes and Host Galaxies. *ARA&A* **51**(1), 511–653 (2013). doi:10.1146/annurev-astro-082708-101811
- T.R. Lauer, K. Gebhardt, S.M. Faber, D. Richstone, S. Tremaine, J. Kormendy, M.C. Aller, R. Bender, A. Dressler, A.V. Filippenko, R. Green, L.C. Ho, The Centers of Early-Type Galaxies with Hubble Space Telescope. VI. Bimodal Central Surface Brightness Profiles. *Astrophys. J.* **664**(1), 226–256 (2007). doi:10.1086/519229
- N.M. Law, S.R. Kulkarni, R.G. Dekany, E.O. Ofek, R.M. Quimby, P.E. Nugent, J. Surace, C.C. Grillmair, J.S. Bloom, M.M. Kasliwal, L. Bildsten, T. Brown, S.B. Cenko, D. Ciardi, E. Croner, S.G. Djorgovski, J. van Eyken, A.V. Filippenko, D.B. Fox, A. Gal-Yam, D. Hale, N. Hamam, G. Helou, J. Henning, D.A. Howell, J. Jacobsen, R. Laher, S. Mattingly, D. McKenna, A. Pickles, D. Poznanski, G. Rahmer, A. Rau, W. Rosing, M. Shara, R. Smith, D. Starr, M. Sullivan, V. Velur, R. Walters, J. Zolkower, The Palomar Transient Factory: System Overview, Performance, and First Results. *Publications of the Astronomical Society of the Pacific* **121**, 1395 (2009). doi:10.1086/648598
- J. Law-Smith, M. MacLeod, J. Guillochon, P. Macias, E. Ramirez-Ruiz, Low-mass White Dwarfs with Hydrogen Envelopes as a Missing Link in the Tidal Disruption Menu. *Astrophys. J.* **841**(2), 132 (2017a). doi:10.3847/1538-4357/aa6ffb
- J. Law-Smith, E. Ramirez-Ruiz, S.L. Ellison, R.J. Foley, Tidal Disruption Event Host Galaxies in the Context of the Local Galaxy Population. *The Astrophysical Journal* **850**(1), 22 (2017b). doi:10.3847/1538-4357/aa94c7. <http://arxiv.org/abs/1707.01559> <http://dx.doi.org/10.3847/1538-4357/aa94c7> <http://stacks.iop.org/0004->

- 637X/850/i=1/a=22?key=crossref.c289c6a61e660d0a15cca0f1b4cddc6e
- G. Leloudas, M. Fraser, N.C. Stone, S. van Velzen, P.G. Jonker, I. Arcavi, C. Fremling, J.R. Maund, S.J. Smartt, T. Kruhlér, J.C.A. Miller-Jones, P.M. Vreeswijk, A. Gal-Yam, P.A. Mazzali, A. De Cia, D.A. Howell, C. Inserra, F. Patat, A.d.U. Postigo, O. Yaron, C. Ashall, I. Bar, H. Campbell, T.-W. Chen, M. Childress, N. Elias-Rosa, J. Harmanen, G. Hosseinzadeh, J. Johansson, T. Kangas, E. Kankare, S. Kim, H. Kuncarayakti, J. Lyman, M.R. Magee, K. Maguire, D. Malesani, S. Mattila, C.V. McCully, M. Nicholl, S. Prentice, C. Romero-Canizales, S. Schulze, K.W. Smith, J. Sollerman, M. Sullivan, B.E. Tucker, S. Valenti, J.C. Wheeler, D.R. Young, The Superluminous Transient ASASSN-15lh as a Tidal Disruption Event from a Kerr Black Hole (2016). <http://arxiv.org/abs/1609.02927>
- G. Leloudas, L. Dai, I. Arcavi, P.M. Vreeswijk, B. Mockler, R. Roy, D.B. Malesani, S. Schulze, T. Wevers, M. Fraser, E. Ramirez-Ruiz, K. Auchettl, J. Burke, G. Cannizzaro, P. Charalampopoulos, T.-W. Chen, A. Cikota, M. Della Valle, L. Galbany, M. Gromadzki, K.E. Heintz, D. Hiramatsu, P.G. Jonker, Z. Kostrzewa-Rutkowska, K. Maguire, I. Mandel, F. Onori, N. Roth, S.J. Smartt, L. Wyrzykowski, D.R. Young, The spectral evolution of AT 2018dyb and the presence of metal lines in tidal disruption events. arXiv e-prints (2019)
- A.J. Levan, N.R. Tanvir, S.B. Cenko, D.A. Perley, K. Wiersema, J.S. Bloom, A.S. Fruchter, A.d.U. Postigo, P.T. O'Brien, N. Butler, A.J. van der Horst, G. Leloudas, A.N. Morgan, K. Misra, G.C. Bower, J. Farihi, R.L. Tunnicliffe, M. Modjaz, J.M. Silverman, J. Hjorth, C. Thöne, A. Cucchiara, J.M.C. Cerón, A.J. Castro-Tirado, J.A. Arnold, M. Bremer, J.P. Brodie, T. Carroll, M.C. Cooper, P.A. Curran, R.M. Cutri, J. Ehle, D. Forbes, J. Fynbo, J. Gorosabel, J. Graham, D.I. Hoffman, S. Guziy, P. Jakobsson, A. Kamble, T. Kerr, M.M. Kasliwal, C. Kouveliotou, D. Kocevski, N.M. Law, P.E. Nugent, E.O. Ofek, D. Poznanski, R.M. Quimby, E. Rol, A.J. Romanowsky, R. Sánchez-Ramírez, S. Schulze, N. Singh, L. van Spaandonk, R.L.C. Starling, R.G. Strom, J.C. Tello, O. Vaduvescu, P.J. Wheatley, R.A.M.J. Wijers, J.M. Winters, D. Xu, An extremely luminous panchromatic outburst from the nucleus of a distant galaxy. *Science* **333**(6039), 199–202 (2011). doi:10.1126/science.1207143. <http://adsabs.harvard.edu/abs/2011Sci...333..199L>
- D. Lin, P.W. Maksym, J.A. Irwin, S. Komossa, N.A. Webb, O. Godet, D. Barret, D. Grupe, S.D.J. Gwyn, An Ultrasoft X-Ray Flare from 3XMM J152130.7+074916: A Tidal Disruption Event Candidate. *Astrophys. J.* **811**(1), 43 (2015). doi:10.1088/0004-637X/811/1/43
- D. Lin, J. Guillochon, S. Komossa, E. Ramirez-Ruiz, J.A. Irwin, W.P. Maksym, D. Grupe, O. Godet, N.A. Webb, D. Barret, B.A. Zauderer, P.-A. Duc, E.R. Carrasco, S.D.J. Gwyn, A likely decade-long sustained tidal disruption event. *Nature Astronomy* **1**, 0033 (2017). doi:10.1038/s41550-016-0033
- D. Lin, J. Strader, E.R. Carrasco, D. Page, A.J. Romanowsky, J. Homan, J.A. Irwin, R.A. Remillard, O. Godet, N.A. Webb, H. Baumgardt, R. Wijnands, D. Barret, P.-A. Duc, J.P. Brodie, S.D.J. Gwyn, A luminous X-ray outburst from an intermediate-mass black hole in an off-centre star cluster. *Nature Astronomy* **2**, 656–661 (2018). doi:10.1038/s41550-018-0493-1
- C.J. Lintott, K. Schawinski, W. Keel, H. van Arkel, N. Bennert, E. Edmondson, D. Thomas, D.J.B. Smith, P.D. Herbert, M.J. Jarvis, S. Virani, D. Andreescu, S.P. Bamford, K. Land, P. Murray, R.C. Nichol, M.J. Raddick, A. Slosar, A. Szalay, J. Vandenberg, Galaxy Zoo: ‘Hanny’s Voorwerp’, a quasar light echo? *Mon. Not. R. Astron. Soc.* **399**(1), 129–140 (2009). doi:10.1111/j.1365-2966.2009.15299.x
- G. Lodato, A.R. King, J.E. Pringle, Stellar disruption by a supermassive black hole: is the light curve really proportional to $t^{-5/3}$? *Mon. Not. R. Astron. Soc.* **392**, 332–340 (2009). doi:10.1111/j.1365-2966.2008.14049.x
- M. MacLeod, J. Guillochon, E. Ramirez-Ruiz, THE TIDAL DISRUPTION OF GIANT STARS AND THEIR CONTRIBUTION TO THE FLARING SUPERMASSIVE BLACK HOLE POPULATION. *The Astrophysical Journal* **757**(2), 134 (2012). doi:10.1088/0004-637X/757/2/134. <http://adsabs.harvard.edu/abs/2012ApJ...757..134M>
- A.-M. Madigan, A. Halle, M. Moody, M. McCourt, C. Nixon, H. Wernke, Dynamical Properties of Eccentric Nuclear Disks: Stability, Longevity, and Implications for Tidal Disrup-

- tion Rates in Post-merger Galaxies. *Astrophys. J.* **853**, 141 (2018). doi:10.3847/1538-4357/aaa714
- J. Magorrian, S. Tremaine, Rates of tidal disruption of stars by massive central black holes. *Monthly Notices of the Royal Astronomical Society* **309**(2), 447–460 (1999). doi:10.1046/j.1365-8711.1999.02853.x. <http://adsabs.harvard.edu/abs/1999MNRAS.309..447M>
- J. Magorrian, S. Tremaine, D. Richstone, R. Bender, G. Bower, A. Dressler, S.M. Faber, K. Gebhardt, R. Green, C. Grillmair, J. Kormendy, T. Lauer, The Demography of Massive Dark Objects in Galaxy Centers. *Astron. J.* **115**, 2285–2305 (1998). doi:10.1086/300353
- W.P. Maksym, M.P. Ulmer, M.C. Eracleous, L. Guennou, L.C. Ho, A tidal flare candidate in Abell 1795. *Mon. Not. R. Astron. Soc.* **435**, 1904–1927 (2013). doi:10.1093/mnras/stt1379
- W.P. Maksym, D. Lin, J.A. Irwin, RBS 1032: A Tidal Disruption Event in Another Dwarf Galaxy? *Astrophys. J.* **792**(2), 29 (2014). doi:10.1088/2041-8205/792/2/L29
- W.P. Maksym, M.P. Ulmer, M. Eracleous, A Tidal Disruption Flare in A1689 from an Archival X-ray Survey of Galaxy Clusters. *Astrophys. J.* **722**, 1035–1050 (2010). doi:10.1088/0004-637X/722/2/1035
- S. Mattila, M. Pérez-Torres, A. Efstathiou, P. Mimica, M. Fraser, E. Kankare, A. Alberdi, M.Á. Aloy, T. Heikkilä, P.G. Jonker, P. Lundqvist, I. Martí-Vidal, W.P.S. Meikle, C. Romero-Canizales, S.J. Smartt, S. Tsygankov, E. Varenus, A. Alonso-Herrero, M. Bondi, C. Fransson, R. Herrero-Illana, T. Kangas, R. Kotak, N. Ramírez-Olivencia, P. Väisänen, R.J. Beswick, D.L. Clements, R. Greimel, J. Harmanen, J. Kotilainen, K. Nandra, T. Reynolds, S. Ryder, N.A. Walton, K. Wiik, G. Östlin, A dust-enshrouded tidal disruption event with a resolved radio jet in a galaxy merger. *Science* **361**, 482–485 (2018). doi:10.1126/science.aao4669
- N.J. McConnell, C.-P. Ma, Revisiting the Scaling Relations of Black Hole Masses and Host Galaxy Properties. *Astrophys. J.* **764**, 184 (2013). doi:10.1088/0004-637X/764/2/184
- J.T. Mendel, L. Simard, M. Palmer, S.L. Ellison, D.R. Patton, A CATALOG OF BULGE, DISK, AND TOTAL STELLAR MASS ESTIMATES FOR THE SLOAN DIGITAL SKY SURVEY. The Astrophysical Journal Supplement Series **210**(1), 3 (2014). doi:10.1088/0067-0049/210/1/3. <http://adsabs.harvard.edu/abs/2014ApJS..210....3M>
- D. Merritt, M.Y. Poon, Chaotic Loss Cones and Black Hole Fueling. *The Astrophysical Journal* **606**(2), 788–798 (2004). doi:10.1086/382497. <http://adsabs.harvard.edu/abs/2004ApJ...606..788M>
- B.D. Metzger, N.C. Stone, A bright year for tidal disruptions. *Mon. Not. R. Astron. Soc.* **461**(1), 948–966 (2016). doi:10.1093/mnras/stw1394
- B. Mockler, J. Guillochon, E. Ramirez-Ruiz, Weighing Black Holes Using Tidal Disruption Events. *Astrophys. J.* **872**, 151 (2019). doi:10.3847/1538-4357/ab010f
- M.M. Pawlik, V. Wild, C.J. Walcher, P.H. Johansson, C. Villforth, K. Rowlands, J. Mendez-Abreu, T. Hewlett, Shape asymmetry: a morphological indicator for automatic detection of galaxies in the post-coalescence merger stages. *Monthly Notices of the Royal Astronomical Society* **456**(3), 3032–3052 (2015). <http://arxiv.org/abs/1512.02000>
- P.J.E. Peebles, Star Distribution Near a Collapsed Object. *Astrophys. J.* **178**, 371–376 (1972). doi:10.1086/151797
- M. Pereira-Santaella, A. Alonso-Herrero, L. Colina, D. Miralles-Caballero, P.G. Pérez-González, S. Arribas, E. Bellocchi, S. Cazzoli, T. Díaz-Santos, J. Piqueras López, Star-formation histories of local luminous infrared galaxies. *Astron. & Astrophys.* **577**, 78 (2015). doi:10.1051/0004-6361/201425359
- F. Pérez, B.E. Granger, IPython: a system for interactive scientific computing. *Computing in Science and Engineering* **9**(3), 21–29 (2007). doi:10.1109/MCSE.2007.53. <http://ipython.org>
- H. Pfister, B. Bar-Or, M. Volonteri, Y. Dubois, P.R. Capelo, Tidal disruption event rates in galaxy merger remnants. arXiv e-prints, 1903–09124 (2019)
- J.L. Prieto, T. Krühler, J.P. Anderson, L. Galbany, C.S. Kochanek, E. Aquino, J.S. Brown, S. Dong, F. Förster, T.W.-S. Holoien, H. Kuncarayakti, J.C. Maureira, F.F. Rosales-Ortega, S.F. Sánchez, B.J. Shappee, K.Z. Stanek, MUSE Reveals a Recent Merger in the Post-starburst Host Galaxy of the TDE ASASSN-14li. *The Astrophysical Journal Letters* **830**(2), 32 (2016). <http://arxiv.org/abs/1609.00013>

- A.D. Quintero, D.W. Hogg, M.R. Blanton, D.J. Schlegel, D.J. Eisenstein, J.E. Gunn, J. Brinkmann, M. Fukugita, K. Glazebrook, T. Goto, Selection and Photometric Properties of K+A Galaxies. *The Astrophysical Journal* **602**(1), 190–199 (2004). doi:10.1086/380601. <http://adsabs.harvard.edu/abs/2004ApJ...602..190Q>
- A. Rau, S.R. Kulkarni, N.M. Law, J.S. Bloom, D. Ciardi, G.S. Djorgovski, D.B. Fox, A. Gal-Yam, C.C. Grillmair, M.M. Kasliwal, P.E. Nugent, E.O. Ofek, R.M. Quimby, W.T. Reach, M. Shara, L. Bildsten, S.B. Cenko, A.J. Drake, A.V. Filippenko, D.J. Helfand, G. Helou, D.A. Howell, D. Poznanski, M. Sullivan, Exploring the Optical Transient Sky with the Palomar Transient Factory. *Publications of the Astronomical Society of the Pacific* **121**, 1334 (2009). doi:10.1086/605911
- M.J. Rees, Tidal disruption of stars by black holes of 106108 solar masses in nearby galaxies. *Nature* **333**(6173), 523–528 (1988). doi:10.1038/333523a0. <http://adsabs.harvard.edu/abs/1988Natur.333..523R>
- J.A. Rich, L.J. Kewley, M.A. Dopita, Galaxy Mergers Drive Shocks: an Integral Field Study of GOALS galaxies. *The Astrophysical Journal Supplement Series* **221**, 28 (2015). doi:10.1088/0067-0049/221/2/28. <http://arxiv.org/abs/1509.08468> <http://dx.doi.org/10.1088/0067-0049/221/2/28>
- N. Roth, D. Kasen, J. Guillochon, E. Ramirez-Ruiz, The X-Ray through Optical Fluxes and Line Strengths of Tidal Disruption Events. *Astrophys. J.* **827**(1), 3 (2016). doi:10.3847/0004-637X/827/1/3
- R.D. Saxton, A.M. Read, P. Esquej, S. Komossa, S. Dougherty, P. Rodriguez-Pascual, D. Barrado, A tidal disruption-like X-ray flare from the quiescent galaxy SDSS J120136.02+300305.5. *Astron. & Astrophys.* **541**, 106 (2012). doi:10.1051/0004-6361/201118367
- R.D. Saxton, A.M. Read, S. Komossa, P. Lira, K.D. Alexander, M.H. Wieringa, XMMSL1 J074008.2-853927: a tidal disruption event with thermal and non-thermal components. *Astron. & Astrophys.* **598**, 29 (2017). doi:10.1051/0004-6361/201629015
- F. Schweizer, P. Seitzer, D.D. Kelson, E.V. Villanueva, G.L. Walth, The [O III] Nebula of the Merger Remnant NGC 7252: A Likely Faint Ionization Echo. *Astrophys. J.* **773**(2), 148 (2013). doi:10.1088/0004-637X/773/2/148
- B.J. Shappee, J.L. Prieto, D. Grupe, C.S. Kochanek, K.Z. Stanek, G. De Rosa, S. Mathur, Y. Zu, B.M. Peterson, R.W. Pogge, S. Komossa, M. Im, J. Jencson, T.W.-S. Holoien, U. Basu, J.F. Beacom, D.M. Szczygiel, J. Brimacombe, S. Adams, A. Campillay, C. Choi, C. Contreras, M. Dietrich, M. Dubberley, M. Elphick, S. Foale, M. Giustini, C. Gonzalez, E. Hawkins, D.A. Howell, E.Y. Hsiao, M. Koss, K.M. Leighly, N. Morrell, D. Mudd, D. Mullins, J.M. Nugent, J. Parrent, M.M. Phillips, G. Pojmanski, W. Rosing, R. Ross, D. Sand, D.M. Terndrup, S. Valenti, Z. Walker, Y. Yoon, The Man behind the Curtain: X-Rays Drive the UV through NIR Variability in the 2013 Active Galactic Nucleus Outburst in NGC 2617. *Astrophys. J.* **788**, 48 (2014). doi:10.1088/0004-637X/788/1/48
- L. Simard, J. Trevor Mendel, D.R. Patton, S.L. Ellison, A.W. McConnachie, VizieR Online Data Catalog: Bulge+disk decompositions of SDSS galaxies (Simard+, 2011). *VizieR Online Data Catalog*, 196–11 (2011)
- L. Simard, C.N.A. Willmer, N.P. Vogt, V.L. Sarajedini, A.C. Phillips, B.J. Weiner, D.C. Koo, M. Im, G.D. Illingworth, S.M. Faber, The DEEP Groth Strip Survey. II. Hubble Space Telescope Structural Parameters of Galaxies in the Groth Strip. *The Astrophysical Journal Supplement Series* **142**, 1–33 (2002). doi:10.1086/341399
- G.F. Snyder, T.J. Cox, C.C. Hayward, L. Hernquist, P. Jonsson, K+A GALAXIES AS THE AFTERMATH OF GAS-RICH MERGERS: SIMULATING THE EVOLUTION OF GALAXIES AS SEEN BY SPECTROSCOPIC SURVEYS. *The Astrophysical Journal* **741**(2), 77 (2011). doi:10.1088/0004-637X/741/2/77. <http://adsabs.harvard.edu/abs/2011ApJ...741...77S>
- D. Stern, R.J. Assef, D.J. Benford, A. Blain, R. Cutri, A. Dey, P. Eisenhardt, R.L. Griffith, T.H. Jarrett, S. Lake, F. Masci, S. Petty, S.A. Stanford, C.-W. Tsai, E.L. Wright, L. Yan, F. Harrison, K. Madsen, Mid-infrared Selection of Active Galactic Nuclei with the Wide-Field Infrared Survey Explorer. I. Characterizing WISE-selected Active Galactic Nuclei in COSMOS. *Astrophys. J.* **753**(1), 30 (2012). doi:10.1088/0004-637X/753/1/30
- N.C. Stone, B.D. Metzger, Rates of stellar tidal disruption as probes of the supermassive black hole mass function. *Mon. Not. R. Astron. Soc.* **455**(1), 859–883 (2016).

- doi:10.1093/mnras/stv2281
- N.C. Stone, S. van Velzen, An enhanced rate of tidal disruptions in the centrally overdense E+A galaxy NGC 3156. *The Astrophysical Journal Letters* **825**, 14 (2016). doi:10.3847/2041-8205/825/1/L14. <http://arxiv.org/abs/1604.02056> <http://dx.doi.org/10.3847/2041-8205/825/1/L14>
- N.C. Stone, M. Kesden, R.M. Cheng, S. van Velzen, Stellar Tidal Disruption Events in General Relativity (2018). <http://arxiv.org/abs/1801.10180>
- C. Tadhunter, R. Spence, M. Rose, J. Mullaney, P. Crowther, A tidal disruption event in the nearby ultra-luminous infrared galaxy F01004-2237. *Nature Astronomy* **1**, 0061 (2017). doi:10.1038/s41550-017-0061. <http://arxiv.org/abs/1702.02573>
- E. Tempel, A. Tamm, M. Gramann, T. Tuvikene, L.J. Liivamägi, I. Suhhonenko, R. Kipper, M. Einasto, E. Saar, Flux- and volume-limited groups/clusters for the SDSS galaxies: catalogues and mass estimation. *Astron. & Astrophys.* **566**, 1 (2014). doi:10.1051/0004-6361/201423585
- B. Trakhtenbrot, I. Arcavi, C. Ricci, S. Tacchella, D. Stern, H. Netzer, P.G. Jonker, A. Horeh, J.E. Mejía-Restrepo, G. Hosseinzadeh, V. Hallefors, D.A. Howell, C. McCully, M. Baloković, M. Heida, N. Kamraj, G.B. Lansbury, L. Wyrzykowski, M. Gromadzki, A. Hamanowicz, S.B. Cenko, D.J. Sand, E.Y. Hsiao, M.M. Phillips, T.R. Diamond, E. Kara, K.C. Gendreau, Z. Arzoumanian, R. Remillard, A new class of flares from accreting supermassive black holes. *Nature Astronomy* (2019). doi:10.1038/s41550-018-0661-3. <https://doi.org/10.1038/s41550-018-0661-3>
- E. Treister, K. Schawinski, C.M. Urry, B.D. Simmons, Major Galaxy Mergers Only Trigger the Most Luminous Active Galactic Nuclei. *Astrophys. J.* **758**, 39 (2012). doi:10.1088/2041-8205/758/2/L39
- S. Tremaine, K. Gebhardt, R. Bender, G. Bower, A. Dressler, S.M. Faber, A.V. Filippenko, R. Green, C. Grillmair, L.C. Ho, J. Kormendy, T.R. Lauer, J. Magorrian, J. Pinkney, D. Richstone, The Slope of the Black Hole Mass versus Velocity Dispersion Correlation. *Astrophys. J.* **574**, 740–753 (2002). doi:10.1086/341002
- C.A. Tremonti, T.M. Heckman, G. Kauffmann, J. Brinchmann, S. Charlot, S.D.M. White, M. Seibert, E.W. Peng, D.J. Schlegel, A. Uomoto, M. Fukugita, J. Brinkmann, The Origin of the Mass-Metallicity Relation: Insights from 53,000 Star-forming Galaxies in the Sloan Digital Sky Survey. *Astrophys. J.* **613**(2), 898–913 (2004). doi:10.1086/423264
- S. Van Der Walt, S.C. Colbert, G. Varoquaux, The numpy array: a structure for efficient numerical computation. *Computing in Science & Engineering* **13**(2), 22–30 (2011)
- S. van Velzen, On the Mass and Luminosity Functions of Tidal Disruption Flares: Rate Suppression due to Black Hole Event Horizons. *Astrophys. J.* **852**, 72 (2018). doi:10.3847/1538-4357/aa998e
- S. van Velzen, G.R. Farrar, S. Gezari, N. Morrell, D. Zaritsky, L. Östman, M. Smith, J. Gelfand, A.J. Drake, OPTICAL DISCOVERY OF PROBABLE STELLAR TIDAL DISRUPTION FLARES. *The Astrophysical Journal* **741**(2), 73 (2011). doi:10.1088/0004-637X/741/2/73. <http://adsabs.harvard.edu/abs/2011ApJ...741...73V>
- M. Volonteri, P. Madau, F. Haardt, The Formation of Galaxy Stellar Cores by the Hierarchical Merging of Supermassive Black Holes. *Astrophys. J.* **593**, 661–666 (2003). doi:10.1086/376722
- J. Wang, D. Merritt, Revised Rates of Stellar Disruption in Galactic Nuclei. *Astrophys. J.* **600**(1), 149–161 (2004). doi:10.1086/379767
- T.-G. Wang, H.-Y. Zhou, S. Komossa, H.-Y. Wang, W. Yuan, C. Yang, EXTREME CORONAL LINE EMITTERS: TIDAL DISRUPTION OF STARS BY MASSIVE BLACK HOLES IN GALACTIC NUCLEI? *The Astrophysical Journal* **749**(2), 115 (2012). doi:10.1088/0004-637X/749/2/115. <http://adsabs.harvard.edu/abs/2012ApJ...749..115W>
- K.-Y. Watarai, K. Ohsuga, R. Takahashi, J. Fukue, Geometrical Effect of Supercritical Accretion Flows: Observational Implications of Galactic Black-Hole Candidates and Ultraluminous X-Ray Sources. *PASJ* **57**, 513–524 (2005). doi:10.1093/pasj/57.3.513
- A.E. Watkins, J.C. Mihos, M. Bershadsky, P. Harding, Discovery of a Vast Ionized Gas Cloud in the M51 System. *Astrophys. J.* **858**(2), 16 (2018). doi:10.3847/2041-8213/aabba1
- T. Wevers, N.C. Stone, S. van Velzen, P.G. Jonker, T. Hung, K. Auchettl, S. Gezari, F. Onori, Black hole masses of tidal disruption event host galaxies II. arXiv e-prints (2019a)

- T. Wevers, D.R. Pasham, S. van Velzen, G. Leloudas, S. Schulze, J.C.A. Miller-Jones, P.G. Jonker, M. Gromadzki, E. Kankare, S.T. Hodgkin, L. . Wyrzykowski, Z. Kostrzewa-Rutkowska, S. Moran, M. Berton, K. Maguire, F. Onori, S. Matilla, M. Nicholl, Evidence for rapid disk formation and reprocessing in the X-ray bright tidal disruption event AT 2018fyk. arXiv e-prints, 1903–12203 (2019b)
- T. Wevers, S. van Velzen, P.G. Jonker, N.C. Stone, T. Hung, F. Onori, S. Gezari, N. Blagorodnova, Black hole masses of tidal disruption event host galaxies (2017). <http://arxiv.org/abs/1706.08965>
- V. Wild, T. Heckman, S. Charlot, Timing the starburst-AGN connection. *Monthly Notices of the Royal Astronomical Society* **405**(2), 933–947 (2010). doi:10.1111/j.1365-2966.2010.16536.x. <http://adsabs.harvard.edu/abs/2010MNRAS.405..933W>
- V. Wild, O. Almaini, J. Dunlop, C. Simpson, K. Rowlands, R. Bowler, D. Maltby, R. McLure, The evolution of post-starburst galaxies from $z=2$ to $z=0.5$. *Monthly Notices of the Royal Astronomical Society* **463**, 832–844 (2016). doi:10.1093/mnras/stw1996. <http://arxiv.org/abs/1608.00588> <http://dx.doi.org/10.1093/mnras/stw1996>
- R.J. Williams, R.W. Pogge, S. Mathur, Narrow-line Seyfert 1 Galaxies from the Sloan Digital Sky Survey Early Data Release. *Astron. J.* **124**(6), 3042–3049 (2002). doi:10.1086/344765
- O.I. Wong, K. Schawinski, S. Kaviraj, K.L. Masters, R.C. Nichol, C. Lintott, W.C. Keel, D. Darg, S.P. Bamford, D. Andreescu, P. Murray, M.J. Raddick, A. Szalay, D. Thomas, J. VandenBerg, Galaxy Zoo: building the low-mass end of the red sequence with local post-starburst galaxies. *Monthly Notices of the Royal Astronomical Society* **420**(2), 1684–1692 (2012). doi:10.1111/j.1365-2966.2011.20159.x. <http://adsabs.harvard.edu/abs/2012MNRAS.420.1684W>
- G. Worthey, D.L. Ottaviani, H γ and H δ Absorption Features in Stars and Stellar Populations. *The Astrophysical Journal Supplement Series* **111**(2), 377–386 (1997). doi:10.1086/313021. <http://adsabs.harvard.edu/abs/1997ApJS..111..377W>
- E.L. Wright, P.R.M. Eisenhardt, A.K. Mainzer, M.E. Ressler, R.M. Cutri, T. Jarrett, J.D. Kirkpatrick, D. Padgett, R.S. McMillan, M. Skrutskie, S.A. Stanford, M. Cohen, R.G. Walker, J.C. Mather, D. Leisawitz, I. Gautier Thomas N., I. McLean, D. Benford, C.J. Lonsdale, A. Blain, B. Mendez, W.R. Irace, V. Duval, F. Liu, D. Royer, I. Heinrichsen, J. Howard, M. Shannon, M. Kendall, A.L. Walsh, M. Larsen, J.G. Cardon, S. Schick, M. Schwalm, M. Abid, B. Fabinsky, L. Naes, C.-W. Tsai, The Wide-field Infrared Survey Explorer (WISE): Mission Description and Initial On-orbit Performance. *Astron. J.* **140**(6), 1868–1881 (2010). doi:10.1088/0004-6256/140/6/1868
- R. Yan, M.R. Blanton, THE NATURE OF LINER-LIKE EMISSION IN RED GALAXIES. *The Astrophysical Journal* **747**(1), 61 (2012). doi:10.1088/0004-637X/747/1/61. <http://iopscience.iop.org/0004-637X/747/1/61/article/>
- R. Yan, J.A. Newman, S.M. Faber, A.L. Coil, M.C. Cooper, M. Davis, B.J. Weiner, B.F. Gerke, D.C. Koo, The DEEP2 Galaxy Redshift Survey: environments of post-starburst galaxies at $\langle z \rangle = 0.1$ and 0.8 . *Monthly Notices of the Royal Astronomical Society* **398**(2), 735–753 (2009). doi:10.1111/j.1365-2966.2009.15192.x. <https://academic.oup.com/mnras/article-lookup/doi/10.1111/j.1365-2966.2009.15192.x>
- C.-W. Yang, T.-G. Wang, G. Ferland, W. Yuan, H.-Y. Zhou, P. Jiang, LONG-TERM SPECTRAL EVOLUTION OF TIDAL DISRUPTION CANDIDATES SELECTED BY STRONG CORONAL LINES. *The Astrophysical Journal* **774**(1), 46 (2013). doi:10.1088/0004-637X/774/1/46. <http://iopscience.iop.org/0004-637X/774/1/46/article/>
- Y. Yang, A.I. Zabludoff, D. Zaritsky, T.R. Lauer, J.C. Mihos, E+A Galaxies and the Formation of Early Type Galaxies at $z=0$. *The Astrophysical Journal* **607**(1), 258–273 (2004). doi:10.1086/383259. <http://adsabs.harvard.edu/abs/2004ApJ...607..258Y>
- Y. Yang, A.I. Zabludoff, D. Zaritsky, J.C. Mihos, The Detailed Evolution of E+A Galaxies into Early Types. *The Astrophysical Journal* **688**(2), 945–971 (2008). doi:10.1086/591656. <http://iopscience.iop.org/0004-637X/688/2/945>
- D.G. York, J. Adelman, J.E. Anderson Jr., S.F. Anderson, J. Annis, N.A. Bahcall, J.A. Bakken, R. Barkhouser, S. Bastian, E. Berman, W.N. Boroski, S. Bracker, C. Briegel, J.W. Briggs, J. Brinkmann, R. Brunner, S. Burles, L. Carey, M.A. Carr, F.J. Castander,

- B. Chen, P.L. Colestock, A.J. Connolly, J.H. Crocker, I. Csabai, P.C. Czarapata, J.E. Davis, M. Doi, T. Dombeck, D. Eisenstein, N. Ellman, B.R. Elms, M.L. Evans, X. Fan, G.R. Federwitz, L. Fiscelli, S. Friedman, J.A. Frieman, M. Fukugita, B. Gillespie, J.E. Gunn, V.K. Gurbani, E. de Haas, M. Haldeman, F.H. Harris, J. Hayes, T.M. Heckman, G.S. Hennessy, R.B. Hindsley, S. Holm, D.J. Holmgren, C. Huang, C. Hull, D. Husby, S. Ichikawa, T. Ichikawa, Ž. Ivezić, S. Kent, R.S.J. Kim, E. Kinney, M. Klaene, A.N. Kleinman, S. Kleinman, G.R. Knapp, J. Korienek, R.G. Kron, P.Z. Kunszt, D.Q. Lamb, B. Lee, R.F. Leger, S. Limmongkol, C. Lindenmeyer, D.C. Long, C. Loomis, J. Loveday, R. Lucinio, R.H. Lupton, B. MacKinnon, E.J. Mannery, P.M. Mantsch, B. Margon, P. McGehee, T.A. McKay, A. Meiksin, A. Merelli, D.G. Monet, J.A. Munn, V.K. Narayanan, T. Nash, E. Neilsen, R. Neswold, H.J. Newberg, R.C. Nichol, T. Nicinski, M. Nonino, N. Okada, S. Okamura, J.P. Ostriker, R. Owen, A.G. Pauls, J. Peoples, R.L. Peterson, D. Petravick, J.R. Pier, A. Pope, R. Pordes, A. Prosapio, R. Rechenmacher, T.R. Quinn, G.T. Richards, M.W. Richmond, C.H. Rivetta, C.M. Rockosi, K. Ruthmansdorfer, D. Sandford, D.J. Schlegel, D.P. Schneider, M. Sekiguchi, G. Sergey, K. Shimasaku, W.A. Siegmund, S. Smee, J.A. Smith, S. Snedden, R. Stone, C. Stoughton, M.A. Strauss, C. Stubbs, M. SubbaRao, A.S. Szalay, I. Szapudi, G.P. Szokoly, A.R. Thakar, C. Tremonti, D.L. Tucker, A. Uomoto, D. Vanden Berk, M.S. Vogeley, P. Wadell, S. Wang, M. Watanabe, D.H. Weinberg, B. Yanny, N. Yasuda, The Sloan Digital Sky Survey: Technical Summary. *Astron. J.* **120**, 1579–1587 (2000). doi:10.1086/301513
- A.I. Zabludoff, D. Zaritsky, H. Lin, D. Tucker, Y. Hashimoto, S.A. Shectman, A. Oemler, R.P. Kirshner, The Environment of “E+A” Galaxies. *Astrophys. J.* **466**, 104 (1996). doi:10.1086/177495